POLYTECHNIQUE MONTRÉAL

affiliée à l'Université de Montréal

Empirical Solution to Estimate the Maximum Allowed Mass of Dumped Waste Rock to Avoid Significant Poor Mixture Between Dumped Waste Rock and Paste Backfill in Stopes

PANTEA KAZEMI

Département des génies civil, géologique et des mines

Mémoire présenté en vue de l'obtention du diplôme de *Maîtrise ès sciences appliquées*

GÉNIE MINÉRAL

Mai 2026

POLYTECHNIQUE MONTRÉAL

affiliée à l'Université de Montréal

Ce mémoire intitulé :

Empirical Solution to Estimate the Maximum Allowed Mass of Dumped Waste Rock to Avoid Significant Poor Mixture Between Dumped Waste Rock and Paste Backfill in Stopes

présenté par **Pantea KAZEMI**

en vue de l'obtention du diplôme de *Maîtrise ès sciences appliquées*

a été dûment accepté par le jury d'examen constitué de :

Pedro CAZZOTO CACCIARI, président

Li LI, membre et directeur de recherche

Louis-Philippe GÉLINAS, membre

DEDICATION

To my family.

ACKNOWLEDGEMENTS

First and foremost, I would like to express my sincere gratitude to my supervisor, Prof. Li Li, for giving me the valuable opportunity to pursue my studies under his supervision. His continuous support and guidance have played a fundamental role in my academic journey. I have been deeply inspired by his strong dedication to research and his passion for his work. Working with him has been a truly enriching experience, and I have learned many important lessons that will benefit my future career.

I would also like to thank Prof. Cazzoto Cacciari and Mr. Gélinas for kindly accepting to serve as members of my thesis examination committee. I truly appreciate the time and effort they devoted to reviewing my work and providing their evaluation.

I would also like to acknowledge the support of Patrick Berneche, Mathieu Robidas, and Noura El-Harrak for their assistance in the preparation of experimental materials and molds. My sincere appreciation is extended to Monica Monzon for her ongoing support and kindness during my studies.

I would like to thank Islem, along with the interns Mohammad and Franck, for their involvement in the laboratory activities and their help with material preparation.

I acknowledge the financial support provided by the Natural Sciences and Engineering Research Council of Canada (NSERC) and the industrial partners of the Research Institute on Mines and the Environment (RIME UQAT – Polytechnique). Their support made this research possible.

Finally, I would like to express my deepest gratitude to my family. I am especially thankful to my parents for providing me with this opportunity, for their constant support. I am truly grateful to my dear Mehrad, who has been by my side during all this time, supporting me, encouraging me, and helping me through every challenge. My heartfelt thanks go to my lovely sister, whose warm smile always helped reduce the distance and made difficult moments easier. I would also like to thank my grandparents for their endless love and kindness.

RÉSUMÉ

Les activités minières génèrent de grandes quantités de rejets miniers, principalement sous forme de roches stériles et de résidus miniers. Traditionnellement, les roches stériles produites dans les mines souterraines sont transportées vers la surface et stockées dans des haldes à stériles. Cette pratique entraîne des coûts d'exploitation élevés, une consommation importante d'énergie et des émissions considérables de gaz à effet de serre. Une approche de plus en plus envisagée dans les méthodes d'abattage par longs trous consiste à déverser directement les roches stériles produites sous terre dans les chantiers en cours de remblayage avec du remblai en pâte cimenté. Cette méthode de codisposition offre plusieurs avantages par rapport à la gestion conventionnelle des roches stériles ou aux procédés de mélange mécanique. Elle permet d'éviter le transport des roches stériles vers la surface ainsi que les opérations de mélange mécanique, ce qui peut réduire la consommation d'énergie, les coûts de main-d'œuvre et les émissions de gaz à effet de serre. De plus, l'utilisation des roches stériles réduit le volume requis de remblai en pâte cimenté, ce qui peut diminuer la consommation de liant et les coûts de production. Un mélange adéquat de roches stériles et de remblai en pâte peut également présenter de meilleures propriétés mécaniques que chacun des matériaux pris séparément.

Malgré ces avantages, cette approche repose sur un processus de mélange naturel et non contrôlé entre les roches stériles déversées et le remblai en pâte déjà en place. Lorsque des quantités excessives de roches stériles sont déposées, un mauvais mélange peut se produire, ce qui peut entraîner l'instabilité de la masse de remblai exposée lors de l'excavation des chantiers adjacents. Il est donc nécessaire de disposer d'un outil fiable permettant de guider la détermination de la quantité maximale admissible de roches stériles à déverser.

Ce mémoire vise à développer une solution empirique permettant d'estimer la masse maximale admissible de roches stériles pouvant être déversée sans provoquer un mauvais mélange significatif entre les roches stériles et le remblai en pâte. Pour atteindre cet objectif, une série d'essais en laboratoire a été réalisée afin d'étudier le comportement de mélange naturel entre les roches stériles et le remblai en pâte. Les effets de paramètres clés, notamment la teneur en solides et l'épaisseur du remblai en pâte, la taille maximale des particules et la hauteur de chute des roches stériles, ainsi que les dimensions du chantier et la surface de réception, ont été analysés de manière systématique.

Les résultats montrent que la masse maximale admissible de roches stériles diminue avec l'augmentation de la teneur en solides du remblai en pâte, tandis qu'elle augmente avec l'augmentation de l'épaisseur du remblai en pâte, de la taille des particules des roches stériles et de la hauteur de chute. Une équation empirique a été développée afin d'estimer cette masse maximale admissible, avec des coefficients déterminés par une analyse de régression basée sur les résultats des essais à petite échelle. La validité et la capacité prédictive de la solution proposée ont été vérifiées à l'aide de résultats expérimentaux indépendants obtenus à partir d'essais à petite et à grande échelle.

La solution proposée peut être considérée comme un outil utile pour soutenir les opérations de déversement des roches stériles et réduire le risque de mauvais mélange entre les roches stériles et le remblai en pâte. Toutefois, une certaine prudence est nécessaire en raison de la nature empirique de cette solution. Elle ne doit pas être utilisée pour estimer le rapport entre les quantités de roches stériles et de remblai en pâte. Des travaux supplémentaires sont nécessaires afin d'intégrer explicitement l'effet de la surface de réception et de valider la solution dans des conditions réelles de terrain en utilisant du remblai en pâte cimenté.

ABSTRACT

Mining activities generate large quantities of mine waste, mainly in the form of waste rock and tailings. Traditionally, waste rock produced in underground mines is transported to the surface and stored in waste rock piles. This practice results in high operational costs, significant energy consumption, and considerable greenhouse gas emissions. An increasingly adopted approach in longhole stoping consists of directly dumping underground-generated waste rock into stopes being filled with cemented paste backfill. This co-disposal method offers several advantages compared to conventional waste rock management or mechanical mixing processes. It eliminates the need for transporting waste rock to the surface and mechanical mixing operations, which may reducing energy consumption, labor costs, and greenhouse gas emissions. In addition, the use of waste rock reduces the required volume of cemented paste backfill, leading to lower binder consumption and reduced production costs. A well-mixed combination of waste rock and paste backfill may also exhibit improved mechanical properties compared to each material alone

Despite these advantages, this approach relies on a natural and uncontrolled mixing process between dumped waste rock and in-place paste backfill. When excessive amounts of waste rock are deposited, poor mixing may occur, which can lead to instability of the exposed backfill mass during the excavation of adjacent stopes. Therefore, a reliable tool is required to guide the determination of the maximum allowable quantity of waste rock to be dumped.

This thesis aims to develop an empirical solution to estimate the maximum allowable waste rock mass that can be dumped without causing significant poor mixing between waste rock and paste backfill. To achieve this objective, a series of laboratory experiments was conducted to investigate the natural mixing behavior between waste rock and paste backfill. The effects of key parameters, including paste backfill solids content and thickness, waste rock maximum particle size and falling height, as well as stope dimensions and receiving area, were systematically analyzed.

The results show that the maximum allowable waste rock mass decreases with increasing solids content of the paste backfill, while it increases with increasing paste backfill thickness, waste rock particle size, and falling height. An empirical equation was developed to estimate this maximum allowable mass, with coefficients determined through regression analysis based on small-scale experimental data. The validity and predictive capability of the proposed solution were verified using independent experimental results obtained from both small-scale and large-scale tests.

The proposed solution can be considered as a useful tool to support waste rock dumping operations and to reduce the risk of poor mixing between waste rock and paste backfill. However, caution is required due to its empirical nature. The solution should not be used to estimate the ratio between waste rock and paste backfill quantities. Further work is needed to explicitly incorporate the effect of receiving area and to validate the solution under real field conditions using cemented paste backfill.

TABLE OF CONTENTS

LIST OF TABLES

LIST OF FIGURES

LISTE OF SYMBOLS AND ABBREVIATIONS

Symbols

a Empirical constant (-)

A' Auxiliary coefficient related to the factor of safety and backfill friction angle (-)

b Empirical constant (-)

B Stope width (m)

B_t Equivalent width of the sliding wedge (m)

B' Auxiliary coefficient related to the sliding-plane geometry and side-wall adherence (-)

c Cohesion (kPa) of backfill in Chapter 2; Empirical constant (-) in Chapter 3

c_b Cohesion along the backfill–side wall interface (kPa)

c_{bb} Interface cohesion between the backfill and the back wall (kPa)

c_{bs} Interface cohesion between the backfill and the side walls (kPa)

c_{final} Required final cohesion of the CPB plug at the completion of backfilling (kPa)

c_{if} Bond cohesion between the final-pour backfill and the side walls (kPa)

c_{ip} Bond cohesion between the plug-pour backfill and the side walls (kPa)

c_p Cohesion of the plug-pour backfill (kPa)

c_s Cohesion along the side walls (kPa)

c_{ss} Self-supporting cohesion required for plug to remain stable without barricade support (kPa)

C_u Coefficient of uniformity (-)

C_w Solids content of paste backfill (%)

C' Auxiliary coefficient related to the exponential arching effect (-)

d Empirical constant (-)

d_{max} Maximum particle size of waste rock (mm)

D_M Mold width (cm)

d_{ts} Thickness of the sill mat (m)

D_{10} Effective particle size corresponding to 10% passing (mm)

D_{60} Effective particle size corresponding to 60% passing (mm)

D' Auxiliary coefficient used in the required cohesion equation (-)

e Empirical constant (-)

f Empirical constant (-)

FS Factor of Safety (-)

g Empirical constant (-)

G' Intermediate parameter used to account for the stress reduction associated with arching in the upper block (kPa)

H Stope height (m)

H^* Equivalent height of the failure block (m)

H_b Height of the plug above the undercut brow (m)

H_f Falling height of wast rock(cm)

H_m Height of the main pour above the plug at a given time (m)

$H_{m,final}$ Final height of the main pour (m)

$H_{m,max}(t)$ Maximum supportable height of the main pour at time t (m)

H_p Paste backfill thickness (cm)

H_s Elevation of the intersection line between the wedge-sliding plane and front-wall plane (m)

h_s Thickness or height of the sill mat (m)

H_t Depth of the potential tension crack (m)

H_{tf} Thickness of the final-pour backfill (m)

H_{tp} Thickness of the plug-pour backfill (m)

H_u Height of the undercut (m)

H' Equivalent height of the plug portion above the sliding plane (m)

K Earth pressure coefficient (-)

L Stope length (m)

L_u Distance between the backfill barricade and the undercut brow (m)

M Arching parameter

M_{remain} Remaining waste rock in the funnel (g)

M_{top} Waste rock remaining on the surface (g)

M_{total} Total mass of waste rock (g)

P_0 Overload applied on the top surface of the backfill (kPa)

p_1 Pressure at the boundary between upper rectangular block and lower triangular wedge (kPa)

p_n Equivalent pressure parameter used to simplify the factor of safety expression (kPa)

p' Equivalent pressure parameter used in the generalized solution for HAR stopes (kPa)

p'' Equivalent pressure parameter used in the generalized solution for LAR stopes (kPa)

R^2 Coefficient of determination (-)

r_{bb} Adherence ratio between the backfill and back wall (-)

r_{bs} Adherence ratio between the backfill and side walls (-)

r_{if} Interface adherence ratio for the final-pour backfill (-)

r_{ip} Interface adherence ratio for the plug-pour backfill (-)

r_p Cohesion ratio between the plug pour and the final pour (-)

r_s Adherence ratio between interface cohesion and backfill cohesion (-)

S_s Shear resistant force along the two side walls (kN)

t Time measured from the start of the plug pour (h)

w Uniform load acting on the sill mat, including overburden and self-weight (kPa)

X Force component associated with the side-wall shear resistance and arching effect (kN)

Y Force component normal-related to the sliding wedge (kN)

Z Force component driving-related to the sliding wedge (kN)

α Inclination angle of the critical failure plane (°)

β Dip angle of the stope (°)

γ Unit weight of the backfill (kN/m³)

γ_p Unit weight of the plug-pour backfill (kN/m³)

δ Interface friction angle between the backfill and the stope wall (°)

ϕ Internal friction angle of the backfill (°)

ϕ_p Internal friction angle of the plug-pour backfill (°)

σ_A Stress difference used to distinguish between crushing and crushing–caving failure modes (kPa)

σ_b Bending-induced stress in the sill mat (kPa)

σ_c Compressive strength of the backfill (kPa)

σ_s Horizontal compressive stress acting on the sill mat, induced by wall closure (kPa)

σ_t Tensile strength of the backfill (kPa)

σ_v Vertical stress applied on the sill mat (kPa)

τ_f Shear strength at the fill–wall interface (kPa)

Abbreviations

AMD Acid mine drainage

ARD Acid rock drainage

CHF Cemented hydraulic fill

CPB Cemented paste backfill

HAR High aspect ratio

LAR Low aspect ratio

LHD Load haul dump

PAF Paste aggregate fill

PSD	Particle size distribution
RPF	Rocky paste fill
UCS	Unconfined compressive strength

CHAPTER 1 INTRODUCTION

1.1 Background and problematics

During underground mining operations, a large volume of waste rock is generated to access ore bodies. Traditionally, a significant portion of this waste rock is transported to the ground surface and then stored in waste rock piles. This process requires a significant amount of energy consumption, workforce, and additional operational costs. An alternative method in longhole stoping is to directly dump waste rock into stopes that are being filled with paste backfill. In this approach, waste rock does not need to be transported to the surface. There is no requirement for mechanical mixers. As a result, energy consumption and operational costs are reduced, greenhouse gas emissions are lowered, and binder consumption decreases because part of the cemented paste backfill is replaced by uncemented waste rock.

Although this method offers several advantages, it presents also a few limitations. For example, waste rock dumping is usually conducted during the final pour stage of cemented paste backfill (CPB), not during the plug pour stage. In addition, the use of waste rock reduces the required volume of cemented paste backfill. As a result, less tailings are placed underground, and a larger volume of tailings may need to be stored on the surface, requiring additional surface storage space. More seriously, if an excessive amount of waste rock is dumped onto the paste backfill, poor mixing between the two materials may occur. In such case, the fill mass may become unstable during the excavation of a neighboring stope, resulting in undesirable and potentially hazardous consequences. To reduce these risks, a practical tool is needed to estimate the maximum allowable quantity of dumped waste rock that can penetrate into the paste backfill.

Until now, most research on underground backfilling has focused on a single type of backfill material, such as hydraulic fill, cemented paste backfill, rockfill, or a mixture of them. A few researchers have examined mixtures of graded waste rock and cemented hydraulic fill or tailings slurry for underground applications (Baldwin & Grice, 2000; Hane et al., 2017; Rask, 2019; Sun et al., 2018). The waste rock was typically crushed, well-graded, and mechanically mixed with the paste backfill to achieve a uniform mixture. It requires additional processing steps, crush waste rocks in to a smaller particles, and mechanical mixing equipment, which increase both energy consumption and operational costs. However, investigations on the mixing behavior between dumped waste rock and paste backfill remain limited.

Recently, Zhang and Li (2023) investigated the natural mixing behavior between dumped waste rock and paste backfill. Their results demonstrated that the degree of mixing can be enhanced by increasing the falling height and maximum particle size of waste rock and by reducing the solid content of the paste backfill. Study on how much waste rock can be dumped into paste backfill without causing poor mixture is still nonexistent in literature.

1.2 Thesis objectives

The main objective of this thesis is to fill the identified gap through developing a practical solution to evaluate the maximum allowable quantity of dumped waste rock that can naturally mix with paste backfill without causing poor mixture conditions. More specifically, this study aims to develop an empirical solution that can be used as a practical tool for mining engineers to control waste rock dumping operations and reduce the risk of poor mixture between the dumped waste rock and paste backfill.

1.3 Hypotheses and methodology

To reach the main objective, the following hypotheses are applied:

- There exists a maximum allowable quantity of dumped waste rock, beyond which poor mixing between waste rock and paste backfill is likely to occur.
- Poor mixture conditions can be avoided or minimized through proper control of the quantity of dumped waste rock.
- The maximum allowable quantity of dumped waste rock to avoid poor mixture with paste backfill depends on several parameters, including the solid content and thickness of the paste backfill, the falling height, the maximum particle size, and the dumping position, and the receiving area of the waste rock as well as stope dimensions.
- The maximum allowable quantity of dumped waste rock to avoid poor mixture with paste backfill in underground mines can be quantitatively described using an empirical equation.

The main objective is then reached through the realization of the following sub-objectives (SO):

- SO1. Obtaining an experimental evaluation of the maximum allowed mass of waste rock to avoid poor mixing between the dumped waste rock and the paste backfill.

To achieve this first SO, a series of controlled laboratory tests were conducted to examine the influence of key parameters on the maximum allowed waste rock mass, including the solid content of the paste backfill, the maximum particle size of the waste rock, the falling height of the waste rock, the thickness of the paste backfill layer, dimensions of stope, and the receiving area of the waste rock on the paste surface.

- SO2. Developing an empirical solution to relate the maximum allowed mass of waste rock with the influencing parameters

  Based on the experimental results obtained in SO1, an empirical equation is proposed to estimate the maximum allowable quantity of dumped waste rock. The equation is derived from laboratory observations and incorporates the key influencing parameters identified during testing. The constant coefficients of the empirical equation are obtained through calibration using the best curve-fitting techniques.

- SO3. Validation or verification of the calibrated empirical solution

  To verify the predictive capability or to evaluate the reliability of the proposed empirical equation, new tests are conducted to obtain additional and independent experimental data. These experimental results, not used during the calibration process, are then used to test the predictive capability of the calibrated empirical solution. In addition, large-scale tests are carried out to examine the applicability of the proposed equation under larger and closer to field conditions.

1.4 Contributions

Through the realization of the three previously defined SOs, this thesis provides a systematic evaluation of the factors affecting the maximum allowable mass of waste rock that can naturally mix with paste backfill. The results demonstrate that this maximum allowable mass depends on paste backfill thickness, solid content of the paste backfill, falling height of the waste rock, receiving area, and the maximum particle size of the waste rock. An empirical equation was for the first time proposed to estimate the maximum allowed waste rock to avoid poor mixture between paste backfill and dumped waste rock. The proposed empirical solution was first calibrated against some experimental results to obtain the empirical constants. The calibrated empirical solution was then validated against two additional and independent sets of experimental data obtained from small -scale tests to large-scale tests. The results demonstrate that the proposed empirical solution can reasonably predict the maximum allowed mass of dumped waste rock at different scales under varying conditions. The outcomes of this research have led to the submission of one journal article and the publication of one conference paper as follows:

- Pantea Kazemi & Li Li (2026) An empirical equation for estimating the maximum allowable waste rock mass to avoid poor mixture between paste backfill and dumped waste rock. Green and Smart Mining Engineering.
- Pantea Kazemi & Li Li (2025) Experimental evaluation of maximum allowed waste rock to avoid poor mixture between paste backfill and dumped waste rock. GeoManitoba 2025.

1.5 Outline of the thesis

The thesis is structured in an article-based format, composed of five chapters.

Chapter 1 presents an introduction of the M.Sc. thesis. The background and problematic were elucidated, followed by the research objectives, hypotheses and methodology, main contributions, and the overall structure of the thesis.

Chapter 2 provides a comprehensive review of the relevant literature. It covers underground mining methods, different types of backfill systems, and previous studies related to mechanical and natural mixtures of waste rock and paste backfill.

Chapter 3 in term of a journal article illustrates the influence of key parameters, such as the solid content of the paste backfill, paste backfill thickness, waste rock falling height, maximum particle size, and stope dimensions, on the maximum allowable mass of dumped waste rock mass to avoid poor mixture between paste backfill and dumped waste rock. An empirical equation is proposed based on first set of experimental results. The predictive capability of the proposed and calibrated solution is evaluated against additional and independent experimental data obtained from small -scale tests to large-scale tests.

A general discussion of the thesis was given in Chapter 4.

Chapter 5 summarizes the principal conclusions of the thesis and outlines recommendations for future research.

CHAPTER 2 LITERATURE REVIEW

Mining has played an essential role in human civilization for thousands of years. Valuable materials such as metals, gold and industrial minerals has been extracted to produce goods, energy, and construction materials. In this chapter, a literature review is presented, covering underground mining methods, the stability and required strength of exposed backfill, mining wastes and their properties and management challenges, different types of mine backfill, and mixtures of waste rock and backfill.

2.1 Underground mining methods and mining backfills

Underground mining methods are generally classified into three main categories based on how the stability of the stope is maintained: unsupported methods (open stopes), supported methods (artificially supported), and caving methods (Darling, 2011). This classification is essential because the need for backfill is directly related to the support mechanism used in each method.

2.1.1 Unsupported mining methods

Unsupported mining methods are those in which the stability of the excavation is mainly maintained by the natural strength of the ore and surrounding rock mass. In these methods, large artificial support systems are generally not required during the extraction stage, although local support may still be necessary in some areas (Brady & Brown, 2006; Hamrin et al., 2001).

These methods include room-and-pillar mining, sublevel stoping, and shrinkage stoping, each of which is applied under specific geological and operational conditions.

Figure 2-1 shows a typical room-and-pillar mining layout. The method is commonly applied to flat-bedded or gently dipping ore deposits with limited thickness (Brady & Brown, 2006; Hamrin et al., 2001). In this method, a series of openings (rooms) are excavated while portions of the ore are intentionally left in place as pillars to support the roof. However, the method often leads to lower overall ore recovery because a significant portion of the ore must remain as support pillars. Backfill is generally not required during primary extraction because the pillars provide sufficient stability. However, if pillar recovery is planned at a later stage, backfill becomes necessary to replace the support provided by the pillars and prevent collapse. Therefore, backfill is not mandatory but becomes operationally necessary during secondary extraction due to the removal of natural support (Brady & Brown, 2006).

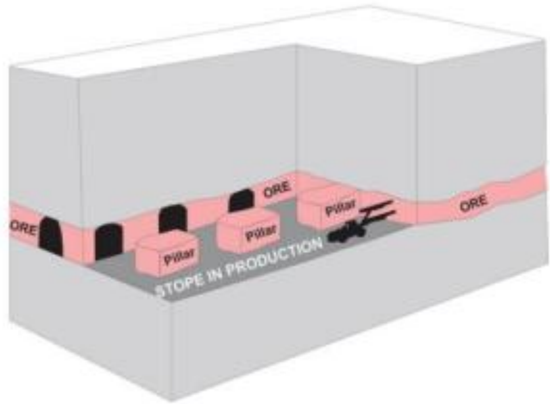

Figure 2-1 Room-and-pillar mining method (reproduced of Abzalov 2016 with permission)

Figure 2-2 shows a typical sublevel stoping layout. This method is widely used for steeply dipping ore bodies with relatively regular geometry, consistent boundaries, and competent ore and wall rock (Hamrin et al., 2001). In this method, the orebody is divided vertically into sublevels from which long blast holes are drilled and blasted to fragment the ore. Broken ore then falls to draw points where it is collected and hauled away. However, because they create large open voids, the surrounding rock must remain stable during ore extraction. Backfill is not always mandatory, but it is often used depending on geomechanical conditions. If the surrounding rock is sufficiently strong, the stope can remain stable without backfill. However, when large unsupported voids create stability concerns or when pillar recovery is required, backfill becomes necessary. Therefore, the need for backfill in this method is conditional and mainly driven by the presence of large voids and the requirement to improve ore recovery (Brady & Brown, 2006; Hustrulid & Bullock, 2001).

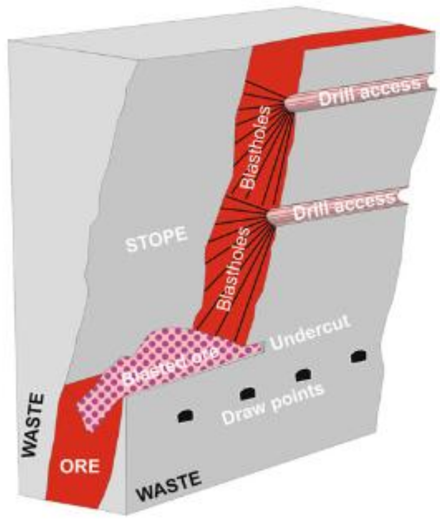

Figure 2-2 Sublevel stoping method (reproduced of Abzalov 2016 with permission)

Longhole stoping is another form of sublevel open stoping method. It is commonly applied to massive or steeply dipping stratiform orebodies. For inclined orebodies, the footwall inclination should be greater than the angle of repose of the broken rock to allow the fragmented ore to flow freely toward the extraction level. The orebody boundaries should be relatively regular, since the method is based on regular stope outlines and the use of long blast holes. In narrow orebodies, drilling inaccuracy may cause blast-hole penetration into the stope walls and increase dilution; therefore, Brady and Brown (2006) reported that the minimum orebody width for open stoping is about 6 m.

Although open stoping is unsupported during the active ore extraction stage, backfill is commonly used after the stope has been mined out. In modern open stoping with delayed backfill, the orebody is often divided into primary and secondary stopes. The primary stopes are mined first and then filled with cemented backfill. This cemented fill forms vertical man-made pillars and must remain stable during the subsequent extraction of adjacent secondary stopes. Figure 2-3 illustrates the cemented backfill in the primary stope and the uncemented backfill placed in the adjacent secondary stope. The cementation of the backfill is generally achieved by adding ordinary Portland cement or other binders, such as fly ash, slag, or pozzolans, to fill materials such as tailings or waste rocks. Liu et al. (2018) explained that delayed backfill improves ground stability, maximizes ore recovery, reduces ground subsidence, and decreases the environmental impacts associated with surface disposal of mine wastes.

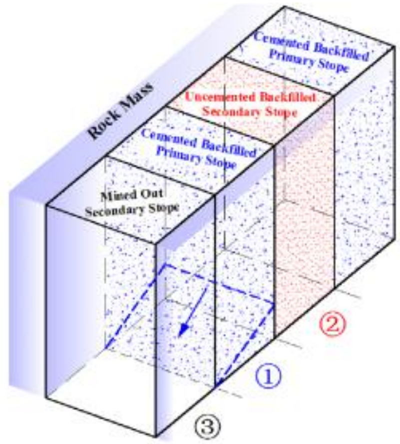

Figure 2-3 Schematic representation of a cemented backfill exposed on one side and subjected to lateral pressure from adjacent uncemented backfill (reproduced from Liu et al., 2018 with permission)

In some longhole stoping operations, backfilling may also be performed in two stages. In this sequence, a cemented paste backfill plug is first placed in the lower part of the stope, close to the extraction level, undercut, or barricade area. This plug must gain enough strength to become self-supporting and to resist the pressure applied by the fill placed above it. After the plug has developed sufficient strength, the remaining volume of the stope is filled with the main or mass fill. The geometry of the CPB plug, the undercut, and the main fill can be seen in Figure 2-4. This two-stage geometry is important because the stability of the plug controls the pressure transferred to the barricade and the overall stability of the backfilled stope. (Grabinsky et al., 2021).

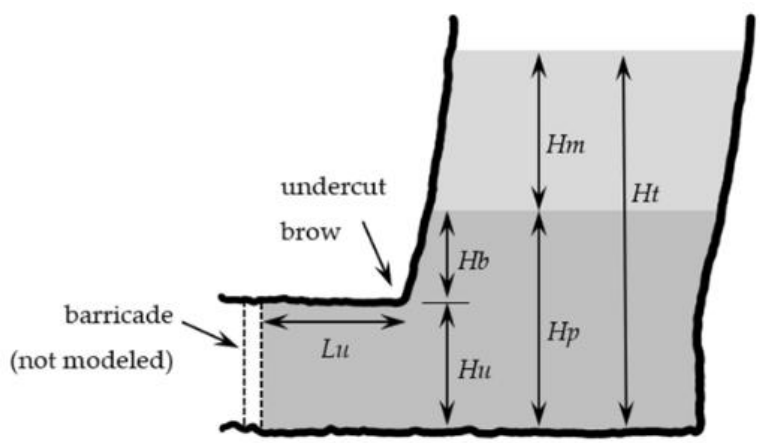

Figure 2-4 CPB plug geometry and model parameters (reproduced of Grabinsky et al. 2021 with permission)

The stability of cemented backfill is therefore a key design issue in open stoping. When a secondary stope is excavated beside a backfilled primary stope, the cemented backfill may become exposed on one side and must act as an artificial support element. If the side-exposed backfill does not have enough strength, it may fail after wall exposure, which can endanger workers and equipment and dilute the blasted ore. Therefore, the required strength of cemented backfill must be properly estimated to ensure stability while avoiding excessive binder consumption (Liu et al., 2018; Wang et al., 2021).

Shrinkage stoping is a selective mining method in which broken ore is temporarily left inside the stope during extraction. This retained ore acts both as a working platform and as temporary support for the stope walls. As a result, this method does not rely on backfill during operation, since the broken ore itself fulfills the supporting function (Brady & Brown, 2006; Hamrin et al., 2001).

2.1.2 Supported mining methods

Supported mining methods are commonly used where the rock mass is not sufficiently stable to remain unsupported during excavation. In these methods, backfill plays an essential role in providing ground support, reducing the exposure of open voids, and offering a safe working platform for continued mining (Potvin et al., 2005; Brady & Brown, 2006).

These methods include bench-and-fill mining method and cut-and-fill mining and its variations such as the Avoca method, drift-and-fill method, post-pillar method.

Bench-and-fill mining was developed as a more productive alternative to conventional cut-and-fill in cases where geotechnical conditions are favorable. In this method, ore is extracted in bench-shaped stopes, often using longhole drilling and blasting, and the mined-out voids are then backfilled. In this method backfill is mandatory because mining creates voids that must be filled to maintain stability and allow operations to continue (Brady & Brown, 2006).

Cut-and-fill is one of the most important underground mining methods for steeply dipping orebodies, especially when the ore zones are irregular or selective mining is required. In this method, ore is extracted in horizontal slices, typically starting from the bottom of the stope and progressing upward. After each slice is removed, the resulting void is filled with backfill material before the next slice is mined. Backfill in cut-and-fill mining serves two main functions. First, it provides support to the stope walls and surrounding rock mass, thereby improving ground stability. Second, it acts as a working platform for workers and equipment during the extraction of the next slice. This working platform created by the backfill during cut-and-fill mining is illustrated in Figure 2-5. Because of the repeated filling process and the use of fill materials, cut-and-fill mining is generally more expensive than many other underground mining methods. Therefore, it is usually applied to high-grade orebodies where selective extraction and good ore recovery justify the higher costs (Belem & Benzaazoua, 2008; Brady & Brown, 2006; Hustrulid & Bullock, 2001).

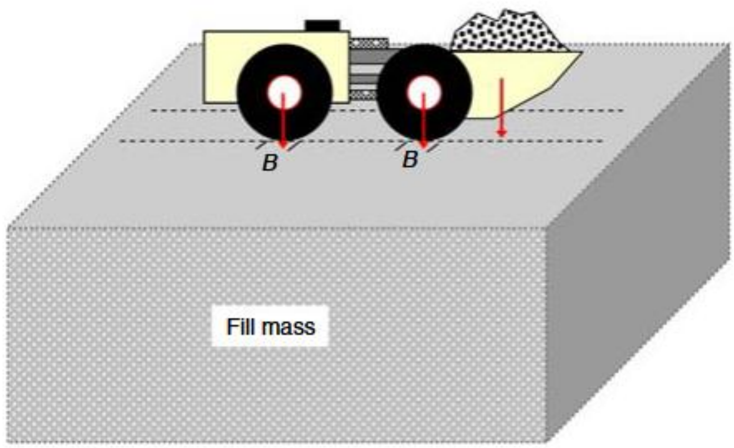

Figure 2-5 Simplified schematic of a working platform (reproduced of Belem & Benzaazoua, 2008 with permission)

Avoca and drift-and-fill methods follow a similar principle of sequential extraction and filling. In all these methods, backfill is mandatory because mining creates voids that must be filled to maintain stability and allow operations to continue. Without backfill, the stope becomes unstable and mining cannot proceed safely. Therefore, the key problems requiring backfill are stope instability and the need for a safe working environment. The Avoca mining method involves dividing the orebody into horizontal slices or levels, with mining generally progressing from the top downward. During the mining process, the stope is continuously backfilled, often using waste rock from adjacent stopes (Brady & Brown, 2006; Hustrulid & Bullock, 2001). The drift-and-fill method is suitable for relatively wide orebodies and involves the excavation of a series of parallel drifts within the orebody. After the ore is removed from primary drifts, these openings are backfilled, commonly using cemented backfill, before the extraction of secondary drifts or remaining pillars (Brady & Brown, 2006; Hustrulid & Bullock, 2001).

The post-pillar mining method combines features of room-and-pillar mining and cut-and-fill stoping. Ore is extracted in horizontal slices while pillars are left in place to support the roof.

However, they may not provide sufficient long-term stability, especially in wide orebodies. In this case, backfill becomes necessary to improve pillar performance and maintain overall stability. Therefore, backfill is not always mandatory at the beginning but becomes necessary when pillar support is insufficient (Brady & Brown, 2006; Hustrulid & Bullock, 2001).

2.1.3 Caving mining methods

Caving mining methods include block caving, sublevel caving, and longwall mining. These methods rely primarily on the natural behavior of the rock mass or on the induced collapse of the surrounding rock during extraction. In such methods, backfill is not required, as the mining process is based on controlled caving or subsidence (Brady & Brown, 2006; Hustrulid & Bullock, 2001). However, backfill can be applied in longwall mining if subsidence is to be avoided or minimized (Li 2024).

2.1.4 Summary

Overall, the review of underground mining methods shows that the need for backfill is directly related to the challenges created by voids during ore extraction. These challenges include the formation of unsupported openings, potential instability of the rock mass, the absence of a stable working platform for equipment, and limitations in ore recovery when support must be left in place. Backfill is generally used to address these issues (Brady & Brown, 2006; Li, 2014a, 2014b; Li & Aubertin, 2012; Li et al., 2005; Li et al., 2003; Ma et al., 2025; Pengyu & Li, 2015; Potvin et al., 2005). In some specific cases, CPB can also play an important role in mine waste management by allowing problematic tailings, such as sulfide-rich tailings that are not suitable for surface storage, to be placed underground as cemented paste backfill.

2.2 Stability and required strength of exposed backfill

2.2.1 Stability and required strength of side-exposed backfill

As discussed in the previous sections, the use of backfill in underground mining is primarily driven by the need to control the stability of excavated voids and to ensure safe and continuous mining operations. However, the use of backfill introduces several engineering challenges that must be addressed in both design and operation. One of the primary challenges is the requirement for sufficient mechanical strength (Li, 2014a; Li & Aubertin, 2012, 2014; Liu et al., 2018; Yang et al., 2017). Backfill must be capable of supporting loads imposed by its own weight, the surrounding rock mass, and mining-induced stresses. In particular, in methods such as cut-and-fill and drift-and-fill, backfill placed in primary stopes must develop adequate strength not only to support subsequent excavation, but also to remain stable when exposed during the extraction of adjacent secondary stopes. Once secondary stopes are mined, the previously placed backfill in primary stopes becomes partially unconfined and must sustain exposed conditions without failure. This side exposure of the primary-stope backfill during secondary-stope extraction is shown in Figure 2-6. Insufficient strength may result in failure modes such as collapse or sliding (Falaknaz et al., 2015; Wang et al., 2021; Yang & Li, 2017).

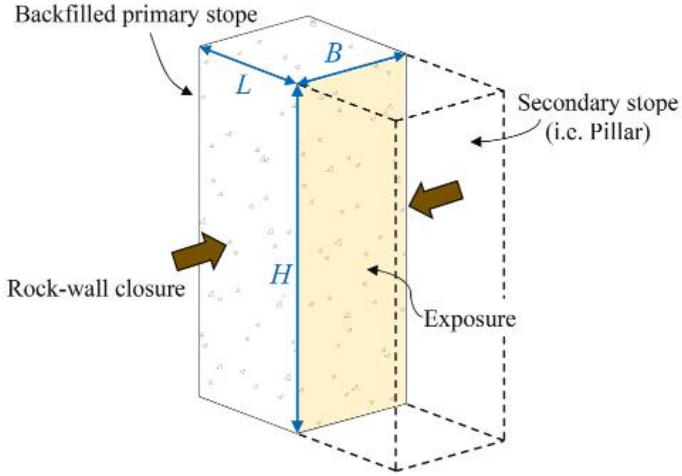

Figure 2-6 Side exposure of backfill in a primary stope during secondary extraction (reproduced from Wang et al., 2021 with permission)

In practice, this requirement is often addressed by increasing the strength of the lower portion of the backfill through the use of a cemented plug. This plug, typically placed at the base of the stope, is constructed with a higher binder content than the remaining fill in order to provide additional resistance against loading, reduce the pressure acting on the barricade at early stages of backfilling, and ensure stability when the backfill becomes exposed during the excavation of adjacent secondary stopes. The cemented plug at the base of the backfilled stope, before and after secondary-stope excavation, is shown in Figure 2-7. Cemented plugs may also be important in underhand stoping, where the lower portion of the fill must provide sufficient support for subsequent mining activities. The presence of a sufficiently strong plug can enhance the overall stability of the backfill system and reduce the risk of failure under exposed conditions (Li, 2014a). It should be noted that the present study focuses on waste rock dumping within the main mass of the backfilled stope, and not within the cemented plug.

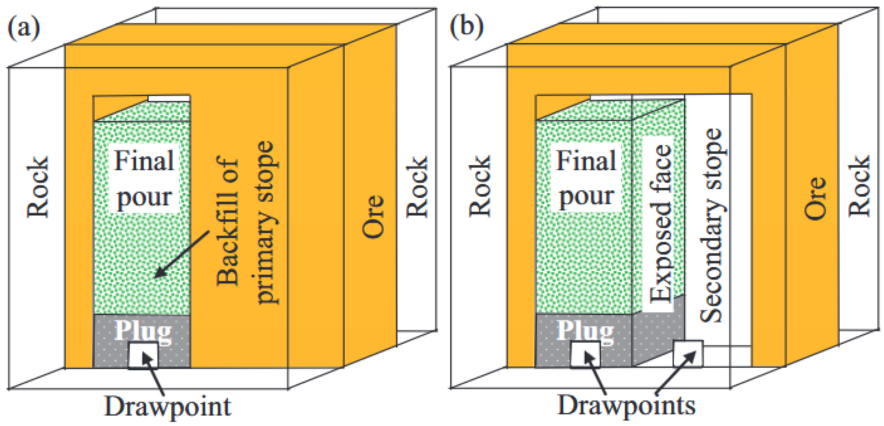

Figure 2-7 Schematic illustration of a cemented plug placed at the base of a backfilled stope (a) before and (b) after excavation of the secondary stope (reproduced from Li, 2014a with permission)

To ensure the stability of backfill under side-exposed conditions, it is necessary to estimate its required strength using quantitative approaches rather than qualitative assessment alone. Over the past decades, several analytical solutions have been developed to evaluate the minimum strength required for backfill exposed during mining operations.

One of the earliest analytical approaches for estimating the required strength of side-exposed backfill was proposed by Mitchell et al. (1982). The model is based on a limit equilibrium approach in which the backfill is treated as a confined block that may fail by sliding along an inclined failure plane. The analysis considers the balance between driving forces due to the self-weight of the backfill and resisting forces provided by cohesion and interaction with the surrounding rock walls (Mitchell et al., 1982).

The model is based on several simplifying assumptions, including the use of the Mohr–Coulomb failure criterion, the neglect of friction at the backfill wall interfaces (δ = 0), and a zero-friction angle for the backfill. In addition, the cohesion at the interface between the backfill and the side walls is assumed to be equal to the internal cohesion of the backfill.

Under these assumptions, the factor of safety (*FS*) of the backfill can be expressed as:

$$FS = \frac{\tan\phi}{\tan\alpha} + \frac{2cL}{H^*(\gamma L - 2C_s)\sin(2\alpha)} \tag{2.1}$$

$$H^* = H - \frac{\mathrm{B}\tan\alpha}{2} \tag{2.2}$$

$$\alpha = 45^\circ + \frac{\phi}{2} \tag{2.3}$$

where c is the cohesion of the backfill, ϕ is the internal friction angle, C_s is the cohesion along the side walls, γ is the unit weight of the backfill, and H, B, and L are the height, width, and length of the stope, respectively.

For design purposes, and under simplified conditions (e.g., ϕ = 0 and FS = 1), the required unconfined compressive strength (UCS) can be estimated as:

$$UCS = 2c = \frac{\gamma}{\frac{1}{H} + \frac{1}{L}} \tag{2.4}$$

Although the model provides a simple and practical design approach, it is generally considered conservative due to the neglect of frictional resistance and interface effects, which may lead to an overestimation of the required backfill strength.

To overcome some of the limitations of the Mitchell et al. (1982) model, Li and Aubertin (2012) proposed a modified analytical solution. In this model, the internal friction angle of the backfill is considered non-zero, and the effect of surcharge applied at the surface of the backfill (P_0) is explicitly taken into account. The failure mechanism is assumed to occur through sliding of a confined backfill block along an inclined failure plane, similar to the Mitchell model, but with more realistic consideration of stress distribution and material behavior. The cohesion at the backfill–wall interface is assumed to be smaller than the internal cohesion of the backfill, while the friction along the interfaces is neglected (δ = 0), and the cohesion at the back wall is taken as zero (C_b =

0). The model can be applied to different stope geometries, including high aspect ratio (HAR) and low aspect ratio (LAR) stopes (Li & Aubertin, 2012).

For high aspect ratio stopes ($H/B \geq \tan\alpha$), the factor of safety (FS) can be expressed as:

$$FS = \frac{\tan\phi}{\tan\alpha} + \frac{2c}{\left[p_0 + H^*\left(\gamma - \frac{2c_s}{L}\right)\right]\sin(2\alpha)} \tag{2.5}$$

$$H^* = H - \frac{\mathrm{B}\tan\alpha}{2} \tag{2.6}$$

$$\alpha = 45° + \frac{\phi}{2} \tag{2.7}$$

where c is the cohesion of the backfill, c_s is the cohesion at the backfill wall interface, ϕ is the internal friction angle, γ is the unit weight of the backfill, P_0 is the surcharge applied at the surface, and H, B, and $L$are the height, width, and length of the stope, respectively.

The required cohesion of the backfill can be estimated as:

$$c = \frac{\frac{p_0 + \gamma H^*}{2}}{\left[\left(FS - \frac{\tan\phi}{\tan\alpha}\right)\sin(2\alpha)\right]^{-1} + r_s\frac{H^*}{L}} \tag{2.8}$$

and the corresponding unconfined compressive strength (UCS) is given by:

$$UCS = 2c\tan\left(45° + \frac{\phi}{2}\right) \tag{2.9}$$

For low aspect ratio stopes ($H/B \leq \tan\alpha$), the factor of safety is expressed as:

$$FS = \frac{\tan\phi}{\tan\alpha} + \frac{2c}{\left[p_0 + H\left(\frac{\gamma}{2} - \frac{c_s}{L}\right)\right]\sin(2\alpha)} \tag{2.10}$$

and the required cohesion becomes:

$$c = \frac{p_0 + \frac{\gamma H}{2}}{2\left[\left(FS - \frac{\tan\phi}{\tan\alpha}\right)\sin(2\alpha)\right] + r_s\frac{H}{L}} \tag{2.11}$$

Compared to the original Mitchell model, the solution proposed by Li and Aubertin (2012) provides a more realistic estimation of the required backfill strength by incorporating the effects of friction, surcharge, and tension crack development, and by considering different stope geometries.

While Li and Aubertin (2012) improved the estimation of the required backfill strength by considering more realistic stress conditions and stope geometries, the backfill was still mainly treated as a single material system. Li (2014a) further extended this framework by considering a two-layer backfill system, in which a stronger cemented plug is placed at the base of the stope to improve stability and an upper backfill layer with lower cement content This two-layer arrangement and the possible failure surfaces within the plug and upper backfill are shown in Figure 2-8. This two-stage filling strategy is commonly used in practice to improve stability and reduce the pressure exerted on barricades. Depending on the stope geometry and the position of the failure surface (Li, 2014a).

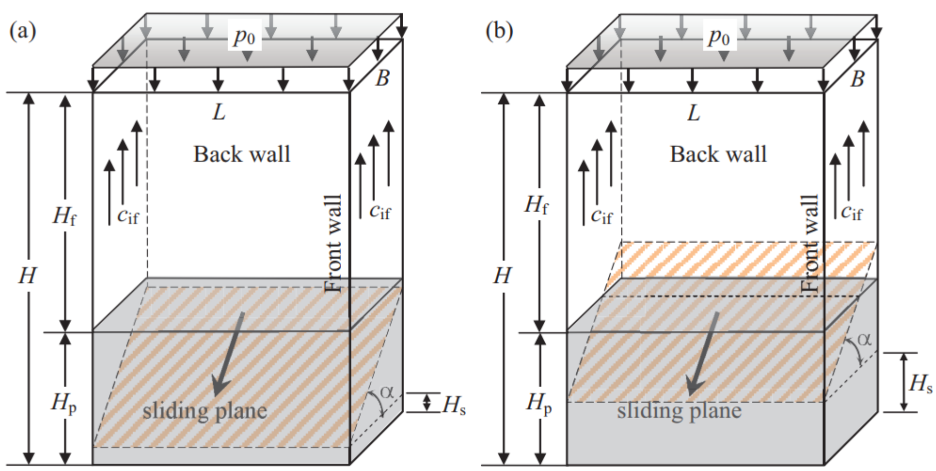

Figure 2-8 Two-layer backfill system with a cemented plug and upper backfill layer showing different failure mechanisms: (a) failure surface within the plug; (b) failure surface extending into the upper backfill (reproduced from Li, 2014a with permission)

For low aspect ratio stopes ($H/B \leq \tan\phi$), where the failure surface develops within the plug, the factor of safety (FS) can be expressed as:

$$FS = \frac{\tan\phi}{\tan\alpha} + \frac{2r_p c}{p_n \sin(2\alpha)} \tag{2.12}$$

where the parameter p_n is introduced to simplify the expression and is defined as:

$$p_n = p_0 + \left(\gamma - \frac{2r_{if}c}{L}\right)H_f + \left(\gamma_p - \frac{2r_{ip}r_p c}{L}\right)H' \tag{2.13}$$

and the equivalent height is given by:

$$H' = H_{tp} - H_s - \frac{\mathrm{B}\tan\alpha}{2} \tag{2.14}$$

The required cohesion of the upper backfill layer can be estimated as:

$$2c = \frac{p_0 + \gamma H_{tf} + \gamma_p H'}{\dfrac{r_p}{\left(FS - \dfrac{\tan\phi}{\tan\alpha}\right)\sin 2\alpha} + r_{if}\dfrac{H_{tf}}{L} + r_{ip}r_p\dfrac{H'}{L}} \tag{2.15}$$

For high aspect ratio stopes (*H/B* ≥ tan ϕ), where the failure surface crosses the plug and extends into the upper backfill, the factor of safety (*FS*) can be expressed as:

$$FS = \frac{\tan\phi}{\tan\alpha} + \frac{c}{\sin^2\alpha} \cdot \frac{\tan\alpha + \left(r_p - 1\right)\dfrac{H_{tp} - H_s}{B}}{p_0 + \left(\gamma - \dfrac{2r_{if}c}{L}\right)H^* + \left(\gamma_p - \dfrac{2r_{ip}r_p c}{L}\right)\dfrac{\left(H_{tp} - H_s\right)^2}{2B\tan\alpha}} \tag{2.16}$$

and the required cohesion of the backfill is given by:

$$c = \frac{p_0 + \gamma H^* + \gamma_p \dfrac{\left(H_{tp} - H_s\right)^2}{2B\tan\alpha}}{\dfrac{\tan\alpha + \left(r_p - 1\right)\dfrac{H_{tp} - H_s}{B}}{\left(FS - \dfrac{\tan\phi}{\tan\alpha}\right)\sin^2\alpha} + \dfrac{2}{L}\left(r_{if}H^* + r_{if}r_p\dfrac{\left(H_{tp} - H_s\right)^2}{2B\tan\alpha}\right)} \tag{2.17}$$

In this formulation, the introduction of a cemented plug allows the model to capture the variation of mechanical properties within the backfill mass and the interaction between different layers. Compared to previous analytical models, this approach provides a more realistic estimation of the required backfill strength, particularly in cases where the failure surface intersects multiple zones with different mechanical properties.

Although the model proposed by Li (2014a) introduced the effect of a cemented plug and heterogeneous backfill properties, some conservative assumptions related to stress distribution and required cohesion still remained. To further improve the analytical prediction of backfill stability, Li and Aubertin (2014) proposed an enhanced analytical solution. proposed an improved analytical solution to overcome the limitations of previous models, particularly the overestimation of required cohesion in Mitchell et al. (1982) and Li and Aubertin (2012). In this model, the cohesion at the backfill–back wall interface is considered non-zero ($C_b \neq 0$), which provides additional shear resistance that was neglected in earlier solutions. This modification leads to a more realistic estimation of the required strength and reduces unnecessary binder consumption. The improved model was validated using numerical simulations, which showed that the backfill mass can be divided into two distinct zones. The upper part behaves as a rectangular block due to vertical shear resistance along the side walls, while the lower part follows an inclined failure surface parallel to the sliding plane defined by $\alpha = 45° + \phi /2$. The displacement pattern of the backfill toward the open face, including the upper rectangular block and the lower inclined failure zone, is shown in Figure 2-9 (Li & Aubertin, 2014).

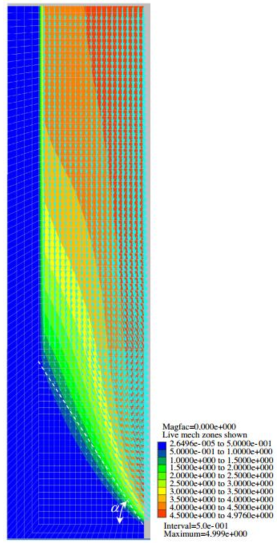

Figure 2-9 Displacement pattern of backfill toward the open face (reproduced from Li and Aubertin, 2014 with permission)

Based on this formulation, the factor of safety (FS) can be expressed as:

$$FS = \frac{\tan\phi}{\tan\alpha} + \frac{c\left(\frac{1}{\cos\alpha} + r_{bs}\frac{H'}{L}\right)\dfrac{\left(\frac{\gamma}{M} - p_1\right)\left[\frac{1-\exp(-MH)}{MH} - 1\right] + \frac{\gamma H'}{2}}{1 + \frac{L}{B}}}{\left(p_1 + \frac{\gamma H'}{2}\right)\sin\alpha} \tag{2.18}$$

where the following parameters are introduced to simplify the expression:

$$H' = \mathrm{B}\tan\alpha \tag{2.19}$$

$$M = 2K\left(\frac{1}{B} + \frac{1}{L}\right)\tan\delta \tag{2.20}$$

$$p_1 = p_0 - G' + (H - H')\gamma - c\left(\frac{2r_{bs}}{L} + \frac{r_{bb}}{B}\right) \tag{2.21}$$

$$G' = \frac{1}{1+\frac{L}{B}}\left[\gamma(H-H') + \left(p_0 - \frac{\gamma}{M}\right)(1-\exp(-(H-H')M))\right] \tag{2.22}$$

The required cohesion of the backfill can be estimated as:

$$c = \frac{D'(p_0 + \gamma(H-H') - G') + \frac{A'\gamma H'}{2}\left(1+\frac{L}{B}\right)\sin\alpha - \gamma\left(\frac{C'}{M} + \frac{H'}{2}\right)}{B'\left(1+\frac{L}{B}\right) + D'(H-H')\left(\frac{2r_{bs}}{L} + \frac{r_{bb}}{B}\right)} \tag{2.23}$$

where the parameters used for simplification are defined as:

$$A' = FS - \frac{\tan\phi}{\tan\alpha} \tag{2.24}$$

$$B' = \frac{1}{\cos\alpha} + r_{bs}\frac{H'}{L} \tag{2.25}$$

$$C' = \frac{1-\exp(-MH')}{MH'} - 1 \tag{2.26}$$

$$D' = A'\left(1+\frac{L}{B}\right)\sin\alpha + C' \tag{2.27}$$

This improved formulation provides a more accurate estimation of the required backfill strength by incorporating the effect of back wall cohesion and a more realistic stress distribution within the backfill mass. Compared to previous analytical models, the solution proposed by Li and Aubertin (2014) reduces the overestimation of required cohesion and leads to a more economical design while maintaining stability.

Although Li and Aubertin (2014) improved the prediction of required cohesion by considering back wall cohesion and a more realistic stress distribution, the treatment of boundary conditions was still further refined in later work. In particular, Li (2014b) generalized the analytical framework by introducing more flexible interface conditions along the side walls and back wall. Li (2014b) proposed a generalized analytical model based on the original formulation of Mitchell et al. (1982), which can be applied to both high aspect ratio (HAR) and low aspect ratio (LAR) stopes. The high and low aspect ratio backfilled stope configurations considered in this generalized solution are shown in Figures 2-10 and 2-11, respectively. In this model, the mechanical behavior at the backfill wall interfaces is treated more realistically by considering non-zero friction along the side walls ($\delta \neq 0$) and different cohesion values for the side walls and the back wall. The cohesion along the side walls is expressed as $c_s = r_s c$, while the cohesion at the back wall is defined as $c_b = r_b c$. Unlike previous models, this approach allows different shear resistances at the boundaries, improving the accuracy of the stability analysis (Li, 2014b)

For high aspect ratio stopes ($H/B \geq \tan\alpha$), the factor of safety (FS) can be expressed as:

$$FS = \frac{\tan\phi}{\tan\alpha} + \frac{2}{\sin(2\alpha)}\left(\frac{p'}{c} - r_a\frac{H'}{B} - 2r_s\frac{H^*}{L}\right)^{-1} \tag{2.28}$$

$$H' = H - B\tan\alpha \tag{2.29}$$

The required cohesion of the backfill can be estimated as:

$$c = p'\left[\frac{2}{\left(FS - \frac{\tan\phi}{\tan\alpha}\right)\sin 2\alpha} + r_a\frac{H'}{B} + 2r_s\frac{H'}{L}\right]^{-1} \tag{2.30}$$

The expression of p' is given by:

$$p' = \frac{L}{2K\tan\delta}\left\{\gamma - \frac{1}{\mathrm{B}\tan\alpha}\left(\frac{\gamma L}{2K\tan\delta} - p_0\right)\left[\exp\left(-\frac{2K\tan\delta}{L}H'\right) - \exp\left(-\frac{2K\tan\delta}{L}H\right)\right]\right\} \tag{2.31}$$

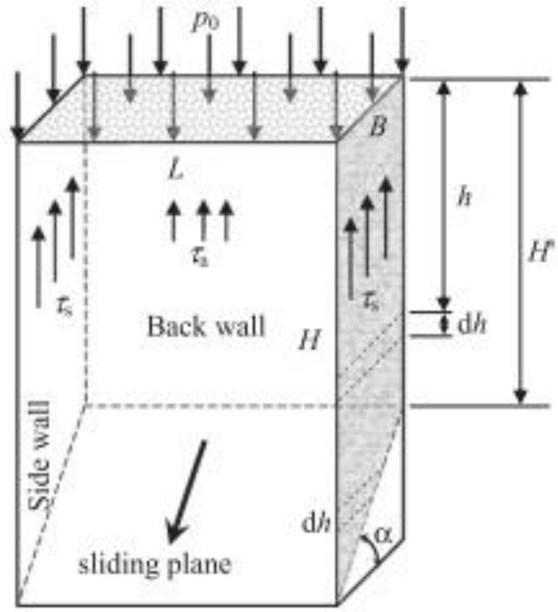

Figure 2-10 High aspect ratio backfilled stope (reproduced from Li, 2014b with permission)

For low aspect ratio stopes ($H/B \leq \tan\alpha$), the factor of safety is expressed as:

$$FS = \frac{\tan\phi}{\tan\alpha} + \frac{2}{\sin(2\alpha)}\left(\frac{p''}{c} - r_s\frac{H}{L}\right)^{-1} \tag{2.32}$$

The required cohesion becomes:

$$c = p''\left[\frac{2}{\left(FS - \frac{\tan\phi}{\tan\alpha}\right)\sin(2\alpha)} + r_s\frac{H}{L}\right]^{-1} \tag{2.33}$$

The expression of p'' is given by:

$$p'' = \frac{L}{2K\tan\delta}\left\{\gamma - \frac{1}{H}\left(\frac{\gamma L}{2K\tan\delta} - p_0\right)\left[1 - \exp\left(-\frac{2K\tan\delta}{L}H\right)\right]\right\} \tag{2.34}$$

where c is the cohesion of the backfill, ϕ is the internal friction angle, δ is the interface friction angle, γ is the unit weight of the backfill, p_0 is the surcharge applied at the surface, H, B, and L are the stope height, width, and length, H' is the equivalent height of the failure block, K is the earth pressure coefficient, and r_a and r_z are parameters related to interface shear resistance.

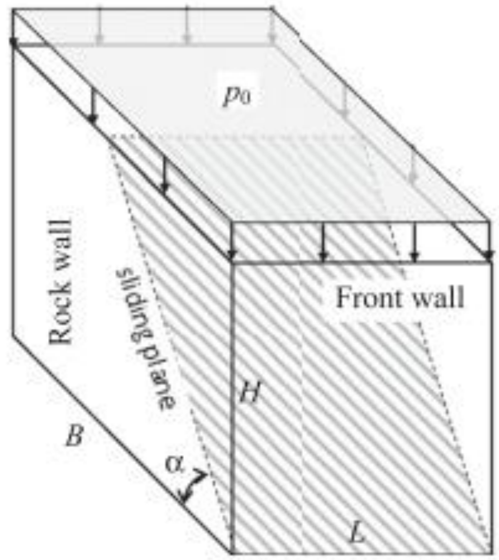

Figure 2-11 Low aspect ratio backfilled stope (reproduced from Li, 2014b with permission)

Compared to previous analytical models, the solution proposed by Li (2014b) provides a more realistic estimation of the required backfill strength by incorporating interface friction, variable cohesion at boundaries, and different stope geometries.

Later, Yang et al. (2017) proposed an improved analytical solution to estimate the required strength of side-exposed backfill, addressing the limitations of previous models. Earlier analytical solutions, including Mitchell et al. (1982) and Li and Aubertin (2012), were found to overestimate the required cohesion, leading to excessive binder consumption and increased operational costs. In contrast, some later models, such as Li and Aubertin (2014), may underestimate the required strength, potentially resulting in instability. To overcome these limitations, Yang et al. (2017) introduced a more realistic failure mechanism by considering tensile stresses at the top of the backfill and allowing the failure surface to evolve with the cohesion of the material.

Their study showed that the failure surface is not always planar. This non-planar, spoon-shaped failure surface of the side-exposed backfill is shown in Figure 2-12. For low cohesion values, failure occurs along a plane passing through the base of the backfill. At higher cohesion values, the backfill remains stable with negligible deformation, while a slight reduction in cohesion leads to a sudden increase in displacement and failure (Yang & Li, 2017).

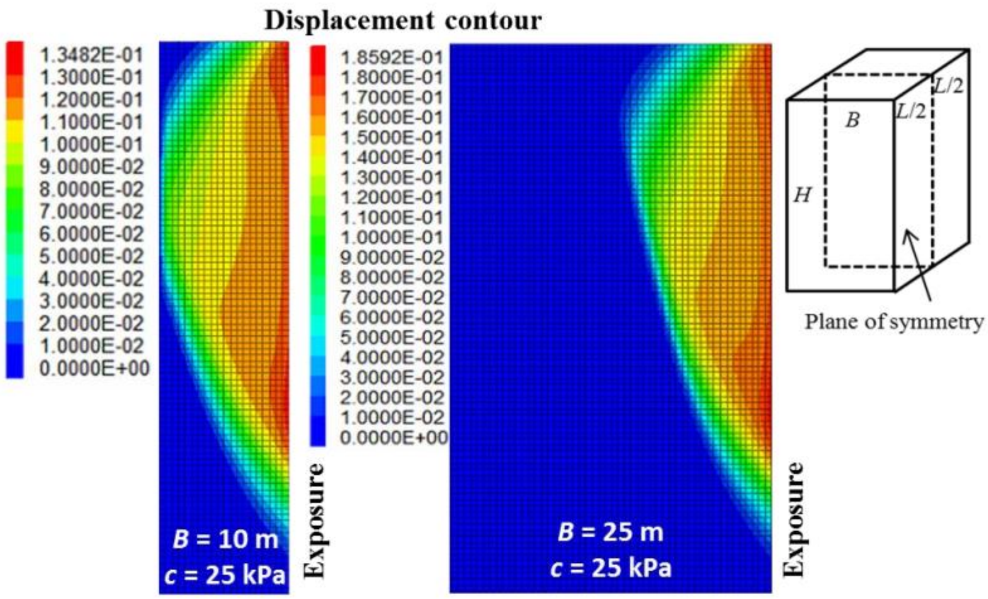

Figure 2-12 Spoon-shaped failure surface of side-exposed backfill (reproduced from Yang et al. 2017 with permission)

Based on this improved understanding of the failure mechanism, the factor of safety (FS) can be expressed as:

$$FS = \frac{\tan\phi'}{\tan\alpha} + \frac{2}{\sin(2\alpha)}\left(\frac{P}{c} - \frac{H_t}{B_t} - r_s\frac{2H - B_t\tan\alpha}{L}\right)^{-1} \tag{2.35}$$

and the required cohesion of the backfill is given by:

$$c = P\left[\frac{2}{\left(FS - \frac{\tan\phi'}{\tan\alpha}\right)\sin 2\alpha} + \frac{H_t}{B_t} + r_s\frac{2H - B_t\tan\alpha}{L}\right]^{-1} \tag{2.36}$$

where P is a simplification parameter defined as:

$$P = \frac{L}{2K\tan\delta}\left\{\gamma - \frac{1}{B_t\tan\alpha}\left(\frac{\gamma L}{2K\tan\delta} - p_0\right)\left[\exp\left(-\frac{2K\tan\delta}{L}H_t\right) - \exp\left(-\frac{2K\tan\delta}{L}H\right)\right]\right\} \tag{2.37}$$

In this formulation, H_t represents the depth of the tension crack, and B_t is the equivalent width of the backfill considering tensile failure. The inclusion of these parameters allows the model to account for tensile effects at the top of the backfill, which were neglected in previous analytical solutions.

Overall, the model proposed by Yang et al. (2017) provides a more accurate estimation of the required backfill strength by incorporating both shear and tensile failure mechanisms. The results show that this approach produces predictions that are much closer to numerical simulations compared to earlier analytical models, making it one of the most reliable methods for evaluating the stability of side-exposed backfill.

Although Yang et al. (2017) improved the representation of the failure mechanism by considering tensile effects and the evolution of the failure surface, the model did not account for additional lateral pressure from adjacent backfilled stopes. This aspect was later addressed by Liu et al. (2018), who extended the analytical framework by considering the pressure exerted by an adjacent uncemented backfill. Liu et al. (2018) proposed an analytical model to estimate the required strength of side-exposed backfill by considering the effect of pressure exerted by adjacent backfilled stopes. This configuration, where the cemented backfill is exposed on one side and laterally pressured by adjacent uncemented backfill, is shown in Figure 2-3. In this configuration, the primary stope filled with cemented backfill is located between two secondary stopes, one excavated and the other filled with uncemented backfill. As a result, the back wall of the primary stope is subjected to horizontal pressure generated by the adjacent secondary stope, which is assumed to be equal to the geostatic pressure of the backfill ($\sigma_h = \gamma_h$). This loading condition introduces an additional destabilizing effect that was not considered in previous analytical solutions (Liu et al., 2018).

Based on this formulation, the factor of safety (FS) can be expressed as:

$$FS = \frac{cL\dfrac{B}{\cos\alpha} + (Y + 2S_s \sin\phi)\tan\phi}{Z - 2S_s \cos\phi} \tag{2.38}$$

and the required cohesion of the backfill is given by:

$$c = \frac{\mathrm{Z}\cos\phi - \mathrm{Y}\sin\phi - 2X}{\frac{LB\ cos\phi}{\cos\alpha} + 2BH^{*}r_s} \tag{2.39}$$

where $\beta = 45° - \phi/2$ and $\alpha - \beta = \phi$, S_s represents the shear force acting along the side walls, and r_s is the adhesion coefficient between the backfill and the surrounding rock mass. The parameters *X, Y,* and *Z* are force components derived from the equilibrium analysis of the backfill block under combined vertical and horizontal loading conditions.

By incorporating the effect of lateral pressure from adjacent backfilled stopes, this model provides a more realistic representation of in-situ conditions. Compared to previous analytical solutions, the approach proposed by Liu et al. (2018) improves the estimation of required backfill strength by considering the interaction between multiple stopes and the additional loading imposed on the backfill mass.

Recently, Grabinsky et al. (2021) proposed an analytical solution to estimate the required strength of plugs under continuous pouring conditions in a two-stage long hole stoping geometry, where a lower plug fill supports the overlying main or mass fill. The plug must become self-supporting and resist the hydrostatic pressure of the overlying main fill. The formulation is based on a limit equilibrium approach using a failure mechanism analogous to a half-Prandtl wedge, supported by numerical calibration and field observations. The limiting equilibrium condition for plug stability is expressed as (Grabinsky et al., 2021):

$$\gamma(H_m + H_b + 0.55H_u) = c\left(4\frac{H_b}{H_u}+3+4\frac{L_u}{H_u}\right) \tag{2.49}$$

where γ is the unit weight of backfill, H_m is the height of the main fill, H_b is the plug height above the brow, H_u is the undercut height, L_u is the distance to the barricade, and c is the undrained cohesion. This equation defines the balance between hydrostatic loading and cohesion-controlled resistance. Figure 2-4 of Grabinsky et al. (2021) presents the geometry of a two-stage backfilling sequence, including the lower cemented paste backfill plug, the overlying main fill, the undercut, and the barricade area.

The corresponding self-supporting condition is given by:

$$\frac{c_{ss}}{\gamma H_u} = \frac{0.55 + \frac{H_b}{H_u}}{3 + 4\frac{H_b}{H_u} + 4\frac{L_u}{H_u}} \tag{2.50}$$

which represents the minimum cohesion required for the plug to remain stable without barricade support.

To account for strength development during curing, the maximum supported height of the main fill is expressed as:

$$H_{m,\max}(t) = \frac{1}{\gamma}\left[c\left(t - t_{ref}\right) - c_{ss}\right]\left(3+4\frac{H_b}{H_u}+4\frac{L_u}{H_u}\right) \tag{2.51}$$

This formulation introduces time-dependent behavior by linking stability to cohesion gain with curing time.

The relationship between cohesion and unconfined compressive strength (UCS) is given by:

$$UCS = \frac{2c\cos\phi}{1 - \sin\phi} \tag{2.52}$$

and the required final cohesion for a given final fill height can be written as:

$$c_{final} = \frac{\gamma\left(H_{m,final}+H_b+0.55H_u\right)}{4\frac{H_b}{H_u} + 3 + 4\frac{L_u}{H_u}} \tag{2.53}$$

Overall, this study provides one of the first analytical frameworks to estimate plug strength based on geometry, loading, and time-dependent strength development, moving beyond purely empirical UCS based design approaches.

2.2.2 Stability and required strength of base-exposed backfill

Base-exposed backfill is mainly encountered when a cemented sill mat becomes exposed after the excavation of the underlying opening. In this condition, the backfill must remain stable without direct support from below and must resist the stresses transferred from the overlying fill and the surrounding rock mass. Several analytical, numerical, and practical design approaches have been proposed to estimate the required strength of base-exposed backfill. These studies show a gradual development from simplified limit-equilibrium models toward more realistic approaches that consider wall closure, stress redistribution, and sill geometry.

Early analytical and practical approaches for sill mat design

Mitchell (1991) investigated the stability of cemented sill mats used in underhand cut-and-fill mining by combining analytical equilibrium approaches with centrifuge model testing. The study focused on understanding the loading conditions and failure mechanisms of sill mats after the removal of the underlying sill pillar, where the backfill becomes base-exposed and must sustain both vertical and horizontal stresses. The typical sill pillar setup and the base-exposed condition of the backfill are shown in Figure 2-13 (Mitchell, 1991).

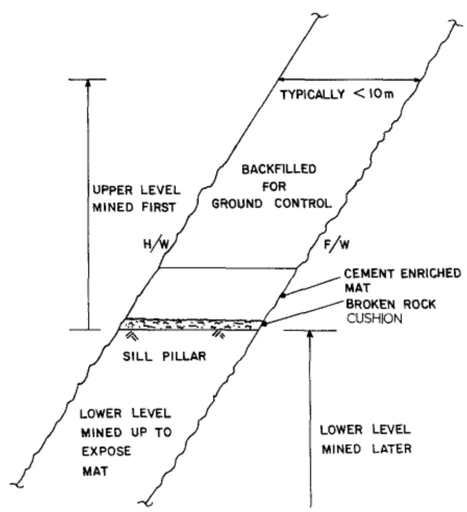

Figure 2-13 Typical setup of sill pillar (reproduced from Mitchell, 1991 with permission)

The loading conditions acting on the sill mat were defined by the vertical stress induced by the overlying uncemented fill and the lateral closure stress resulting from rock mass deformation. The vertical stress was estimated using an arching-based approach derived from soil mechanics, expressed as:

$$\sigma_v = \frac{\gamma L}{2K \tan \phi} \tag{2.40}$$

where γ is the unit weight of the fill, L is the span of the opening, K is a coefficient related to stress transfer, and ϕ is the internal friction angle of the fill. This formulation accounts for the reduction of vertical stress due to arching between the hanging wall and footwall, and serves as the primary load applied to the sill mat.

Based on these loading conditions, the study analyzed several potential failure mechanisms of the sill mat using limit equilibrium formulations. Flexural failure was considered as a dominant mode for wide and thin sill mats due to the relatively low tensile strength of cemented backfill. This mode was evaluated using beam theory, leading to the following failure condition:

$$\left(\frac{L}{d_{ts}}\right)^2 > \frac{2(\sigma_t + \sigma_c)}{w} \tag{2.41}$$

where d_{ts} is the sill mat thickness, σ_t is the tensile strength of the backfill, σ_c represents compressive strenght, and w is the uniform load acting on the sill mat, including both overburden and self-weight. This equation highlights the strong influence of the span-to-thickness ratio on flexural stability.

Caving failure was also examined by assuming the formation of a stable arch within the sill mat. Under this assumption, failure occurs when the vertical load exceeds the tensile capacity of the material, expressed as:

$$L\gamma > 2.5\sigma_t \tag{2.42}$$

indicating that increased span or unit weight promotes instability, while higher tensile strength improves resistance.

In addition, shear failure along the contact between the sill mat and surrounding rock was analyzed. The condition for sliding failure is given by:

$$(\sigma_v + \gamma d_{ts}) > 2\left(\frac{\tau_f}{\sin^2\beta}\right)\left(\frac{d_{ts}}{L}\right) \tag{2.43}$$

where τ_f is the shear strength at the fill wall interface and β is the dip angle of the stope. This formulation emphasizes the importance of interface properties and stope geometry in controlling shear stability.

Rotational (torsional) failure was also considered, particularly in cases where the hanging wall provides limited resistance. This mode was described by:

$$(\sigma_v + \gamma d_{ts}) > \frac{{d_{ts}}^2 \sigma_t}{2L(L - d_{ts}\cot\beta)\sin^2\beta} \tag{2.44}$$

which indicates that instability may occur due to combined effects of geometry, tensile strength, and boundary conditions.

Furthermore, the study highlighted that crushing failure may occur when the lateral closure stress exceeds the unconfined compressive strength (UCS) of the cemented backfill, linking the stress state directly to material strength capacity.

Overall, Mitchell (1991) provided a comprehensive analytical framework to evaluate sill mat stability by identifying multiple failure mechanisms and corresponding limit conditions. This work proposed a set of failure criteria that must be satisfied to ensure stability. This work represents one of the earliest systematic efforts to model sill mat behavior and has served as the foundation for many subsequent developments in backfill design. Although Mitchell's model provided the fundamental basis for sill mat stability analysis, it was based on simplified loading and boundary conditions. Later studies therefore attempted to improve the practical applicability of this approach by considering field observations, design charts, and more realistic loading conditions.

Following the early analytical framework proposed by Mitchell (1991), Pakalnis et al. (2005) investigated the design of sill mats in underhand cut-and-fill mining with a strong emphasis on practical applicability. Their study combined analytical concepts, numerical modeling, and field observations from several underground mines to better understand the loading conditions acting on sill mats.

A key contribution of this work is the improved estimation of vertical stress acting on the sill mat by considering arching effects, stope geometry, fill height, and stope inclination. Compared to simplified analytical approaches, this leads to a more realistic representation of the load distribution within the backfill.

In addition, practical design charts were developed to relate the unconfined compressive strength (UCS) of the backfill to stope span and sill thickness, providing a direct and convenient tool for engineering design. This design chart, which relates the required UCS to the stope span and sill thickness, is shown in Figure 2-14. These charts are typically associated with a factor of safety of approximately 2 and are consistent with observed field performance.

The study also highlights the importance of several practical factors that are not explicitly included in simplified analytical models, such as seismic loading, stope closure, fill placement quality (e.g., cold joints), and wall contact conditions, all of which can significantly influence sill stability.

Overall, although no new analytical failure mechanism is introduced, Pakalnis et al. (2005) improve the practical applicability of existing approaches by providing a more realistic estimation of loading conditions and by linking analytical understanding with numerical modeling and field observations (Pakalnis et al., 2005).

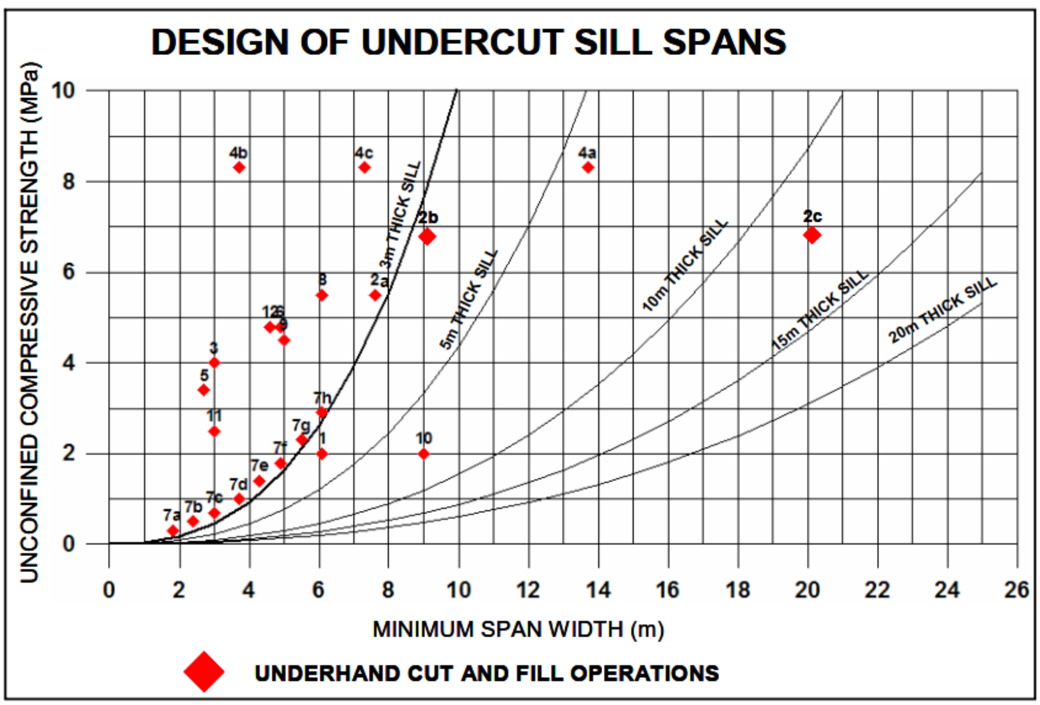

Figure 2-14 Design chart relating UCS to stope span and sill thickness (reproduced from Pakalnis et al., 2005 with permission)

However, both early analytical and practical design approaches still provide a limited representation of rock wall movement and stress redistribution around the exposed sill mat. This limitation motivated later numerical and analytical studies that explicitly considered wall closure and its effect on the governing failure mechanism.

Influence of wall closure and stress redistribution

Pagé et al. (2019) performed a numerical investigation to evaluate the stability and minimum required strength of base-exposed sill mats using finite element modeling. Unlike analytical solutions such as Mitchell (1991), which assume that the sill mat behaves as an isolated beam supported by rigid and immobile walls, this study explicitly considered the effect of rock wall closure induced by the excavation of the underlying stope.

The results showed that the apparent failure mechanism of sill mats may be caving or rotation, while the actual governing mechanism is crushing or shear failure caused by increased horizontal stresses within the sill mat. It was demonstrated that the minimum required strength increases with parameters that enhance horizontal stress, such as mine depth, in-situ stress ratio, and sill stiffness, and decreases with increasing span and thickness due to reduced horizontal stress induced by wall closure (Pagé et al., 2019).

This study represents a significant improvement over Mitchell (1991) by introducing a more realistic stress state governed by wall closure, thereby shifting the interpretation of failure mechanisms from bending-controlled to stress-controlled behavior, based on numerical modeling.

Consistent with the numerical findings of Pagé et al. (2019), Fan et al. (2025) developed an analytical model to estimate the minimum required strength of base-exposed sill mats by explicitly incorporating the effect of rock wall closure induced by undercutting.

Fan et al. (2025) developed an analytical model to estimate the minimum required strength of base-exposed sill mats by explicitly incorporating the effect of rock wall closure induced by undercutting. In contrast to earlier analytical approaches, particularly Mitchell (1991), which assumed immobile rock walls and neglected lateral deformation, this study recognized that wall convergence generates significant horizontal compressive stresses within the sill mat that directly control its stability and failure mechanism (Fan et al., 2025).

A key contribution of the study is the formulation of the horizontal compressive stress induced by wall closure, denoted as σ_s, which depends on rock mass stiffness, sill stiffness, stope geometry, and in-situ stress conditions. This stress represents the dominant load acting on the sill mat and replaces the simplified loading assumptions used in earlier models. Based on this, the required strength of the sill mat is evaluated using the Mohr–Coulomb failure criterion, linking stress to material strength as:

$$\sigma_s = UCS = \frac{2c\cos\phi}{1-\sin\phi} \tag{2.45}$$

which leads to the expression for the minimum required cohesion:

$$c_{min} = \frac{\sigma_s(1-\sin\phi)}{2\cos\phi} \tag{2.46}$$

These equations provide a direct and practical way to estimate the required strength of the sill mat under realistic stress conditions.

In addition to redefining the loading conditions, Fan et al. (2025) also revisited the governing failure mechanisms. While Mitchell (1991) primarily considered flexural, sliding, and rotational failures based on beam-like behavior, the new model demonstrated that the dominant failure mode is compressive, specifically crushing induced by horizontal stress. Furthermore, a new combined failure mechanism, referred to as crushing caving, was identified, reflecting the interaction between compressive stress and geometric instability. This mechanical model of the sill mat under crushing caused by wall closure is shown in Figure 2-15.

To distinguish between these failure modes, the study introduced a criterion based on the comparison between bending-induced stress and horizontal compressive stress:

$$\sigma_A = \sigma_b - \sigma_s \tag{2.47}$$

where the bending stress is expressed as:

$$\sigma_b = \frac{\gamma B^2}{2h_s} \tag{2.48}$$

If $\sigma_A < 0$, crushing governs the failure, whereas $\sigma_A \geq 0$ indicates a combined crushing–caving mechanism. This criterion provides a clear and practical tool for identifying the governing failure mode during design.

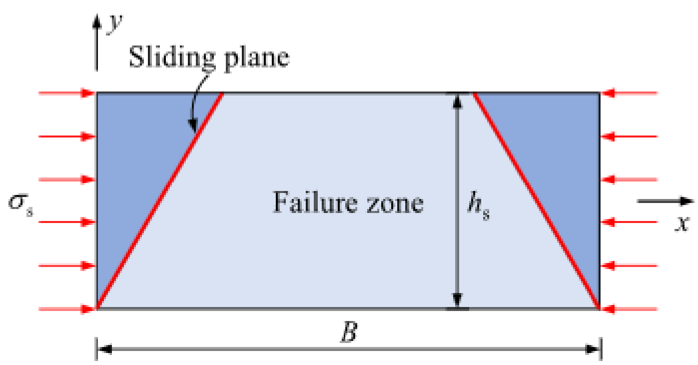

Figure 2-15 Mechanical model of sill mat under crushing due to wall closure (reproduced from Fan et al., 2025 with permission)

Overall, this study significantly improves upon the work of Mitchell (1991) by replacing the assumption of rigid rock walls with a realistic representation of wall closure, introducing horizontal stress as the primary driving factor, and providing analytical expressions for estimating the minimum required strength. Unlike earlier models that relied on multiple independent failure checks, the proposed framework offers a unified and physically consistent approach for evaluating sill mat stability under base-exposed conditions.

Geometry-based effects

In addition to stress redistribution caused by wall closure, the geometry of the sill mat can also affect the required strength and the governing failure mode. Keita et al. (2021) extended the numerical investigation of sill mat stability by proposing a novel concept of arched sill mats as a means to reduce tensile stresses and improve stability. Using finite element simulations (RS2), the study evaluated the influence of sill mat geometry on the minimum required cohesion and failure mechanisms.

The results indicated that arched sill mats significantly reduce tensile stresses at the base, thereby mitigating flexural failure, which is critical due to the low tensile strength of cemented backfill materials. It was shown that the minimum required cohesion increases with span but decreases with increasing curvature of the sill mat, demonstrating that geometry plays a key role in stability (Keita et al., 2021).

This concept is mainly applicable when flexural failure governs the stability of sill mats. Compared to previous studies (Mitchell, 1991; Pagé et al., 2019), this work introduced a new design strategy by modifying geometry rather than only adjusting material strength, providing a more economical solution by reducing the need for high binder content or reinforcement systems.

2.3 Mining wastes

Mining operations generate large quantities of waste materials, mainly in the form of waste rock and tailings (Lottermoser, 2010; Hudson-Edwards et al., 2011). Waste rock is excavated during mine development and ore extraction to access the ore body, whereas tailings are produced during mineral processing after valuable minerals have been separated from the ore.

2.3.1 Waste rock

Physical, mechanical and hydraulic properties

In underground mining operations, accessing ore bodies requires the construction of various development openings such as shafts, drifts, raises, and declines in underground mines. Figure 2-16 presents a schematic illustration of the longhole underground mining layout, including the access ramp, sublevel drives, and the arrangement of primary and secondary stopes (Joughin, 2017). These activities produce large volume of excavated material that do not contain sufficient amount of valuable mineral for economic processing and therefore classified as waste rock (Hamrin, 1980; Hartman & Mutmansky, 2002; Hustrulid & Bullock, 2001; Lottermoser, 2010). The amount of waste rock produces in mining operations can be very significant, mainly due to the high waste-to-ore ratio observed in both underground and open-pit mines. The amount of waste rock produced depends on several factors including the geometry and location of the ore body, the mining method, and the geotechnical stability of the surrounding rock mass (Lèbre et al., 2017; Lottermoser, 2010).

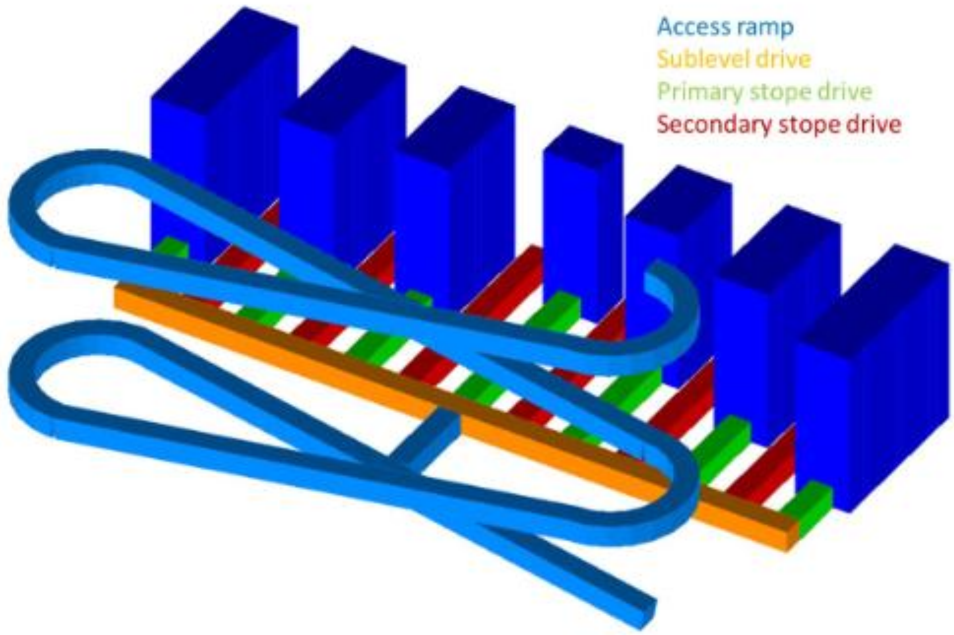

Figure 2-16 Schematic illustration of the longhole underground mining layout, including the access ramp, sublevel drives, and the arrangement of primary and secondary stope (reproduced from Joughin, 2017 with permission)

The characteristics of waste rock used in underground backfilling are strongly influenced by the mining method, excavation geometry, blasting pattern, and handling system. In contrast, open-pit waste rock is commonly produced by large-scale blasting and bulk excavation, which may generate highly heterogeneous material with a wide particle size distribution, they may contain particles ranging from fine materials to very large blocks, sometimes exceeding 2 m. In some mining operations, waste rock generated from open-pit blasting can also be transported underground through waste passes and used for underground backfilling applications (Arteaga et al., 2014; Kumar et al., 2023; Mining, Minerals and Sustainable Development Project, 2002; Zhang & Liu, 2017).

In contrast, underground mining waste rock is produced in more confined spaces and is usually subject to additional fragmentation and handling construction, since the waste rock is often loaded, transported, and dumped multiple times. The presence of tunnels, loading system and handling equipment limits the allowable particle size, as oversized fragments can obstruct movement, reduce loading efficiency and increase mining cycle time. As a result, the crushing process is usually controlled to avoid the production of large blocks that may create operational difficulties in underground openings. Figure 2-17 shows representative underground waste rock materials after being transported to the surfac (Hartman & Mutmansky, 2002; Hustrulid & Bullock, 2001; Sainsbury et al., 2021).

Figure 2-17 Representative waste rock materials from an underground mine in Australia (reproduced from Sainsbury et al., 2021 with permission)

The particle size distribution of underground waste rock directly affects its geotechnical and hydraulic behavior when it is used as backfill material. Compared with very coarse open-pit waste rock, underground waste rock generally has a more controlled maximum particle size and therefore typically exhibits lower permeability.

The grain size distribution also affects key geotechnical parameters such as porosity, permeability, and uniformity coefficient. Studies have shown that the uniformity coefficient (C_u) in waste rock is usually greater than 20 and can ever reach 440 (Aubertin, 2013; Fala et al., 2005; Gamache-Rochette, 2004). The bulk density of waste rock deposits typically ranges between approximately 1600 and 2700 kg/m³ depending on compaction conditions and specific gravity (Hustrulid & Bullock, 2001; Maknoon, 2016). At the particle scale, the specific gravity of waste rock fragments generally ranges between approximately 2.4 and 4.8 depending on the mineral composition and rock type (Maknoon, 2016).

In addition to physical properties, hydraulic characteristics are important when waste rock is placed in underground stopes, because they control drainage and pore water pressure development within the backfilled area. Because of the wide range of particle sizes, shapes, and void ratios, the hydraulic conductivity of waste rock materials can vary significantly (Aubertin, 2013; Smith, 2021). Laboratory and field investigations have reported that the saturated hydraulic conductivity of waste rock materials typically ranges between approximately $10^{-5}$and 10^{-3}m/s depending on particle size distribution, compaction conditions, and internal structure (Aubertin, 2013; Peregoedova, 2012).

Management and challenges

As mining operations progress, large volume of waste rock are generated that need to be managed properly through the life cycle of the mine. In practice, waste rock is usually disposed on the surface in waste rock piles. This is the most common disposal method because it is relatively simple to implement and can accommodate very large volume of material. However it requires a large area of land, long term monitoring and may cause significant land disturbance and landscape deformation (Lottermoser, 2010).

Surface waste rock piles can be constructed using a variety of methods, including end dumping, push dumping, and free dumping. These methods differ primarily in the way the material is placed and redistributed on the surface of the pile, which directly affects particle segregation, density, and internal structure.

In end-dumping, trucks transport the waste rock to the edge of the pile and simply dump the material over the slope. The rock then flows downward under gravity, forming the pile naturally. The internal layering and stratigraphy commonly formed in waste rock piles are illustrated in Figure 2-18. This method is easy to operate but often leads to strong particle segregation, where coarse particles travel further downslope while finer particles remain near the top (Aubertin, 2013; Hawley & Cunning, 2017; Pearce et al., 2016; Tomaschitz et al., 2018). This approach generally produces a loose slope structure since the material is placed without mechanical compaction (Boakye, 2008).

In push dumping, waste rock is first dumped near the crest of the pile, and then bulldozers push the material down the slope. Because the movement is controlled by equipment rather than only gravity, this method generally reduces segregation compared to end dumping and allows better control of the slope shape (Moffitt, 2000; Nichols, 1986; Pearce et al., 2016; Raymond et al., 2021; Tomaschitz et al., 2018).

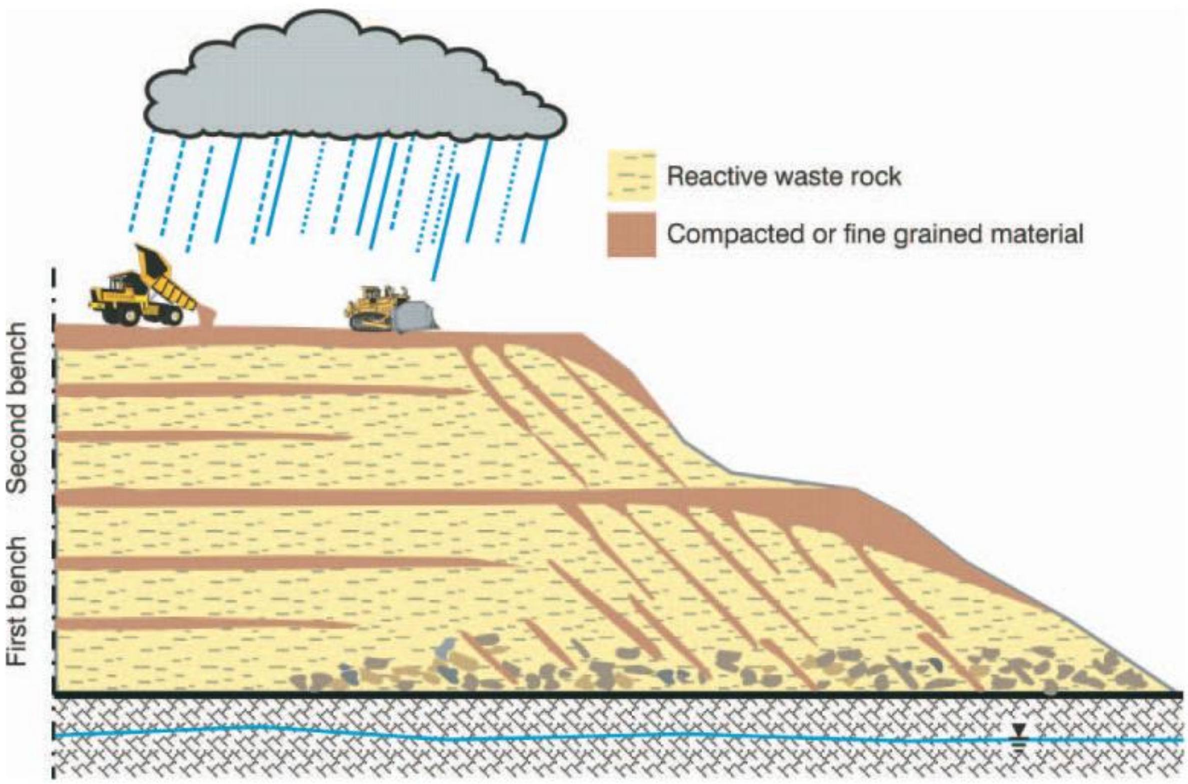

Figure 2-18 Schematic cross-section of a waste rock pile showing internal layering and stratigraphy (reproduced from Bussiere, 2007 with permission)

The free dumping method is commonly used to place waste rock in the form of small piles on the surface, after which dozers and compactors are employed to level and compact the material (Fala et al., 2003). This approach is generally applied during the early stages of pile construction, particularly for forming relatively low-height deposits. As the operation progresses, it is often replaced by end dumping or push dumping methods to continue deposition on an already leveled surface. Although this method does not lead to significant segregation, considerable variations in the physical properties of the waste rock, such as bulk density, may occur due to differences in compaction levels (Tachie-Menson, 2006).

Despite differences in construction methods, waste rock piles generally develop heterogeneous internal structures due to segregation and stratification. This heterogeneity can significantly influence their mechanical and hydraulic behavior and may increase the risk of hydro geotechnical instability. In addition to these physical and operational challenges, long-term storage of such large volumes of material can lead to several environmental challenges, particularly related to the generation of acid rock drainage (ARD), also known as acid mine drainage (AMD). This process occurs when sulfide minerals present in waste rock, such as pyrite and pyrrhotite, react with oxygen and water, producing sulfuric acid and releasing dissolved metals into surrounding water systems (Akcil & Koldas, 2006; Blowes et al., 2003; Lottermoser, 2010; Nordstrom & Alpers, 1997). The acidic conditions generated during this process can mobilize heavy metals and contaminate groundwater and surface water resources. An example of acid mine drainage generated at an abandoned metalliferous mine is shown in Figure 2-19. Elevated concentrations of metals such as copper, zinc, nickel, and cobalt have been observed in drainage waters associated with waste rock piles, posing potential risks to ecosystems and water quality (Akcil & Koldas, 2006; Nordstrom & Alpers, 1997).

Figure 2-19 Example of acid mine drainage (AMD) at an abandoned metalliferous mine in South Africa (reproduced from Akcil & Koldas, 2006 with permission)

Moreover, the transportation of excavated material, including waste rock, represents an essential stage of the mining operation. After blasting and fragmentation, the broken rock must be loaded, transported, and hoisted to the surface using a combination of underground haulage systems and lifting equipment (Tatiya, 2005).

Overall, although surface disposal of waste rock is widely practiced due to its simplicity, it is associated with significant land use, long-term management requirements, operational costs, and environmental impacts. These challenges have encouraged the mining industry to explore alternative waste management strategies that can reduce surface disposal and improve overall efficiency.

2.3.2 Tailings

Physical, mechanical and hydraulic properties

Tailings are generated during ore processing after the valuable minerals have been separated from the parent ore. Tailings are crushed rock particles produced or deposited in slurry form, and they mainly consist of the finely ground waste material that remains after mineral extraction. A typical tailings slurry deposit in an impoundment is shown in Figure 2-20. Their production involves crushing and grinding of the ore, followed by concentration processes such as gravity separation, magnetic separation, or froth flotation, in which the valuable particles are recovered as concentrate and the remaining low-value particles become tailings. After mineral recovery, the tailings are commonly dewatered in thickeners to recover part of the process water, but they are still typically discharged and transported as a thickened slurry to the tailings impoundment. Vick (1990) notes that this slurry transport method is used almost universally because the tailings are already mixed with water in the mill and complete drying is generally uneconomic. The final characteristics of the generated tailings depend strongly on the ore type, processing method, and degree of grinding, which is why tailings can differ widely in grain size, specific gravity, plasticity, and chemical composition (Vick, 1990).

The physical properties of tailings are closely related to the milling and grinding processes used in mineral processing. Since milling practices vary from one mine to another, the particle size distribution (PSD) of tailings can also differ significantly between sites and ore types. Figure 2-21 illustrates the particle size distribution (PSD) curves of tailings obtained from nine hard-rock mines in Canada, as reported by Bussière (2007). The results indicate that the particle sizes of these tailings generally vary between approximately 0.1 and 400 μm. Compared with the values reported by Potvin et al. (2005), the tailings from these mines contain a relatively larger proportion of fine particles. The characteristic particle sizes show that the D_{10} values range between 0.001 and 0.004 mm, whereas the D_{60} values vary from 0.01 to 0.05 mm. In addition, the coefficient of uniformity (C_u) is reported to fall within the range of 8 to 18 (Bussiere, 2007).

Figure 2-20 Tailings slurry deposit in an impoundment (reproduced from Bussiere, 2007 with permission)

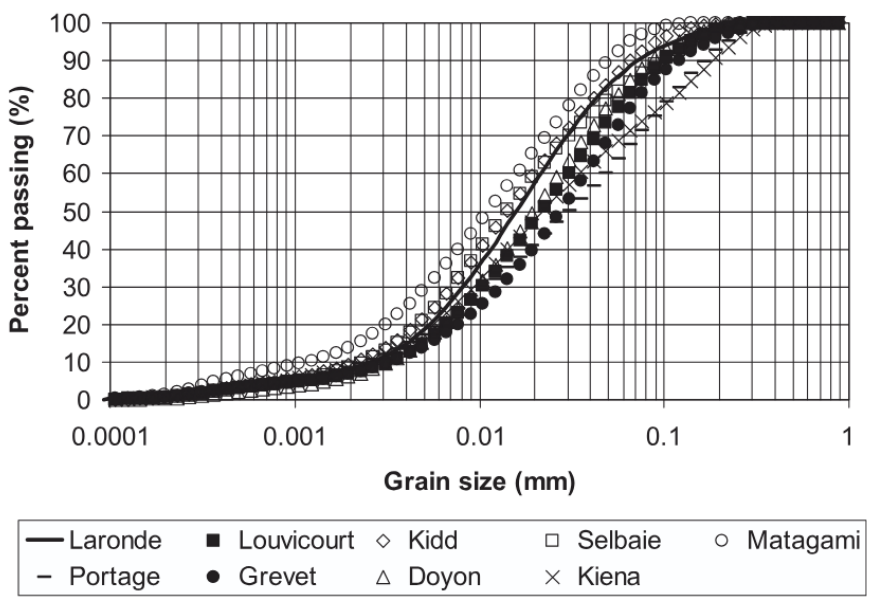

Figure 2-21 Particle size distribution of nine tailings from Canadian hard rock mines (reproduced from Bussiere, 2007 with permission)

From a hydraulic perspective, tailings exhibit relatively low permeability due to their fine particle size. The saturated hydraulic conductivity of hard rock tailings typically ranges between approximately 10^{-8} and 10^{-6} m/s for fine-grained materials, while coarser tailings may show higher values ranging from about 10^{-6} to 10^{-4} m/s (Bussiere, 2007). From a mechanical point of view, the effective friction angle of tailings under drained conditions generally varies between 30° and 42°, while the effective cohesion is typically close to 0 kPa, indicating that shear strength is mainly governed by frictional resistance (Bussiere, 2007; Matyas et al., 1984; Pettibone & Kealy, 1971). Under undrained conditions, the friction angle decreases to approximately 14° to 25°, and the apparent cohesion may range between 0 and 100 kPa depending on the consolidation state of the material (Bussiere, 2007; Vick, 1990).

Management and challenges

Because of tailings complex hydro-geotechnical behavior, including slow consolidation, low strength, and susceptibility to liquefaction, the management of tailings represents a major technical and environmental challenge.

A range of tailings management methods has been developed to address these challenges, depending on site conditions, operational constraints, and environmental considerations. The most widely used approach is conventional slurry-based storage, in which tailings containing approximately 20 to 40% solids are hydraulically transported and deposited behind containment structures. This method is operationally simple, cost-effective, and can maintain saturated conditions, which is beneficial for controlling acid rock drainage (ARD) (Berger, 2017). However, it requires complex long-term water management and is associated with significant risks, particularly related to dam stability and potential catastrophic failure. In addition, particle segregation during deposition may create localized unsaturated and permeable zones, which facilitate oxygen ingress and promote acid generation (Berger, 2017; Investigation & Panel, 2015).

To reduce these limitations, alternative technologies based on dewatered tailings have been developed, including thickened or paste tailings and filtered (dry stack) tailings. Thickened or paste tailings, typically containing 60 to 75% solids, exhibit higher yield stress and reduced segregation during deposition. This method allows improved water recovery and results in more uniform deposits with lower hydraulic conductivity. It may also reduce the size of containment structures and can be used as underground backfill (Berger, 2017). However, it requires more complex operation and control, specialized equipment, sensitive to variations in tailings properties, insufficient drying in wet climates, and the requirement for external water management (Berger, 2017).

Filtered tailings (dry stacking), with solids content typically exceeding 80%, behave similarly to unsaturated soil and can be transported and compacted to form stable deposits. This method offers the highest level of water recovery and significantly reduces the risk of catastrophic failure, as failures are generally localized. It also allows progressive reclamation and improved closure performance (Berger, 2017). Despite these advantages, dry stacking involves high capital and operational costs, increased energy consumption, and may be challenging under wet or cold climatic conditions. In addition, it may not be suitable for all tailings types, particularly those with high clay content (Berger, 2017).

Historically, tailings were often discharged directly into rivers, lakes, or wetlands, leading to widespread contamination of aquatic environments (Lewin et al., 1977). Even today, the erosion of tailings deposits and waste rock piles can transport contaminated sediments into surrounding water systems, increasing turbidity and sedimentation while introducing metals, metalloids, and radionuclides into river channels, floodplains, and lake sediments (Lewin et al., 1977).

Despite the availability of these different management Wind erosion from tailings surfaces can generate dust that disperses contaminants into surrounding soils and the atmosphere (Jakubick et al., 2003). In addition, seepage through tailings embankments or through the base of tailings deposits can introduce dissolved contaminants into groundwater and nearby surface waters (Jakubick et al., 2003). In addition, the failure of tailings dams represents one of the most critical risks in mining, as demonstrated by historical accidents such as the Aznalcóllar–Los Frailes dam failure in southwestern Spain in 1998, which caused severe environmental damage and contamination metals (Grimalt et al., 1999; Turner et al., 2008).

Because of these environmental and geotechnical risks, tailings management is subject to strict regulatory frameworks in many jurisdictions. In Québec, the Directive 019 on the mining industry provides guidelines for the design, operation, and monitoring of tailings storage facilities, including requirements related to water quality, environmental protection, and long-term stability. Recent updates to this directive have introduced stricter controls on environmental performance, water management, and risk mitigation, reflecting the increasing emphasis on safe and sustainable tailings management (MELCCFP, 2025).

Overall, the environmental and operational challenges associated with the surface disposal of tailings have increased the interest in using these materials as underground backfill in modern mining practice. This approach can reduce the volume of mine waste stored on the surface, limit the need for tailings impoundments, and at the same time contribute to ground support within underground excavations. Therefore, it is necessary to first review the main types of underground backfill used in mining practice. This provides the background needed to understand how tailings and waste rock are used underground as backfill.

2.4 Mining backfills

Mining backfill is widely used in underground mines to fill mined-out openings and improve the stability of excavations. It can help support the surrounding rock mass, reduce ground movement, improve ore recovery, and provide a safe working environment. In addition, backfilling allows part of the mine waste, such as tailings and waste rock, to be used underground as backfill materials, reducing the amount of mine waste stored on the surface. Different types of mine backfill have been developed depending on the material used, the method of placement, the required strength, and the mining conditions. The most common types include hydraulic fill, paste backfill, and rockfill.

2.4.1 Hydraulic Fill

Hydraulic fill is one of the earliest mining backfill used in underground mines. It was first applied in underground mines in 1884 and has since been widely used in many mining operations worldwide (Potvin et al., 2005). Hydraulic fill is typically produced from deslimed tailings, sand, or their mixtures, and transported to underground stopes as a slurry through pipelines. Figure 2-22 showes an example of hydraulic fill placement in an underground mine (Cacciuttolo & Marinovic, 2023). Hydraulic fill often contains a substantial amount of water to satisfy the requirements of delivery. The large amount of this water drains out of stopes and needs to be pumped to the surface.

Figure 2-22 Example of hydraulic fill in an underground mine in Peru (reproduced of Cacciuttolo & Marinovic 2023 with permission)

Hydraulic fill is generally prepared with a solids content of about 60 to 70%, and a water content of approximately 42 to 67% (Belem & Benzaazoua, 2008; Potvin et al., 2005; Sivakugan et al., 2015b). Because fine particles are removed, it usually consists of relatively coarse particles and is classified as silty sand or sandy silt (Sivakugan et al., 2015b). The maximum particle size is typically limited to about 1 mm, while particles finer than 10 μm should remain below 10% by weight (Potvin et al., 2005). The uniformity coefficient C_u commonly ranges from 5 to 10, and the specific gravity ranges between 2.9 and 4.4 (Sivakugan et al., 2015b).

In order to minimize the potential failures of hydraulic fill induced by liquefaction, water should be allowed to drain as quickly as possible after the placement of hydraulic fill in the stopes. Therefore, a high conductivity is important for hydraulic fill after placed into a stope. The hydraulic conductivity of hydraulic fill typically ranges from 10^{-6} to 10^{-5} m/s (Grice, 2001; Potvin et al., 2005; Rankine, 2005).

The strength of hydraulic fill depends on several factors, including binder content, binder type, curing conditions, and water content. cement content plays the crucial role in the unconfined compressive strength (UCS). When cement is added, the strength increases significantly. For example, hydraulic fill with 4% cement may reach a UCS of about 1 MPa after 28 days (Darling, 2011; Saw & Villaescusa, 2013).

Despite its widespread application, hydraulic fill presents several limitations when evaluated against the key challenges of underground backfilling. One of the limitation is related to the desliming process used to prepare hydraulic fill. Since hydraulic fill is mainly produced from the coarse fraction of tailings, the removed fine fraction still needs to be managed separately. This fine portion is often stored on the surface, which reduces the overall benefit of returning tailings underground. In addition, fine tailings can be difficult to drain and consolidate because of their low hydraulic conductivity, creating additional geotechnical challenges for surface storage facilities. Due to its high water content, hydraulic fill is prone to segregation during placement, where fine particles and binders tend to migrate upward while coarse particles settle at the bottom. This results in a heterogeneous fill structure, with stronger upper layers and weaker lower zones. Such weak layers may become unstable when the backfill is exposed during the extraction of adjacent secondary stopes, compromising the overall stability of the stope (Liu et al., 2017; Yang & Li, 2017).

In addition, the large amount of water in hydraulic fill requires efficient drainage systems, typically through barricades constructed at the entrance of the stope. However, inadequate drainage may lead to the development of excess pore water pressure and the formation of water columns, which significantly increase the loading on barricades. This can result in barricade failure, potentially causing catastrophic consequences such as uncontrolled flow of backfill into drifts, equipment damage, and safety hazards. Therefore, both segregation and drainage-related issues must be carefully considered in the design and application of hydraulic fill systems (Li & Aubertin, 2011; Yang, 2016).

2.4.2 Paste backfill

To address part of the limitations associated with hydraulic backfill, paste backfill was developed to allow a larger portion of mill tailings, including fine particles, to be used underground as backfill material. This is an important advantage compared with hydraulic fill (Potvin et al., 2005; Robinsky, 1975). Paste backfill is prepared by thickening the tailings and, in some cases, by further filtration or pressure filtration to reach a high solids concentration, typically 70 to 85%, thereby improving their handling and performance in underground conditions (Fall et al., 2009; Potvin et al., 2005). Figure 2-23 presents an example of cemented paste backfill placement in an underground mine (Cacciuttolo & Marinovic, 2023). A paste backfill is much thicker than hydraulic backfill.

Figure 2-23 Example of cemented paste backfill in an underground mine in Peru (reproduced of Cacciuttolo & Marinovic 2023 with permission)

Uncemented paste backfill presents several fundamental limitations that restrict its use in underground mining applications, particularly in exposed stopes. First, it has negligible cohesion and low shear strength, which prevents it from behaving as a load-bearing material. As a result, it cannot maintain stability when exposed during adjacent stope extraction or undercutting operations. Second, due to its high fine content and water retention, uncemented paste is prone to liquefaction and flow under static or dynamic loading, especially before significant consolidation occurs. Third, it is unable to form stable structural elements such as plugs or sill mats, which are essential for controlling stresses and ensuring the stability of backfilled stopes. To overcome this limitation, binders are commonly added to paste backfill, resulting in what is known as cemented paste backfill (CPB). The binders typically used include cement, slag, fly ash, or their mixtures, with contents ranging from 2 to 10% of the dry solids mass. The first underground application of CPB was reported at Kidd Creek Mine in 1987. Figure 6 of Pornillos (2009) schematically shows the cemented paste backfill preparation and transport to underground stopes through pipelines (Lee & Pieterse, 2005; Pornillos, 2009; Potvin et al., 2005).

Cemented paste backfill, which belongs to the broader category of thickened tailings, was initially proposed for the surface disposal of concentrated tailings in the mid-1970s (Robinsky, 1975). Its first underground application was reported at the Bad Grund Mine in Germany in 1979. Following successful implementations in several mines in Canada and Australia during the 1990s, CPB became widely accepted as a practical alternative to rock fill and hydraulic fill (Rankine & Sivakugan, 2007). The technology was later introduced in China in the late 1990s and further developed with advanced thickening systems in the 2000s (Wu et al., 2017), leading to its widespread adoption in modern mining operations.

From a physical perspective, cemented paste backfill (CPB) is characterized by a high solids content, typically ranging from 70% to 85%, and a relatively low water content (Fall et al., 2009; Potvin et al., 2005). The presence of sufficient fine particles, at least 15% passing 20 μm, plays a key role in ensuring homogeneous flow behavior during transport and prevention of particle segregation. (Landriault, 1995).

From a mechanical perspective, CPB behaves as a non-Newtonian material with a distinct yield stress is commonly reported to range from about 250 to 800 Pa, and usually transported using positive displacement or volumetric pumps. Lower yield stress values, generally below 200 Pa, may be required for centrifugal pump transport (Sadrossadat et al., 2020). The development of mechanical strength in CPB is primarily governed by the binder content and water-to-cement ratio, with lower water content improving binder efficiency and resulting in higher strength. Experimental studies have indicated that a minimum cement content of approximately 1 to 3% is required to reduce the risk of liquefaction (Potvin et al., 2005).

Overall, cemented paste backfill (CPB) has been developed to overcome many of the limitations associated with hydraulic fill, particularly in terms of strength and stability under complex loading conditions. The addition of binders significantly improves the mechanical strength of CPB, allowing it to satisfy the requirements of primary stopes and maintain stability when exposed during adjacent stope extraction. In addition, the relatively low water content of CPB reduces the risk of excess pore water pressure buildup compared to hydraulic fill, which is beneficial for maintaining effective stress and ensuring barricade stability. However, the performance of CPB is highly dependent on proper mix design and curing conditions, and its application is associated with significant economic and operational challenges. The high consumption of binders, which can account for a major portion of operating costs, as well as the need for complex infrastructure and processing systems, represent key limitations of this method. Therefore, while CPB provides improved mechanical performance and stability under exposed conditions, its use requires careful optimization to balance technical performance and economic feasibility.

2.4.3 Rockfill

Rockfill is one of the main materials used for backfilling underground mine voids. It is generally composed of coarse granular materials such as underground waste rock, quarry rock, coarse rejects from heavy medium separation plants, smelter slag, leach pad residues, and in some cases natural river gravels. Representative laboratory-produced rockfill samples are shown in Figure 2-24 (Potvin et al., 2005). In its simplest form, rockfill is dumped directly into mined-out stopes to fill the voids and reduce the deterioration of the surrounding rock mass. This practice can improve ground stability and provide a practical way to manage mine waste underground instead of transporting it to the surface for disposal (Potvin et al., 2005). Rockfill can be classified as uncemented rockfill or cemented rockfill depending on whether a binder is absent or present. Uncemented rockfill is commonly used where later exposure of the fill is not required, while cemented rockfill is used where the fill must remain stable after exposure during the mining of adjacent stopes (Potvin et al., 2005).

Figure 2-24 Laboratory-produced rockfill samples (reproduced of Sainsbury et al. 2021 with permission)

In practice, rockfill can be used in both unmodified and modified forms. Unmodified rockfill refers to coarse granular fill that has not been adjusted by particle size optimisation and does not contain any binder. Underground development waste rock is a typical unmodified rockfill. Because it is a loose and cohesionless material, it cannot stand vertically when exposed and therefore usually requires confinement by stope walls or the presence of a diaphragm wall if adjacent mining is planned (Potvin et al., 2005). For this reason, unmodified rockfill is generally more suitable in situations where fill exposure is not critical. In contrast, modified rockfill is produced by improving the particle size distribution and/or adding binders such as Portland cement. Modification may also include blending with fine materials such as tailings, sand, or slurry in order to reduce porosity, improve particle packing, and increase strength. When the porosity is reduced, the fill mass becomes denser and more competent, which improves its ability to remain stable during vertical exposure (Potvin et al., 2005).

The physical behavior of rockfill is strongly controlled by its granular nature. Rockfill is typically made of coarse particles with common particle sizes ranging from about 1 to 100 mm, and waste-rock-based fills usually need to be well graded in order to improve interlocking between particles. The coefficient of uniformity (C_u) of rockfill is commonly reported to range between 8 and 18. Reported dry density values generally range from 1500 to 2300 kg/m^3, while the void ratio varies from about 0.48 to 0.85 (Williams & Kuganathan, 1992; Williams & Walker, 1985). One of the most important physical characteristics of rockfill is the angle of repose, which represents the slope formed when the material is dumped. Depending on the particle grading, maximum particle size, dumping method, dumping height, moisture content, and the effect of the surrounding rock walls, the angle of repose may vary from 35° to 55° for rockfill. For dry, nearly single-sized rockfill, the angle of repose is often around 38 to 40° (Potvin et al., 2005). These values show that rockfill in its natural state is a loose material and cannot maintain a vertical face without confinement or cementation.

The mechanical properties of rockfill depend on whether the fill is cemented or uncemented. For uncemented rockfill, the shear strength is mainly frictional and is controlled by particle interlocking and relative density. The friction angle is commonly reported to range from 35° to 55°, with higher values corresponding to denser and more dilative materials for rockfill (Potvin et al., 2005). Apparent cohesion may develop in densely packed rockfill because of particle interlocking, but the material remains fundamentally granular. For cemented rockfill, strength is strongly influenced by particle size distribution, binder content, rock type, particle angularity, placement method, and water content. Among these factors, binder content is usually the most important. With a typical cement content of about 4 to 8%, the unconfined compressive strength (UCS) of cemented rockfill generally varies between 1 and 10 MPa (Annor, 1999). The addition of binder also increases stiffness, and therefore the elastic modulus of the fill tends to increase with cementation (Pierce et al., 1998). However, the field strength of placed rockfill can be lower than laboratory values because of segregation, scale effects, and variations in quality control during placement

The hydraulic behavior of rockfill is also important in mine backfilling. Because rockfill is composed of coarse particles and usually contains a relatively large interconnected pore structure, it generally has a much higher hydraulic conductivity than hydraulic fill or cemented paste backfill. Reported hydraulic conductivity values for rockfill range from 4×10^{-5} to 3×10^{-3} m/s (Peregoedova, 2012).

Overall, rockfill presents several limitations when evaluated against the key challenges of underground backfilling, particularly in terms of strength distribution and stability under exposed conditions. One of the major concerns is the segregation of cemented rockfill during placement, where fine particles with higher cement content tend to accumulate near the center of the fill, while coarse particles roll toward the edges, resulting in poorly cemented outer zones. This leads to a non-homogeneous fill structure, in which weak zones may develop and become unstable when exposed during the excavation of adjacent stopes (Annor, 1999). In addition, due to its granular nature, rockfill cannot maintain a uniform structure without proper grading and mixing, and achieving full coating of particles with cement slurry is difficult in practice. As a result, zones with little or no cementation may form, further reducing the overall stability of the backfill mass under exposed conditions. Therefore, while rockfill offers advantages in terms of drainage and material availability, its performance is strongly affected by segregation, heterogeneity, and operational constraints, particularly in mining methods requiring stable backfill under exposure conditions.

2.5 Mixtures of waste rock and paste backfill

Although conventional backfills made from a single material such as hydraulic fill, rock fill, or cemented paste backfill are widely used, many mining operations also employ combinations of different materials, for example waste rock and tailings, as backfill. These mixed materials are generally considered to provide improved mechanical and hydraulic performance compared to single-material backfills.

2.5.1 Mechanical mixing

Mechanical mixing refers to the blending of waste rock and tailings backfill using dedicated equipment, such as a concrete mixer, under controlled conditions. In this method, the waste rock is usually crushed and properly graded before mixing. The mixing operation is commonly carried out on the ground surface, after which the prepared mixture is transported to the underground stope using trucks, conveyors, or boreholes.

Several studies have investigated the influence of incorporating waste rock into cemented tailings paste backfill, with a focus on its mechanical and hydraulic behavior. Overall, the results consistently show that the addition of waste rock can significantly improve the performance of cemented tailings backfill, although this improvement depends strongly on the proportion and particle size of the waste rock. However, one of the main challenges reported for such mixtures is their transportability, particularly through pipelines, because the presence of coarse waste rock particles can increase flow resistance and create a risk of blockage or segregation during transport.

Hane et al. (2017) reported that increasing the waste rock content (up to 50% by volume) generally leads to higher unconfined compressive strength (UCS), particularly when well-graded particle sizes (e.g., 0 to 15 mm) are used. However, the use of coarser particles (e.g., 0 to 20 mm) may introduce segregation and reduce mixture uniformity. Similarly, Qiu et al. (2020) showed that, for a given cement-to-sand ratio, the UCS first increases with increasing waste rock content and then decreases beyond an optimal threshold. This behavior is explained by the balance between particle packing and bonding: moderate amounts of waste rock reduce the specific surface area and improve cement efficiency, while excessive amounts hinder proper coating of particles and weaken the cementitious matrix. Consistent trends were also observed by Qiu et al. (2022). They found that both strength and permeability are strongly influenced by waste rock content and cement-to-sand ratio. For a fixed cement ratio, both UCS and permeability initially increase with increasing waste rock content and then decrease after a certain level. The peak strength was observed at relatively low waste rock content (around 10%), while maximum permeability occurred at higher contents (around 30%). These results highlight the role of waste rock in modifying pore structure, where moderate additions improve particle packing, while excessive coarse particles increase porosity and micro-cracking. Overall, these studies indicate that the inclusion of waste rock can enhance strength and alter permeability characteristics of cemented tailings backfill, but only within an optimal range of content and particle size. Beyond this range, issues such as segregation, insufficient particle coating, and increased porosity may reduce performance. Therefore, careful control of mixture design parameters, including waste rock content, particle size distribution, and binder proportion, is essential to achieve the desired mechanical and hydraulic properties (Hane et al., 2017; Qiu et al., 2020; Qiu et al., 2022).

In addition to laboratory-based studies, several field-scale applications have been reported in underground mines, demonstrating the practical implementation of mechanical mixing systems.

At the Mount Isa Mine, a rocky paste fill (RPF) was developed by mixing cemented tailings with graded rockfill, resulting in a non-segregating and cohesive material. The mixture, with a solids content of 70 to 74% and a maximum particle size of 50 mm, was designed to improve dewatering and reduce segregation. The reported unconfined compressive strength (UCS) reached approximately 1.07 MPa after 28 days (Kuganathan & Sheppard, 2001). Similarly, at the Olympic Dam Mine, a rock–paste fill system was produced by mixing tailings, sand, crushed waste rock, and binder in a pug mill, generating a homogeneous mixture with good flowability (slump of 150 to 180 mm) and strength ranging from 0.5 to 5 MPa (Baldwin & Grice, 2000).

A comparable approach was implemented at the Loulo Mine, where a paste aggregate fill (PAF) composed of approximately 50% tailings and 50% crushed waste rock was prepared using a twin-shaft mixer. The mixture was designed to meet high strength requirements, achieving up to 7 MPa after 28 days and 9.5 MPa after 90 days (Lee & Gillot, 2014). In addition, the inclusion of coarse particles improved particle size distribution and reduced binder consumption. At the Tong Keng Mine, a similar mixture of waste rock, tailings, and cement was used, with a high solids content of 81 to 83% and waste rock content of 25 to 35% and cement content of 2 to 5%. The resulting fill exhibited a strength of about 3 MPa and relatively high hydraulic conductivity (10^{-6} to 10^{-5} m/s), facilitating drainage (Sun et al., 2018). However, the Loulo case also highlights an important operational limitation of paste aggregate fill. Although the addition of crushed waste rock can improve strength, the transport and distribution of such coarse mixtures through pipelines may be difficult and can increase the risk of plugging in the backfill distribution system. For this reason, later operation may favor conventional cemented paste backfill over paste aggregate fill where reliable pipeline transport is required.

Overall, these studies demonstrate that mechanical mixing of waste rock with tailings can produce a homogeneous backfill with enhanced strength, and reduced binder demand. However, these benefits are associated with several practical limitations. In this method, waste rock generated underground must first be transported to the surface, where it is crushed, graded, and mixed with tailings under controlled conditions. The prepared mixture is then transported back to underground stopes for placement. This multi-stage process significantly increases operational complexity and energy consumption. In addition, as mining depth increases, the distance required to transport materials to the surface and back underground becomes longer, leading to higher haulage costs and reduced overall efficiency. Therefore, although mechanical mixing can improve backfill performance, its application requires careful consideration of processing requirements, material handling logistics, and associated costs operations (Hartman & Mutmansky, 2002; Salama, 2014; Skawina, 2017).

2.5.2 Codisposal of waste rock and cemented paste backfill

Veenstra & Grobler (2021) presented a design methodology for maximizing underground disposal of waste rock by placing it within primary stopes at the Dead Bullock Soak underground mine in Australia. In this approach, waste rock is deposited within the stope and encapsulated by cemented paste backfill (CPB), forming a composite backfill system. Due to the coarse nature of run-of-mine waste rock, the material is placed by truck dumping or rock chutes, while CPB is delivered through conventional pipelines. The resulting backfill structure consists of a central waste rock zone surrounded by CPB. As a consequence of this configuration, a transition zone, referred to as a "halo," develops at the interface between the waste rock and the surrounding CPB. Figure 6 of Veenstra and Grobler (2021) presents a co-disposal configuration consisting of a waste rock core, cemented paste backfill, and a surrounding halo zone. Despite this approximation, the presence of this interface leads to a heterogeneous structure within the backfill mass and acts as a mechanically weaker region that controls the overall stability of the system (Veenstra & Grobler, 2021).

Therefore, although co-disposal enables increased underground waste rock storage and reduces surface handling, the absence of true mixing and the formation of a distinct interface zone limit its effectiveness. The resulting heterogeneity and the development of a weak transition region may compromise the structural integrity of the backfill, making this method less reliable compared to approaches that promote more uniform mixing between waste rock and paste backfill.

2.5.3 Natural mixture

The concept of natural mixtures refers to the formation of a composite material by directly pouring waste rock into a stope being filled with cemented paste backfill without any prior crushing, grading, or mechanical mixing. In this approach, the waste rock and paste backfill interact and mix naturally within the stope under gravity. This practice eliminates the need to transport underground-produced waste rock to the surface, thereby reducing energy consumption and operational costs associated with haulage and hoisting. Although natural mixing is commonly practiced in underground mines, particularly in Canada, it remains poorly documented and not well understood in the literature.

Lee and Gu (2017) reported that co-disposal of waste rock with cemented backfill can provide several operational advantages, including reducing some waste rock handling requirements and increasing the amount of waste rock placed underground, and decreasing the consumption of cemented backfill. They also showed that the inclusion of coarse waste rock particles can improve the mechanical performance of the fill mass through particle interlocking, while the paste matrix fills the voids and ensures overall cohesion. The economic benefit of this approach is mainly related to reducing waste rock handling and transportation requirements. For example, the combined costs of hoisting, haulage, and surface disposal of waste rock can reach approximately CAD 6 per ton, which may result in several million dollars annually for large-scale mining operations with high waste-to-ore ratios (Lee & Gu, 2017). However, this advantage should be interpreted with caution. If the use of waste rock reduces the amount of cemented paste backfill placed underground, a larger volume of tailings may still need to be stored on the surface. This is an important consideration because tailings storage facilities are generally associated with high construction, operation, monitoring, and closure costs, mainly due to the need for careful water management, long-term stability control, and environmental protection measures.

In addition, Lee and Gu (2017) proposed operational solutions, such as a slinger-based system, to simultaneously place waste rock and paste backfill into stopes. However, their work did not investigate how the two materials naturally mix or how the mixing quality evolves in space and time.

The experimental study by Zhang and Li (2023) provided a clear understanding of this phenomenon through laboratory tests. They showed that the natural mixing between waste rock and paste backfill is highly dependent on key parameters such as the solids content of the paste backfill, the particle size of waste rock, and the falling height during dumping. Specifically, a lower solids content allows deeper penetration of waste rock and leads to a more homogeneous mixture, whereas a higher solids content results in poor mixing and accumulation of waste rock on the surface. In addition, larger particle sizes and higher falling heights increase the impact energy of particles, thereby improving the mixing degree. This study also introduced, for the first time, quantitative indicators such as the mixing degree to evaluate the quality of the natural mixture (Zhang & Li, 2023). Building on this preliminary laboratory work, Zhang et al. (2026a, 2006b) extended the investigation by combining laboratory testing with numerical modeling to analyze the natural mixing behavior between dumped waste rock and paste backfill. The laboratory setup used to examine the natural mixing of dumped waste rock and paste backfill without mechanical mixing is shown in Figure 2-25. The validated model was applied to predict the natural mixing behavior under different test scales and particle sizes, and it was able to show the distribution of waste rock within the paste backfill. The numerical predictions showed generally good agreement with the experimental observations and confirmed that larger waste rock particles and larger-scale conditions can lead to deeper penetration and greater mixing potential. These results demonstrate that numerical modeling can be used as a useful tool to evaluate and predict natural mixing behavior while accounting for the effects of particle size and stope scale. However, the authors also reported discrepancies between some numerical predictions and laboratory results, highlighting limitations in both the experimental setup and the numerical model (Zhang et al., 2026a, 2006b).

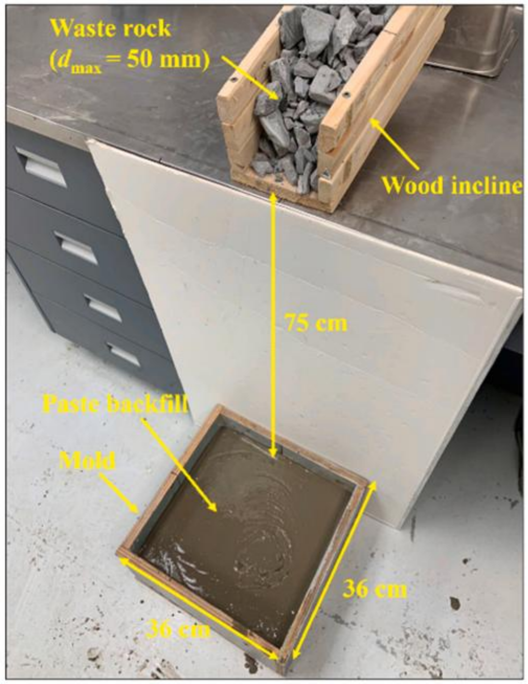

Figure 2-25 Laboratory setup for natural mixing of waste rock and paste backfill without mechanical mixing (reproduced of Zhang et al., 2026b with permission)

Although these studies have improved the understanding of natural mixing behavior and mixing degree, a practical and easy-to-use tool is still lacking for mining engineers and dumping operator to estimate the maximum allowable waste rock mass that can be dumped without causing poor mixture. Predictive tools are necessary but non existant to guide waste rock dumping operations in stopes filled with paste backfill.

CHAPTER 3 Article 1: An empirical solution for estimating the maximum allowable waste rock mass to avoid poor mixture between paste backfill and dumped waste rock

Pantea Kazemi, Li Li

Submitted to *Green and Smart Mining Engineering* on March 23, 2026

Contributions: Pantea Kazemi: Conceptualization, Methodology, Experimental tests, Investigation, Data curation, Formal analysis, Validation, Visualization, Writing original draft**. Li Li:** Conceptualization, Methodology, Resources, Funding acquisition, Project administration, Supervision, Review & editing.

Abstract

Abstract

Traditionally, waste rock generated in underground mines is transported to the ground surface and stored in waste rock piles. This process requires significant energy consumption and leads to additional operational costs. In Canada, an alternative practice is to directly dump waste rock into stopes that are being filled with paste backfill. This method eliminates the need for surface transportation of waste rock. It also removes the necessity for crushing large rock blocks into smaller particles, using special mixers for mechanically mixing two materials. As a result, energy consumption and greenhouse gas emissions are reduced. In addition, binder consumption decreases because part of the cemented paste backfill is replaced by dumped uncemented waste rock. Although this method offers several advantages, a practical tool is absent to guide backfill engineers in the waste rock dumping operation. As such, an excessive quantity of waste rock may be dumped into paste backfill, resulting in poor mixture between the two materials. Upon side exposure during the excavation of neighboring stope, the fill mass can fail and lead to undesirable consequences. To fill this gap, a series of laboratory tests were conducted to evaluate the effect of different factors such as solids content and thickness of paste backfill, falling height, maximum particle size of waste rock, and stope dimensions on the maximum allowed mass of waste rock studied. An empirical solution was established to estimate the maximum allowed waste rock mass to avoid poor mixture between dumped waste rock and paste backfill. The predictability of the proposed solution was successfully con-firmed with additional and independent experimental results.

Keywords: Paste backfill; Waste rock; Empirical solution; Natural mixing; Underground backfilling; Co-disposal

3.1 Introduction

Underground mining activities generate large quantities of solid waste materials, mainly in the form of waste rock and tailings (Iqbal et al., 2025; James et al., 2013; Lottermoser, 2010; Manaviparast et al., 2024; Vick, 1990). Tailings consist of water and fine particles produced during the milling process and are usually stored in impoundments where they settle and consolidate (Aubertin, Bussière, Bernier, et al., 2002; Azam & Li, 2010; Rico et al., 2008; Vick, 1990). Tailings impoundments may pose geotechnical risks, including seismic-induced liquefaction and potential structural failure (Azam & Li, 2010; Lyu et al., 2019; Martin & McRoberts, 1999; Rico et al., 2008). Environmental impact such as environmental footprint, acid mine drainage, and contaminated neutral drainage is another major concern of surface disposal of mine waste (Bernd & Bernd, 2007; Blowes et al., 2003; Johnson & Hallberg, 2005; Nordstrom & Alpers, 1997). Using mine wastes as backfill material to fill underground mining stopes helps to increase ore recovery and reduce the environmental impact of mining industry (Fan, Li, Liu, et al., 2025; Fan, Li, Yang, et al., 2025; Ma et al., 2025; Pengyu & Li, 2015).

Traditionally, underground generated waste rock is transported to the surface and stored in waste rock piles (Aubertin, Bussière, & Bernier, 2002; Bernd & Bernd, 2007; James & Aubertin, 2012; Tatiya, 2005). This practice requires substantial energy for hauling and handling, significant workforce involvement, additional operational costs, and increasing greenhouse gas emissions (Lee & Gu, 2017).

On the other hand, an increasingly adopted approach in Canadian underground mines is to directly dump waste rock into stopes that are being filled with paste backfill. Energy consumption, operational costs, and greenhouse gas emissions are substantially reduced because crushing large waste rock blocks into smaller particles, mechanical mixing between waste rock and paste backfill as well as transportation of waste rock from underground to surface disposal infrastructures is not needed. In addition, binder usage can be decreased because a portion of cemented paste backfill is effectively replaced by uncemented waste rock (Lee & Gu, 2017; Zhang et al., 2026a, 2006b). Moreover, a good mixture of waste rock and cemented paste backfill can have higher mechanical strength than either material alone (Hane et al., 2017; Qiu et al., 2020; Qiu et al., 2022).

Despite the several advantages, the waste rock dumping onto cemented paste backfill operation in stopes can also involve severe risks. When an excessive quantity of waste rock is dumped onto the cemented paste backfill, poor mixture between the two materials may take place. The fill mass upon side-exposure during the excavation of neighboring stopes may collapse, resulting in undesirable consequences such as ore dilution or loss, equipment damage, and in some cases personal injury or death. Therefore, the waste rock dumping onto cemented paste backfill operation in stopes must be adequately managed. This requires a tool to guide the waste rock dumping operations.

Over the past decades, a large number of publications has been devoted to study on underground backfilling with a single backfill (Béket Dalcé et al., 2019; Fan, Li, Liu, et al., 2025; Fan, Li, Yang, et al., 2025; Liu et al., 2017; Pengyu & Li, 2015; Qin et al., 2021; Yang et al., 2017). In contrast, few studies have focused on the concept of natural mixing, where waste rock is directly dumped onto paste backfill without mechanical blending. Several studies have examined mechanically mixed materials such as graded waste rock and tailings slurry or graded waste rock and cemented backfill (Hane et al., 2017; Kuganathan & Sheppard, 2001; Lee & Gillot, 2014; Potvin et al., 2005; Qiu et al., 2020; Qiu et al., 2022; Sun et al., 2018). Waste rock typically needs to be crushed, well-graded, and mechanically mixed with tailings or cemented backfill to produce a uniform and controlled composite material. Dedicated equipment is necessary for these operations. Increase in energy consumption, operational costs, and greenhouse gas emissions is another non negligible limitation of these mechanical mixture operations.

Recently, Zhang and coworkers (Zhang, 2024; Zhang & Li, 2023; Zhang et al., 2026a, 2006b) investigated the natural mixing behavior between dumped waste rock and paste backfill. Their results demonstrated that the degree of mixing can be enhanced by increasing the falling height and maximum particle size of waste rock and by reducing the solids content of the paste backfill (Zhang & Li, 2023). However, an important gap remains because no study has provided a practical and quantitative tool for estimating what quantity of waste rock can be safely dumped onto paste backfill in stope without causing substantial poor mixture between the two materials.

To fill this gap, a series of laboratory tests were conducted to evaluate the effect of different factors such as solids content and thickness of paste backfill, falling height and maximum particle size of waste rock, and stope dimensions on the maximum allowed mass of waste rock. A solution in terms of an empirical equation is proposed to estimate the maximum allowed waste rock mass to avoid substantial poor mixture between dumped waste rock and paste backfill. The empirical solution along with empirical constants was established using a set of experimental test results. The predictability of the proposed solution is verified with new and independent test results.

3.2 Small-scale laboratory tests

3.2.1 Materials

The tailings used in this study for paste backfill were collected from an underground mine (named Mine A) located in Québec, Canada. The tailings are non-sulfidic. They have a spe-cific gravity of 2.77 and a dry density of approximately 1 550 kg·m^{-3}. The particle size dis-tribution (PSD) curve is presented in Figure 3-1. The maximum particle size (d_{max}) of the tail-ings is about 0.6 mm, with approximately 75% of the particles smaller than 80 µm.

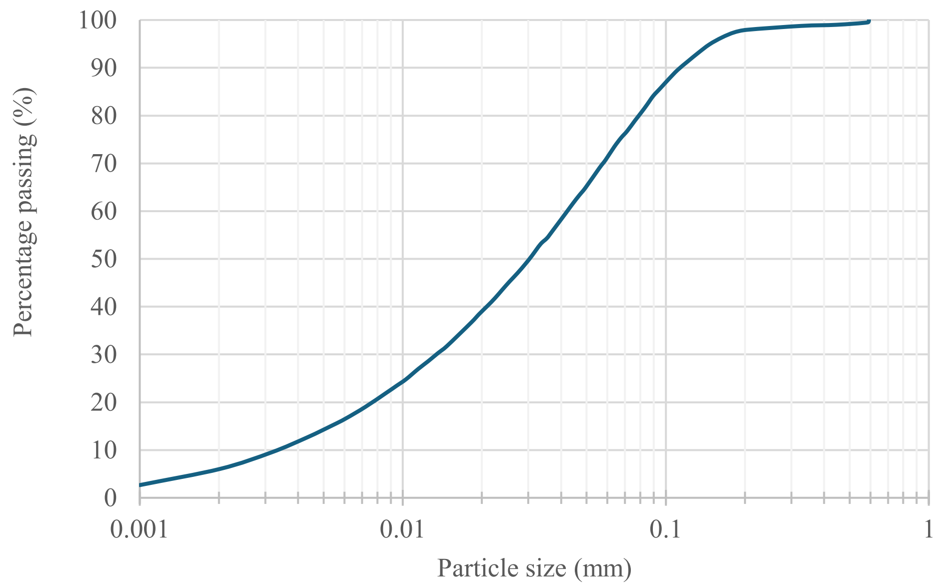

Figure 3-1 Particle size distribution of tailings used in small-scale tests

Waste rock was obtained from an open pit mine (named Mine B) also in Québec, Canada. The waste rock samples were prepared by applying a double truncation to the original material (Deiminiat & Li, 2022; Zhang & Li, 2024; Zhang et al., 2026a, 2006b). Particles larger than 10 mm and smaller than 1 mm were removed. The oversized particles were excluded to facilitate cutting of the hardened mixture samples during post-test analysis. The fine particles were excluded to ensure that all waste rock particles in the waste rock and paste backfill mixtures can be easily distinguished from the paste backfill by visual observation. Five samples of waste rock with maximum particle sizes (d_{max}) of 2 mm, 3.35 mm, 4.75 mm, 8 mm, and 10 mm using double scalping technique were tested. Figure 3-2 shows their PSD curves.

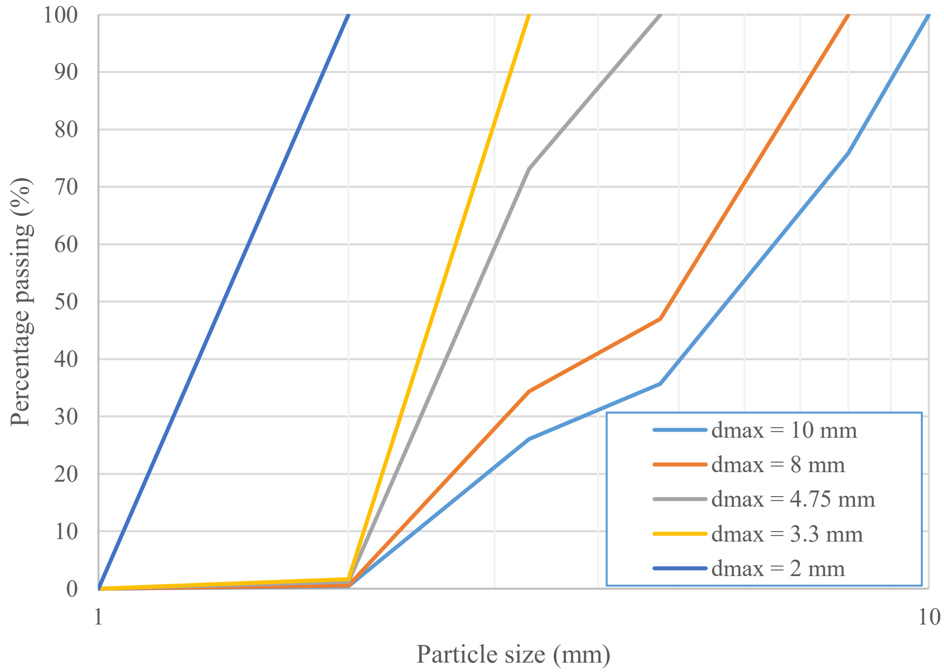

Figure 3-2 PSD of waste rock samples used to investigate the effect of maximum particle size on the maximum allowable waste rock mass

3.2.2 Experimental setup

Figure 3-3 illustrates the small-scale experimental setup used in this study after a few improvements (see details given in Appendix A). Figure 3-3(a) presents a schematic representation of the system, while Figure 3-3(b) shows a photograph of the physical model.

A mold with internal dimensions of 15 cm × D_M × D_M was used to represent a simplified mine stope at laboratory scale. A funnel with a top diameter of 19 cm, a bottom outlet diameter of 4.0 cm, and a height of 12 cm was positioned, vertically centered above the mold. The parameter H_p (cm) represents the thickness of the paste backfill layer placed inside the mold. The falling height of the waste rock, denoted as H_f (cm), is defined as the vertical distance between the funnel outlet and the surface of the paste backfill.

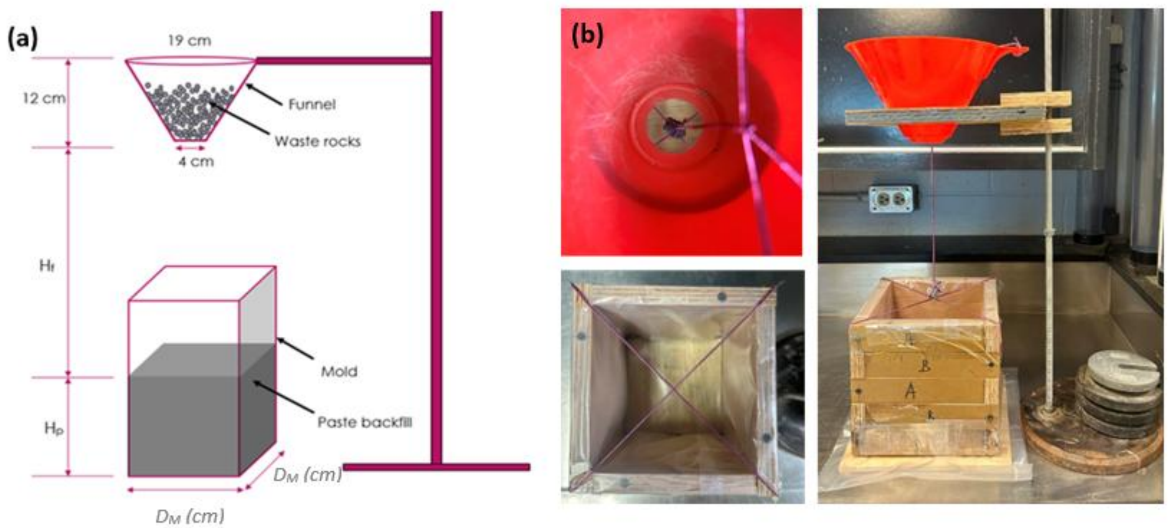

Figure 3-3 A small-scale physical model used to study the natural mixing of waste rocks poured into paste backfill: (a) schematic presentation; (b) photograph

3.2.3 Test procedure

Prior to testing, the tailings were oven-dried for 24 hours and then allowed to cool to room temperature. This step was necessary to prevent unintended water evaporation during preparation and to ensure accurate control of the solids content. The dried tailings were manually mixed with water to prepare paste backfill with the desired solids content by mass (C_w), as shown in Figure 3-4. Mechanical mixing was initially tested but not adopted as it resulted in incomplete homogenization, with some tailings remaining at the bottom of the container. Manual mixing provided a more uniform mixture.

Figure 3-4 Manual mixing of the paste backfill

Paste backfill was mixed for a minimum of 15 minutes at room temperature to ensure consistency between tests. For each experiment, the paste backfill with a given solids content (C_w) was poured into the mold with a width (D_M) to a predefined thickness (H_p). The paste backfill was continuously mixed until the moment it was poured into the mold in order to prevent tailings sedimentation and to maintain a homogeneous mixture. The funnel was then positioned to have a specified falling height (H_f) above the paste backfill surface. A total mass of waste rock (M_{total}) with a specified maximum particle size (d_{max}) was weighed and placed into the funnel. Waste rock was poured onto the paste backfill surface until visual observation of waste rock remaining on the surface of the paste backfill.

The remaining waste rock in the funnel (M_{remain}) was measured. The paste backfill and waste rock samples were left in the mold to dry under natural laboratory conditions for 7 to 10 days. After that curing time, the waste rock remaining on the surface (M_{top}) of the paste backfill was carefully removed and weighed. The mass of the waste rock that had penetrated into the paste backfill but remained unmixed with the paste backfill ($M_{unmixed}$) was also taken out and weighed. The mixture samples were then cut vertically through the center to examine the internal texture structure and to evaluate the mixture quality. The maximum allowable waste rock mass that successfully mixed with the paste backfill was calculated as:

$$M_{mixture} = M_{total} - M_{remail\ in\ funnel} - M_{top} - M_{unmixed} \tag{3.1}$$

To evaluate the individual influence of each parameter, a controlled experimental strategy was adopted. In each test series, only one parameter was varied at a time, while all other parameters were kept constant at predefined values. This one-factor-at-a-time approach allowed the independent effect of each parameter on the maximum allowable waste rock mass to be assessed. The overall testing program is summarized in Table 3-1.

Table 3-1 Experimental testing program

Case	Paste backfill		Waste rock		Stop width
	C_w (%)	H_p (cm)	d_{max} (mm)	H_f (cm)	D_M (cm)
1	63, 66.5, 68, 70, 74	7	4.75	35	15
2	70	2, 7, 10, 13, 20	4.75	35	15
3	70	7	2, 3, 4.75, 8, 10	35	15
4	70	7	4.75	15, 35, 50, 75, 100, 120, 150, 200	15
5	70	7	4.75	35	10, 15, 35

3.2.4 Test results

Effect of solids content of paste backfill, C_w

Figure 3-5 illustrates the distribution of waste rock within the paste backfill of different solids contents along a vertical center section with different solids contents of paste backfill. One sees that waste rock occupies a large volume through almost all space with a paste backfill solids content of 63%, while a V-shaped of waste rock distribute through the mixture with a paste backfill solids content of 74%. These results indicate that a thinner paste backfill with a low solids content facilitate the mixture, allowing a larger volume of waste rock to be dumped into paste backfill without significate poor mixture between the two materials.

For the sample with a solids content of 63%, the paste backfill exhibited a relatively fluid behavior, allowing the waste rock particles to sink deeply into the paste backfill. In this case, the waste rock penetrated to the bottom of the mold and reached the side-walls, forming a concrete texture and dense internal structure with a relatively uniform distribution of particles. Of course, at such low solids content, the uncemented paste backfill is mostlly called thickened tailings than paste backfill. The same thing for the uncemente dpaste backfill at a solids content of 66.5% or higher. The question is: at which solids content the backfill can be named as paste backfill? If one applies all the criteria of paste backfill specified in mining backfill handbooks (Hassani and Archibald 1998;

Potvin et al. 2005), the paste backfill applied in a largr number of mines cannot be called paste backfill because the solids content does not meet the criterion by which the backfill should not bleed of water uopon their deposition on a floor. As indicated by Zheng and Li (2020), the only possibility for a backfill not bleeding is that it is unsaturated. In such case, the backfill would be too thick for traporation by pipes. That is why more water has to be added to increase the fluidity and facilitate the tranportation. The criteraion of paste backfill in terms of solids content is not satified and the backfill is still largely called “paste backfill” in mining industry (Zheng and Li 2020).

When the solids content increased to 66.5%, the paste backfill became thicker. Under these conditions, the maximum allowable waste rock mass decreased to 1000 g. The waste rock particles penetrated into the paste backfill until the bottom. Some zones remained free of waste rock particles.

At the highest solids content of 74%, the paste backfill exhibited the highest consistency. The paste backfill strongly resisted particle penetration, and the waste rock remained mainly near the surface. Only a small quantity of waste rock was able to penetrate into the paste backfill, resulting in a maximum allowable waste rock mass of 69 g.

These observations are consistent with the findings reported by Zhang and Li (Zhang & Li, 2023), who also showed that the degree of natural mixing between dumped waste rock and paste backfill decreases as the solids content of the paste backfill increases. Their study indicated that lower solids content promotes deeper particle penetration and higher mixing efficiency, while higher solids content restricts waste rock penetration. The present results therefore confirm the important role of paste backfill solids content in controlling the natural mixing behavior between dumped waste rock and paste backfill.

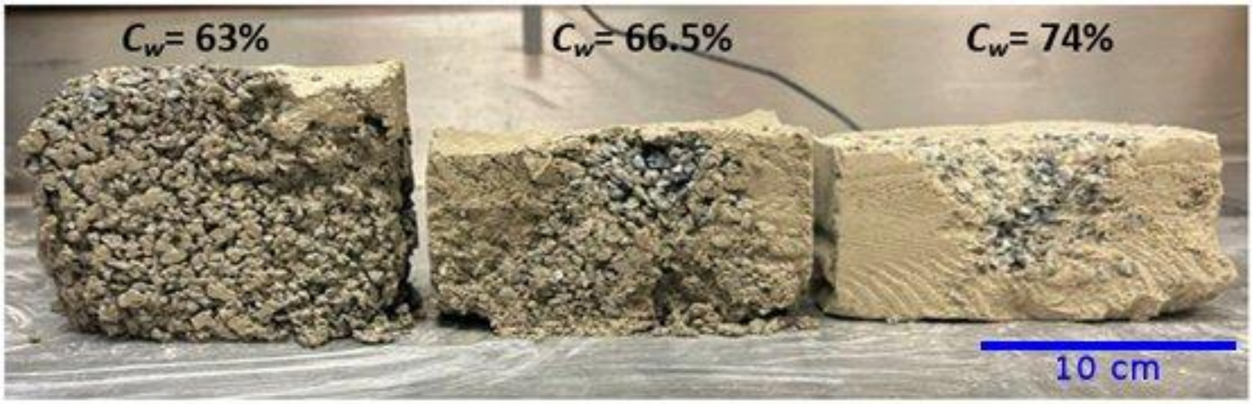

Figure 3-5 Internal texture structure of samples with solids contents of 63%, 66.5%, and 74% (from left to right) of paste backfill; details given in Table 3-1 for Case 1

Figure 3-6 shows the variation of the maximum allowable waste rock mass as a function of solids content of the paste backfill. One sees that the maximum allowable waste rock mass decreases with increasing solids content. When the solids content increased from 63% to 74%, the maximum allowable waste rock mass dropped from 2891.8 g to 69 g. The repeated tests (orange markers) follow the same curve trend, confirming the repeatability and reliability of the experimental results (reasons for repeated tests given in Appendix B).

The observed trend can be explained by the rheological behavior of paste backfill. Increasing the solids content increases the yield stress and viscosity of the paste backfill, which significantly reduces the penetration ability of waste rock particles into the paste backfill. At lower solids contents, the paste backfill behaves more like a fluid, allowing waste rock particles to sink more easily and mix with the paste backfill. In contrast, at higher solids contents the paste backfill behaves as a stiffer material, which resists particle penetration and limits the mixing between the two materials.

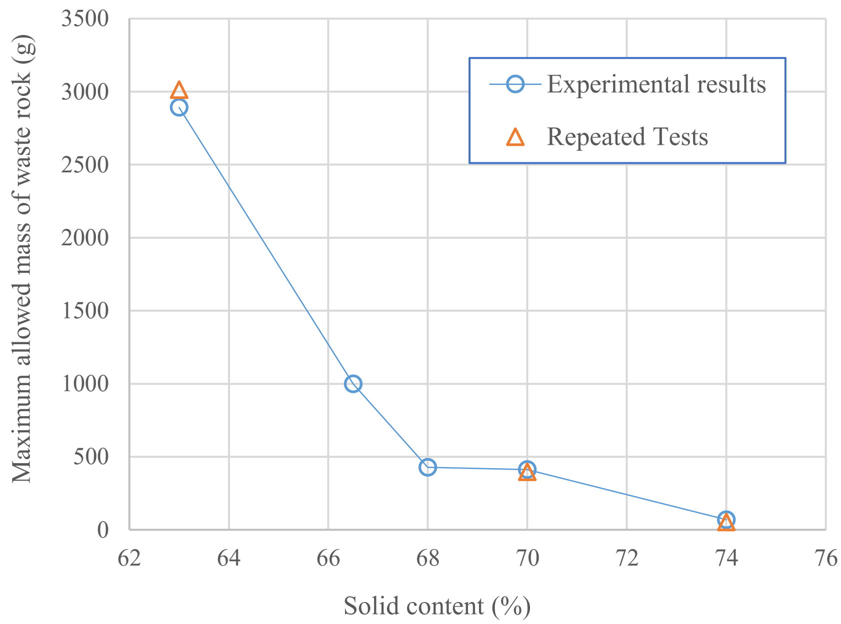

Figure 3-6 Variation of the maximum allowable waste rock mass as a function of solids content of the paste backfill; details given in Table 3-1 for Case 1

Effect of paste backfill thickness H_p

Figure 3-7 illustrates the internal texture structure of the paste backfill and waste rock samples along a vertical center section with paste backfill thickness (H_p) of 2 cm, 10 cm, and 20 cm, respectively.

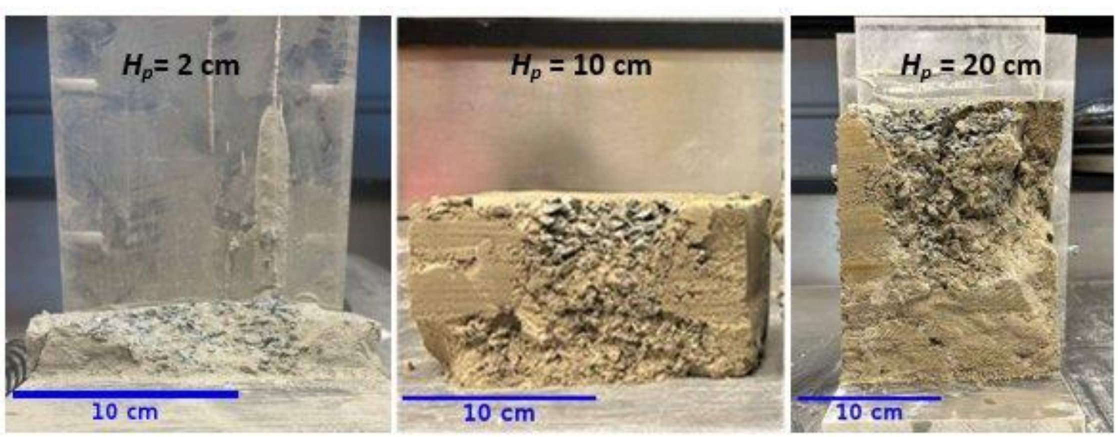

Figure 3-7 Internal texture structure of the paste backfill and waste rock samples along a vertical cen-ter section with paste backfill thickness (H_p) of 2 cm, 10 cm, and 20 cm (from left to right), respectively; details given in Table 3-1 for Case 2

For the sample with a paste backfill thickness of 2 cm, the available space for waste rock penetration was very limited. Under this condition, the waste rock particles quickly reached the bottom of the mold, which restricted further penetration. As a result, the maximum allowable waste rock mass was limited. When the paste backfill thickness increased to 10 cm, a larger space was available for waste rock penetration. The waste rock particles were able to sink deeper into the paste backfill and reach the bottom of the mold, resulting in a higher allowable waste rock mass.

A further increase in paste backfill thickness to 20 cm provided an even larger space for particle penetration, allowing more waste rock particles penetrating into the paste backfill. However, due to the relatively high solids content of the paste backfill ($C_w = 70\%$), the paste backfill exhibited a relatively stiff consistency. The waste rock particles did not reach the bottom of the mold and were mainly distributed within the upper and middle portions of the paste backfill layer.

Figure 3-8 shows the variation in the maximum allowable waste rock mass as a function of paste backfill thickness. One sees that the maximum allowable waste rock mass increases as the paste backfill thickness increases. This is quite straightforward. With a thicker paste backfill layer, the sinking particles of waste rock driven by the kinetic energy can have longer distance before touching the bottom, resulting in a larger volume of waste rock penetrating into the paste backfill.

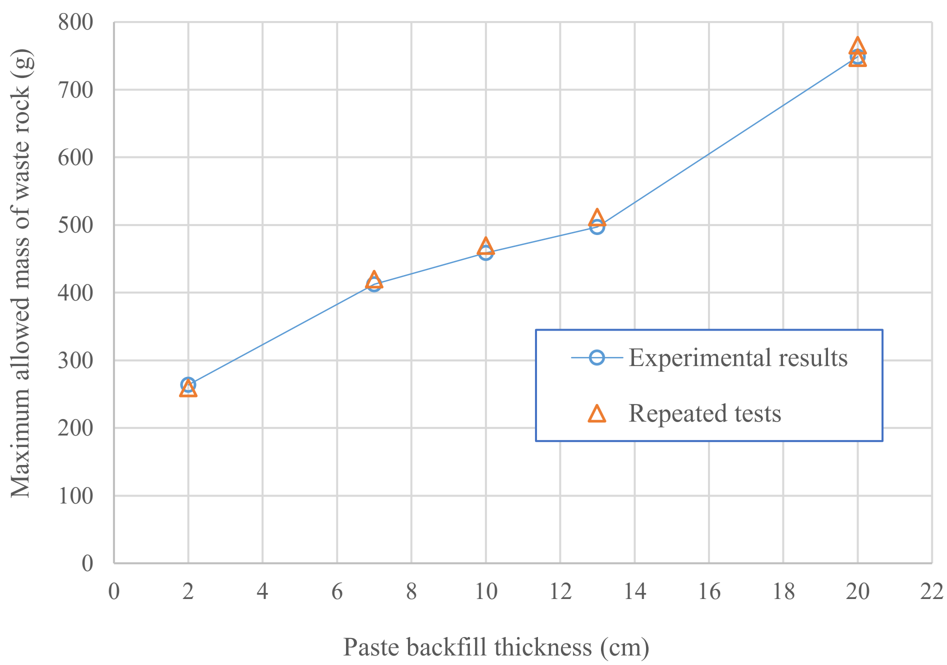

Figure 3-8 Variation in the maximum allowable waste rock mass as function of paste backfill thickness; details given in Table 3-1 for Case 2

Effect of maximum particle size (d_{max}) of waste rock

Figure 3-9 illustrates the internal texture structure of the paste backfill and waste rock samples along a vertical center section. For the sample containing waste rock with a maximum particle size of 2 mm, the particles mainly accumulated in a cone-shaped zone directly beneath the pouring point. For the sample containing waste rock with a maximum particle size of 8 mm, the particles penetrated much deeper into the paste backfill and spread toward the bottom of the mold, filling most of the base region. For both cases, some areas near the side-walls remained free of waste rock particles.

Similar observations were reported by Zhang and Li, who showed that larger waste rock particles penetrate deeper into paste backfill and increase the degree of natural mixing between the two materials (Zhang & Li, 2023).

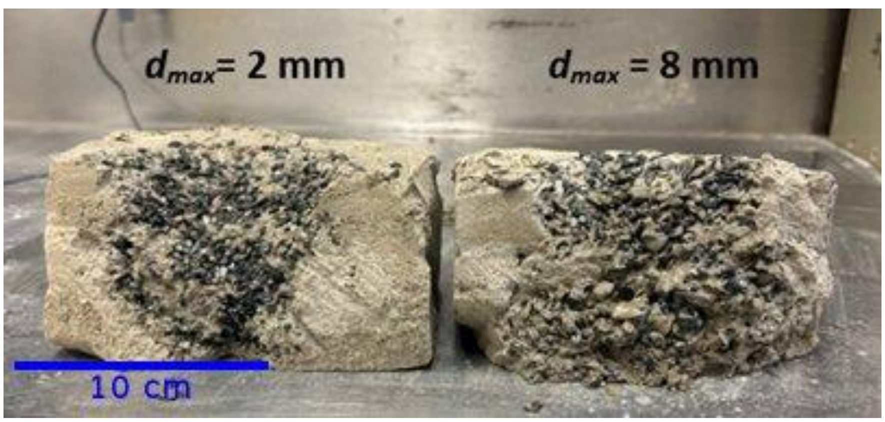

Figure 3-9 Internal texture structure of paste backfill and waste rock with maximum particle sizes of 2 mm (left) and 8 mm (right), respectively; details given in Table 3-1 for Case 3

Figure 3-10 shows the variation in the maximum allowable waste rock mass as a function of maximum particle size of waste rock. When the maximum particle size increased from 2 mm to 8 mm, the maximum allowable waste rock mass increased from approximately 202.5 g to about 711 g. The repeated tests (orange markers) follow the same curve trend, indicating good repeatability and reliability of the experimental results.

The observed trend can be explained by the kinetic energy of falling particles of waste rock. Larger particles have a larger mass and therefore higher kinetic energy when falling onto the paste backfill surface. This higher kinetic energy allows the particles to overcome the resistance of the paste backfill and penetrate deeper into the paste backfill, resulting in a larger quantity of waste rock mixing with the paste backfill. However, when the maximum particle size increased from 8 mm to 10 mm, the maximum allowable waste rock mass increased only slightly from about 711 g to 718.4 g. This indicates that beyond a certain particle size, the influence of maximum particle size on the maximum allowable waste rock mass becomes limited.

To better understand the constant trend observed in the maximum allowable waste rock mass with further increase in the maximum particle size from 8 mm to 10 mm, one should note the (truncated) cone-shaped waste rock distribution, as shown in Figure 3-9. The (truncated) cone was formed by the dumping of waste rock particles, similar to repose angle pile tests. Using the same waste rock as this study, Zhang have shown that the angle of repose of the waste rock does not depend on the maximum particle size as long as the quantity of waste rock is sufficiently large (Zhang, 2024). As the base size of the stope is fixed, the volume of the waste rock in a (truncated) cone shape does not change significantly with the increase in maximum particle size of waste rock. Consequently, the almost constant value in the maximum allowable waste rock mass with further increase in the maximum particle size larger than 8 mm is well explained.

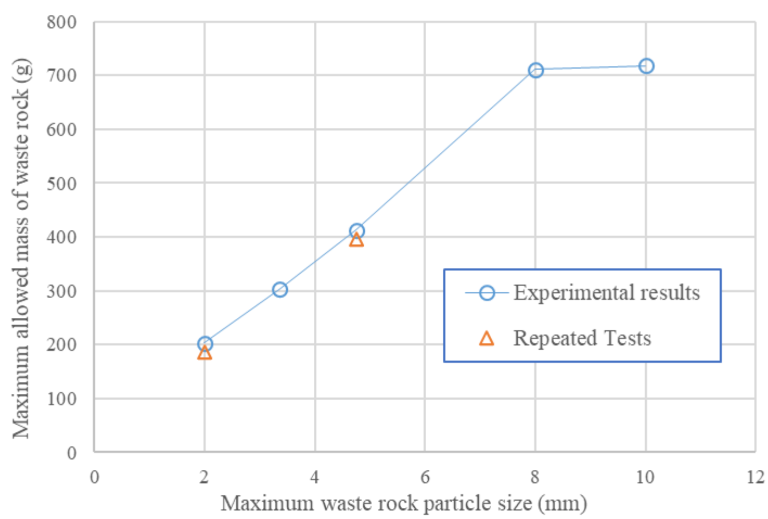

Figure 3-10 Variation of the maximum allowable waste rock mass as a function of maximum particle size of waste rock; details given in Table 3-1 for Case 3

Effect of falling height of waste rock, H_f

Figure 3-11 illustrates the internal texture structure of the paste backfill and waste rock samples along a vertical center section with different falling height of waste rock. One sees that at a falling height of 50 cm, the waste rock particles mainly penetrated vertically toward the bottom of the mold but did not reach the side walls. A similar penetration pattern was observed at a falling height of 100 cm, where the particles remained concentrated in a relatively localized region beneath the pouring point.

When the falling height increased to 150 cm, the waste rock particles penetrated deeper into the paste backfill and spread closer to the mold walls compared with the samples obtained at lower falling heights. At the highest falling height of 200 cm, the particles reached the mold walls and spread over a much larger area within the paste backfill. However, some zones within the sample still remained free of waste rock particles.

As more waste rock penetrates into the paste backfill, a larger volume of the paste backfill becomes occupied by waste rock particles, which results in a thicker mixed zone between the waste rock and the paste backfill.

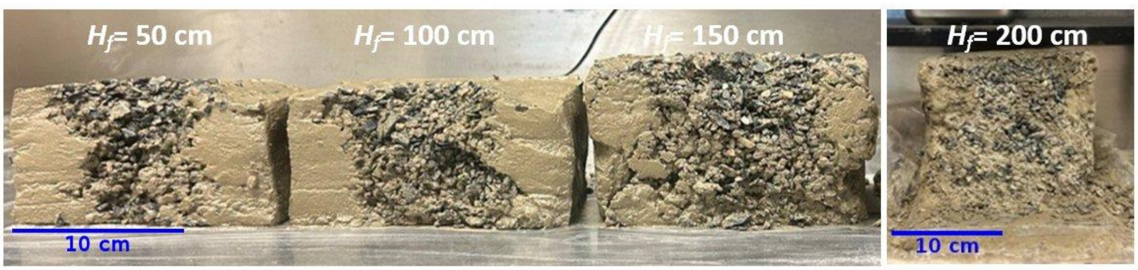

Figure 3-11 Internal texture structure of the paste backfill and waste rock samples along a vertical cen-ter section with waste rock falling heights of 50 cm, 100 cm, 150 cm, and 200 cm (from left to right), respectively; details given in Table 3-1 for Case 4

Figure 3-12 shows the variation in the maximum allowable waste rock mass as a function of waste rock falling height. In general, the maximum allowable waste rock mass increases as the waste rock falling height increases as what has been reported by Zhang and Li (Zhang & Li, 2023). More specifically, one notes that the maximum allowable waste rock mass initially increased and then tended to remain nearly constant when the falling height increased from 15 cm to 100 cm. This is still straightforward. When the falling height is not very large, an increase in the falling height of waste rock results in higher kinetic energy, deeper penetration, and larger volume of waste rock particles penetrates into the paste backfill. When the falling height increases to a certain critical point, the drag force balances the gravity force. Further increase in height does not result in significant increases in the falling velocity and kinetic energy as well as the maximum allowed waste rock mass.

However, a sharp increase in the maximum allowable waste rock mass with further increase in the falling height of waste rock was observed when the falling height exceeded approximately 100 cm. The reliability of the test results is confirmed through new tests, presented in orange points on the figure 3-12. At a falling height of 100 cm or less, the waste rock particles mainly fell in the center part. At a falling height of 150 cm or higher, the waste rock particles fell and spread over a much larger area on the surface of the paste backfill. Thus, the further increase in the maximum allowable waste rock mass with further increase in the falling height of waste rock beyond 100 cm can be partly attributed to the increase in the waste rock receiving area on top of the paste backfill with increasing falling height of the waste rock. The effect of receiving area on the maximum allowable waste rock mass is further addressed in section "Discussion".

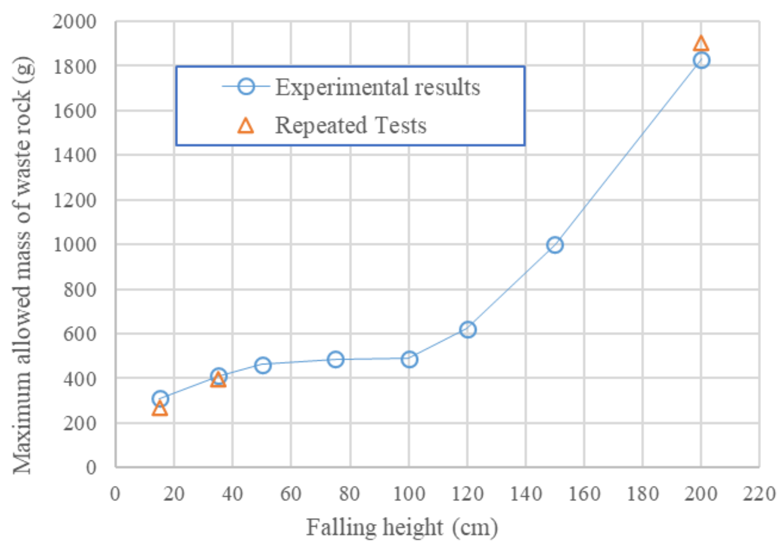

Figure 3-12 Variation in the maximum allowable waste rock mass as a function of falling height of waste rock; details given in Table 3-1 for Case 4

Effect of stope dimensions D_M

Figure 3-13 illustrates the internal texture structure of the paste backfill and waste rock samples along a vertical center section with different stope dimensions. One sees that the waste rocks in samples with mold dimensions of 15 cm and 35 cm are distributed with a similar pattern in both tests. Most of the waste rock particles mainly penetrated downward toward the bottom of the mold and did not reach the side walls. Therefore, increasing the mold dimensions does not significantly affect the results, since the waste rock particles cannot reach the side walls and thus the mold boundaries do not influence the penetration and distribution of waste rock within the paste backfill.

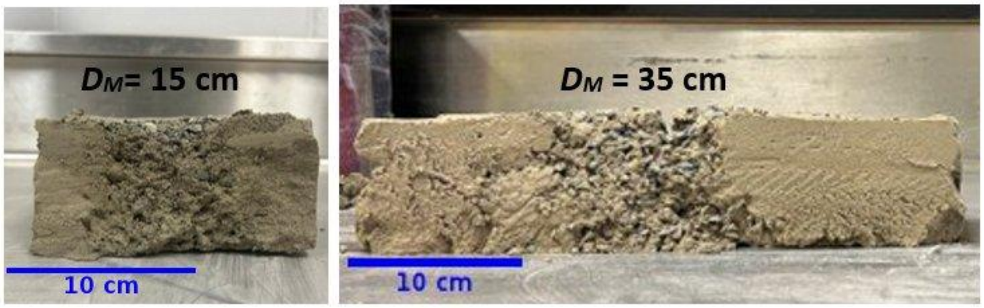

Figure 3-13 illustrate the internal texture structure of the paste backfill and waste rock samples along a vertical center section with different stope dimensions; details given in Table 3-1 for Case 5

Figure 3-14 shows the variation in the maximum allowable waste rock mass as a function of mold size. Despite the substantially larger volume of the paste backfill due to larger cross section in horizontal plane, the measured values of allowable waste rock mass remained almost constant, indicating that the amount of waste rock that can penetrate and mix with the paste backfill is not sensitive to the variation of stope width. This observation can be explained by the constant receiving area with different mold dimensions, as shown in Figure 3-15 as well as the similar distributions of waste rock with the paste backfill with different stope dimensions, as shown in Figure 3-13.

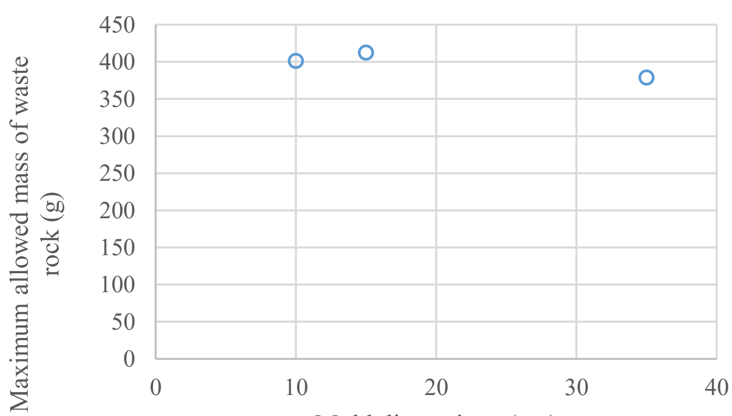

Figure 3-14 Variation in the maximum allowable waste rock mass as a function of mold dimension and maximum allowable waste rock mass; (b) top-view photograph of samples with mold dimensions of 10 cm (left) and 35 cm (right) ; details given in Table 3-1 for Case 5

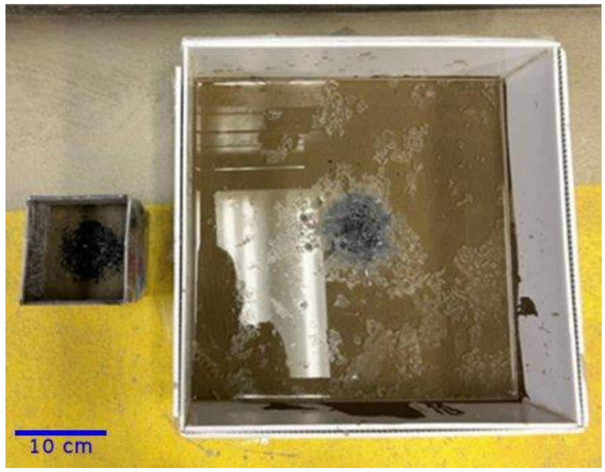

Figure 3-15 Top-view photograph of samples with mold dimensions of 10 cm (left) and 35 cm (right); details given in Table 3-1 for Case 5

3.3 Proposed solution

Based on the experimental results presented in Section 3.2, an empirical solution was developed to estimate the maximum amount of waste rock that can mix naturally with the paste backfill as follows:

$$M_c = a \exp\left(b\, C_w + c\, H_f\right)\left(d\, d_{max} + e\right)\left(f\, H_p + g\right) \tag{3.2}$$

where M_c represents the maximum allowed waste rock mass (g), C_w represents the solids content of the paste backfill (–), H_p is the thickness of the paste backfill (cm), H_f is the falling height of the waste rock (cm), and d_{max} is the maximum particle size of the waste rock (mm). The coefficients *a,b,c,d,e,f,* and *g* are empirical constants obtained through a curve-fitting procedure based on the experimental data presented in Section 3.2 as follows:

a =1345996.74, b= -30.4, c= 0.0098, d =41.88, e = -4.97, f= 137.22, and g= 668.15.

Equation 3.2 alongside with a =1345996.74, b= -30.4, c= 0.0098, d =41.88, e = -4.97, f= 137.22, and g= 668.15 constitute the proposed solution for estimating the maximum allowable waste rock mass to avoid poor mixture between paste backfill and dumped waste rock. Figure 3-16 shows the variation of the maximum allowable waste rock mass as function of paste backfill solids content (Figure 3-16a), paste backfill thickness (Figure 3-16b), maximum particle size of waste rock (Figure 3-16c), and falling height of waste rock (Figure 3-16d) obtained by measured and calculated by applying the proposed solution (i.e. Equation 3.2 with a =1345996.74, b= -30.4, c=

0.0098, d =41.88, e = -4.97, f= 137.22, and g= 668.15). Overall, the proposed solution describes well the experimental data.

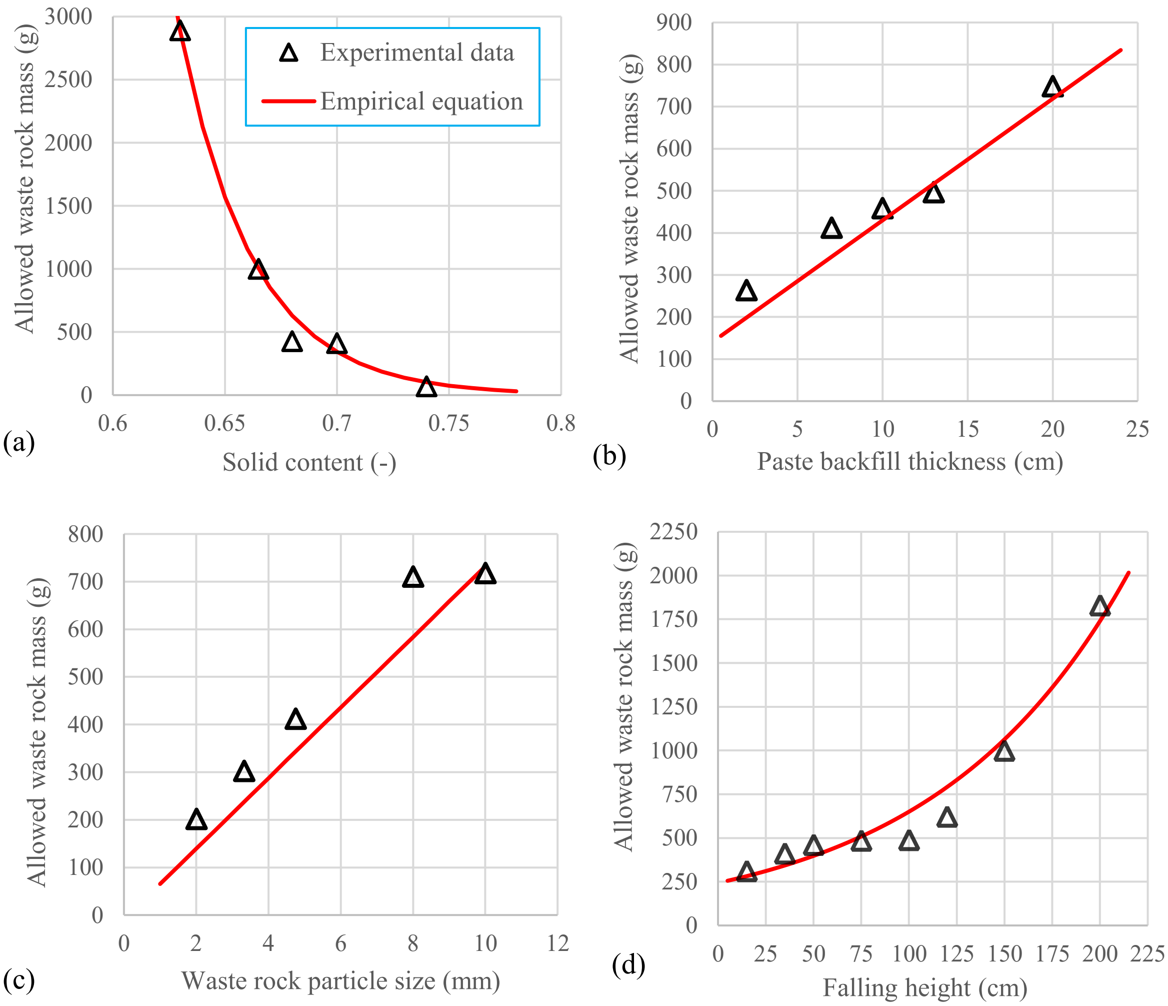

Figure 3-16 Variation of the maximum allowable waste rock mass as function of (a) paste backfill solids content, (b) paste backfill thickness, (c) maximum particle size of waste rock, and (d) falling height of waste rock obtained by measured and calculated by applying the proposed solution (i.e. Equation 3.2 with a =1345996.74, b= -30.4, c= 0.0098, d =41.88, e = -4.97, f= 137.22, and g= 668.15)

Although the agreement between the proposed solution and the laboratory results is good, the capability of prediction of the proposed solution remains unknown. New and independent test results are needed to evaluate the predictive ability of the proposed solution.

Table 3-2 shows additional laboratory tests with the waste rock having a d_{max} value of 4.75 mm. The comparison between the predicted and measured values of the maximum allowable waste rock mass is illustrated in Figure 3-17. To quality of the predictive performance of the proposed solution is evaluated using the coefficient of determination (R^2) defined as follows:

$$R^2 = 1 - \frac{\sum_{i=1}^{n}(y_i - \hat{y}_i)^2}{\sum_{i=1}^{n}(y_i - \bar{y})^2} \tag{3.3}$$

One sees that the predicted values agree very well with the measured experimental results with a R^2 of 0.997.

Table 3-2 Additional laboratory tests with waste rock having a d_{max} value of 4.75 mm

Test	H_f (cm)	H_p (cm)	C_w (%)
1	20	7	70
2	35	4	70
3	36	7	72
4	165	7	70
5	35	7	64

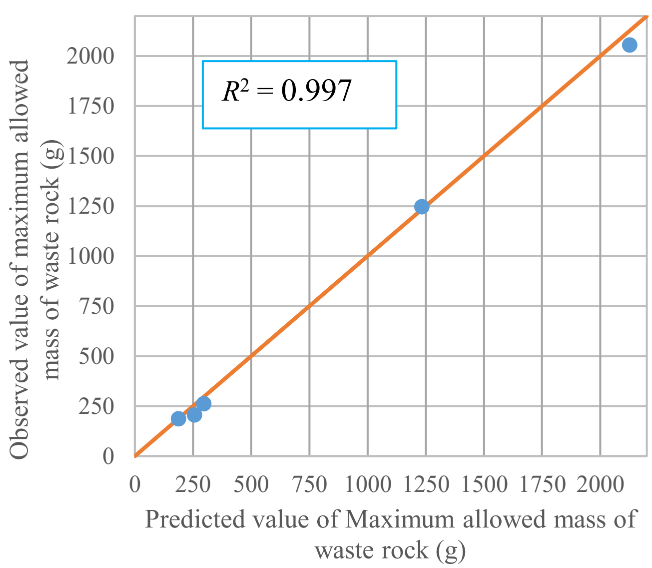

Figure 3-17 Comparison between the predicted and measured values of maximum allowable waste rock mass obtained from the additional experimental tests.

3.4 Large-scale tests

During the small-scale tests, tailings and waste rock available in our laboratory for other projects were used. The waste rock samples were obtained by applying double scalping technique with both undersized fine particles and oversized coarse particles excluded. The waste rock samples may not be fully representative of underground generated waste rock. To evaluate the applicability and predictability of the proposed solution (Equation 3.2 with a =1345996.74, b= -30.4, c= 0.0098, d =41.88, e = -4.97, f= 137.22, and g= 668.15) under a condition closer to the field one, additional tests were conducted with tailings and waste rock, both provided by an underground mine.

3.4.1 Test materials

The paste backfill was made from 75% non-sulfate tailings and 25% sulfate tailings, obtained from underground mine A in Quebec, Canada. Figure 3-18 shows the two types of tailings delivered from the mine in separate containers. To ensure homogeneity, each type of tailings was first blended individually in its own container to obtain a uniform material. The solids content of each tailings batch was carefully adjusted so that both materials had identical solids content. Then, the two types of tailings were mixed to produce a paste backfill composed of 25% sulfate tailings (Figure 3-18a) and 75% non-sulfate tailings (Figure 3-18b), which is representative of the field conditions of Mine A. Before each test, the final mixture was blended for 30 minutes before placement in the mold to ensure a uniform and homogeneous material. This long mixing time was necessay because the large-scale tests required a relatively large volume of paste backfill, and the tailings stored in a paste-like state likely underwent partial sedimentation and consolidation before testing.

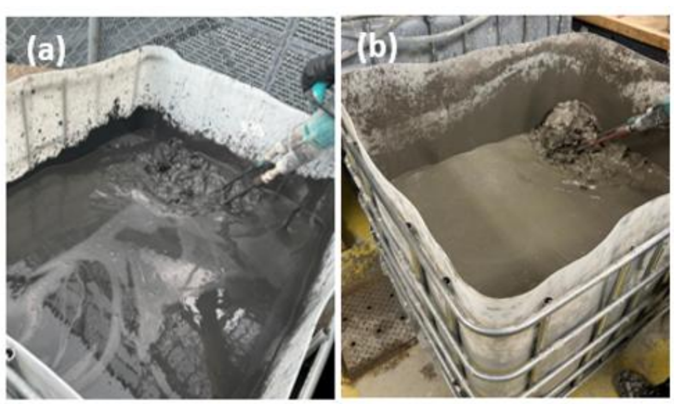

Figure 3-18 Pictures of (a) sulfate tailings and (b) non sulfate tailings

The waste rock was also provided by underground mine A, but delivered in several barrels. The size distribution could vary from one barrel to another.

To minimize this variability, the waste rock of all barrels was first thoroughly mixed together. As shown in Figure 3-19, the combined material was then quartered, meaning it was divided into four equal portions. This procedure ensured that the final waste rock sample used in the experiments had a uniform and representative particle size distribution. Finally, a sieve analysis was performed on the prepared waste rock to determine its PSD.

Figure 3-20 shows the PSD curves of the paste backfill and waste rock, used in the large scale-tests. The maximum particle size of the waste rock is 50 mm. Unlike the small-scale tests, the fine fraction of the waste rock was retained in the large-scale tests to better represent the gradation of field underground-generated waste rock. This choice was important because removing fine particles can modify the PSD and the mechanical property of the waste rock. These factors may influence the spreading of waste rock on the paste backfill surface, the penetration depth of particles, and the mixing pattern between waste rock and paste backfill. Therefore, retaining the fine particles in the large-scale tests rendered the laboratory testing conditions closer to the field ones. Compared to the paste backfill used in the small-scale tests, the paste backfill made from the mixture of non-sulfate and sulfate tailings used in the large-scale tests has the same maximum particle size, but contains a much higher proportion of fine particles.

Figure 3-19 Waste rock of underground mine A used for the large-scale tests

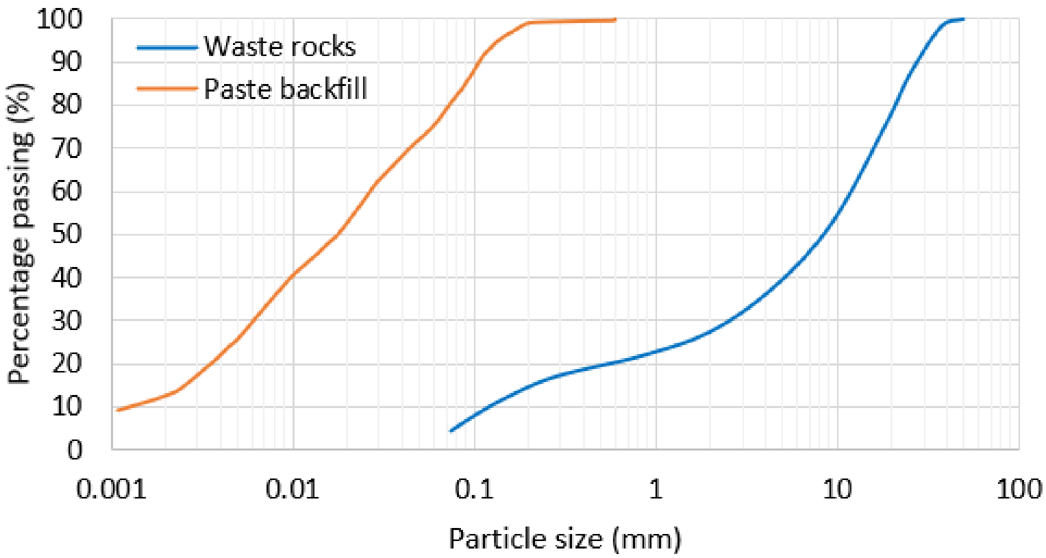

Figure 3-20 PDS curves of waste rocks and paste backfill used for large scale tests

3.4.2 Test setup

Figure 3-21 illustrates the large-scale experimental setup. Figure 3-21(a) shows a schematic representation of the system, and Figure 3-21(b) presents a photograph of the physical model. A rectangular mold with internal dimensions of 80 cm × 50 cm × 100 cm (length × width × height) was used to simulate a stope at a larger scale. The mold was constructed from reinforced wooden panels to ensure structural stability. A drainage system consisting of several small holes installed at the bottom of the mold and covered with a geotextile filter layer was incorporated to allow excess water from the paste backfill to drain during the tests, facilitating the drying process. A bucket with a base diameter of 24 cm and a height of 30 cm was positioned above the mold to allow controlled deposition of waste rock. The bucket was supported by two vertical rigid supports fixed to the mold frame. This large-scale configuration allowed assessment of the scalability of the experimental observations obtained from small-scale tests.

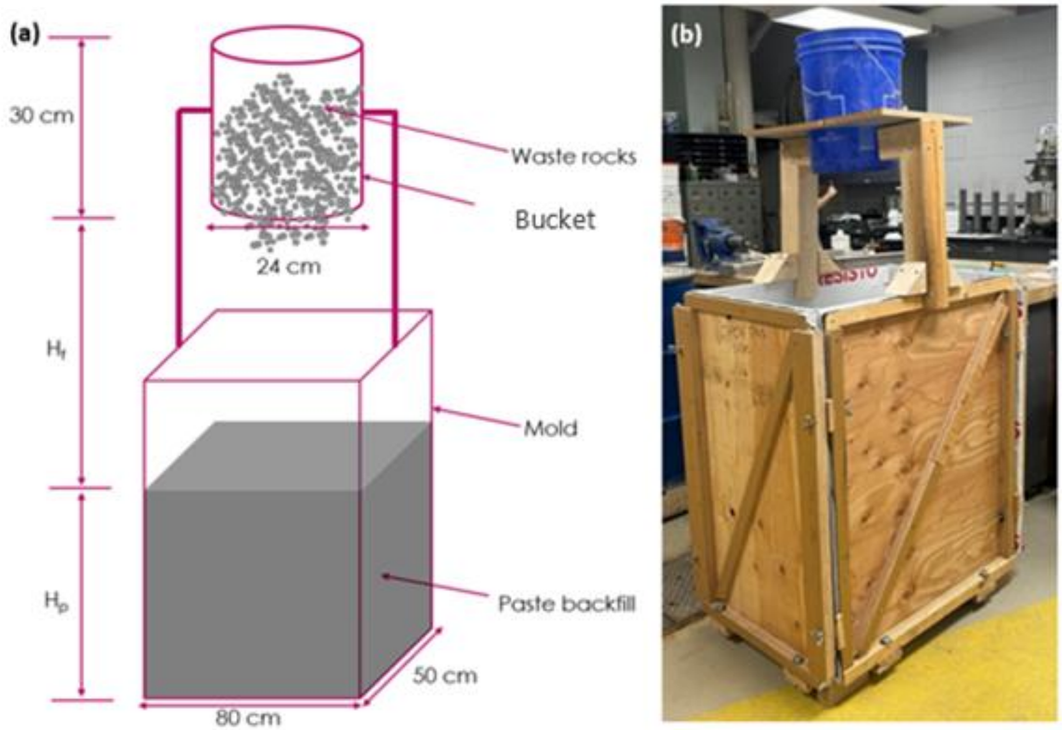

Figure 3-21 : A large-scale physical model used to study the natural mixing of waste rocks poured into paste backfill: (a) schematic presentation; (b) photograph.

3.4.3 Test procedure

The same test procedure used for small-scale tests was adopted for the large-scale tests. The only difference relies on the curing time before exposed the paste backfill – waste rock mass: Longer period was necessary before the mixture becoming hard enough to be exposed. Table 3-3 presents the large-scale tests with the waste rock having a d_{max} value of 50 mm.

Table 3-3 Large-scale tests with the waste rock having a d_{max} value of 50 mm

Test	H_f (cm)	H_p (cm)	C_w (%)
1	100	30	72
2	80	40	66
3	100	35	70

3.4.4 Test results

Figure 3-22 presents the internal texture structure of the samples cut through the center after thirty days, once the samples had become hard and dry. For Test 1 (see Table 3-3), the waste rock penetrated into the paste backfill in a V-shaped pattern, reaching the bottom of the mold but not extending to the side-walls. For Test 2 (see Table 3-3), the waste rock penetrated more extensively, reaching the bottom of the mold and partially contacting the side-walls.

Figure 3-22 Photographs of inner textures of large-scale test samples: Left, Test 1; Right, Test 2

Figure 3-23 shows a comparison between the measured values and those predicted by applying the proposed solution (Equation 3.2 with a =1345996.74, b= -30.4, c= 0.0098, d =41.88, e = -4.97, f= 137.22, and g= 668.15). The strong agreement with a R^2 value of 0.985 indicates once again that the proposed solution can be used to estimate the maximum allowable waste rock mass to avoid poor mixture between paste backfill and dumped waste rock in underground mine stopes.

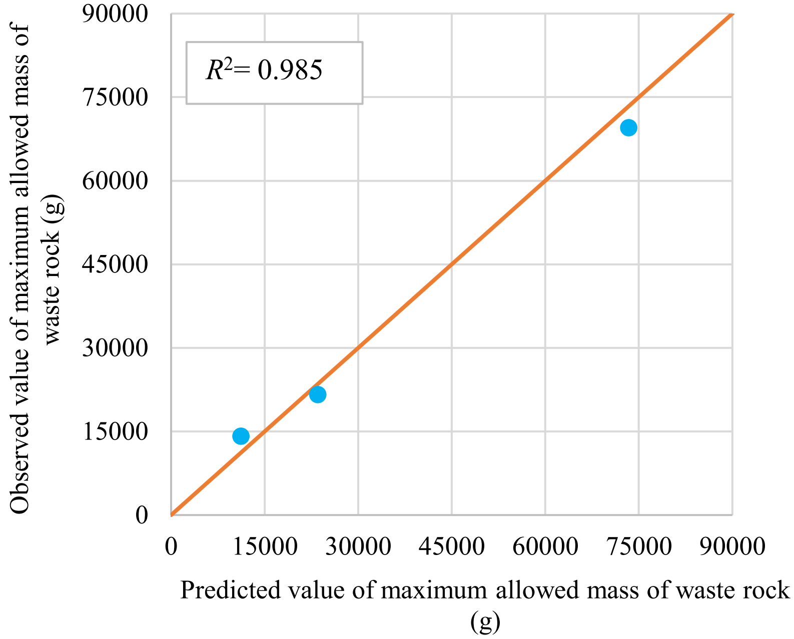

Figure 3-23 Comparison between predicted and measured values of maximum allowable waste rock mass in large-scale tests

3.5 Discussions

In this study, the natural mixing behavior between dumped waste rock and paste backfill was investigated through a series of laboratory experiments. The results showed that the maximum allowable waste rock mass is influenced by the solids content and thickness of the paste backfill as well as the maximum particle size and falling height of waste rock, but non-sensitive to the variation of horizontal cross section of stope. Based on these key pa-rameters, an empirical solution was proposed with several empirical coefficients was pro-posed to estimate the maximum allowable waste rock mass that can naturally mix with paste backfill. The validity and predictability of the proposed solution were verified with additional experimental results obtained from new and independent small-scale and large-scale tests, indicating that the proposed solution can be used to estimate the maximum allowable waste rock mass to be dumped in stope being filled with paste backfill without significant poor mixture between the two materials. Despite these promising results, several limitations in-volved in this study should be highlighted.

For instance, the test results showed that the receiving area of waste rock particles on the surface of the paste backfill can significantly influence the maximum allowable waste rock mass. This effect was observed in Case 4, which investigated the influence of falling height of dumped waste rock on the maximum allowable waste rock mass. With increasing falling height above 100 cm, the receiving area of waste rock particles on the paste backfill surface increased, which consequently led to sharply increase in the maximum allowable waste rock mass. At a falling height of 15 cm, the waste rock particles fell within a small and concentrated area near the center of the mold. In contrast, at a falling height of 150 cm, the particles spread more randomly and over a much larger area, allowing more waste rock particles to penetrate into the paste backfill through a larger cross-sectional region (Figure 3-24).

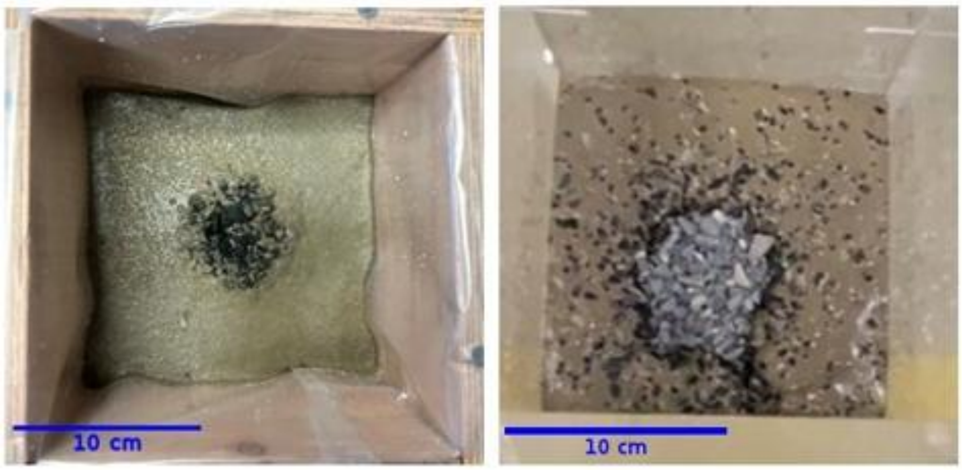

Figure 3-24 Top view of samples with falling heights of 15 cm (left) and 150 cm (right), respectively; details given in Table 3-1 for 3; the difference in color between the two samples is due to difference in photograph time. The right one was taken immediately at the end of the dumping operation, while the left one was made 4 days after the dumping operation.

The effect of receiving area parameter has been implicitly accounted for in the proposed solution (Equation 3.2 with a =1345996.74, b= -30.4, c= 0.0098, d =41.88, e = -4.97, f= 137.22, and g= 668.15) as long as the dumping of waste rock is conducted at one point. When spreading equipment (e.g., slinger truck) is used to increase the receiving area, the maximum allowable waste rock mass can be expected to significantly increase.

In this study, the experimental procedure was simplified to represent a controlled single-point dumping condition. The paste backfill was first placed in the mold, and the waste rock was then dumped incrementally at one location on the paste backfill surface. However, field backfilling operations can be more complex. In underground stopes, paste backfill and waste rock may be placed in several stages, and part of the unmixed waste rock remaining on the paste surface after one dumping stage may later be covered by a new layer of paste backfill. In addition, waste rock may be dumped from several locations or spread over the paste backfill surface using equipment such as a slinger. These placement conditions can increase the receiving area and may allow a larger amount of waste rock to penetrate and mix with the paste backfill. In general, the maximum allowable waste rock mass increases almost linearly with receiving area (Kazemi 2026). Nevertheless, further work is still required to fully evaluate multi-stage dumping, multi-point placement, and equipment-assisted spreading to incorporate these effects into the proposed empirical solution.

The results also showed that mold width did not directly affect the maximum allowable waste rock mass under the tested conditions. In these tests, the selected solids content, falling height, paste backfill thickness, and waste rock particle size produced a relatively limited penetration zone, and the waste rock particles did not reach the mold side walls. Therefore, the direct influence of the side walls on the mixing behavior remained limited. However, the mold width may still have an indirect effect through its interaction with other parameters. For example, lower solids content, greater falling height, larger paste backfill thickness, or larger waste rock particles can increase the penetration depth and lateral spreading of waste rock. Under such conditions, the waste rock may reach the side walls, and the mold boundaries may then influence the final mixing pattern. Therefore, mold width is not included as a direct parameter in the proposed empirical solution, but its possible effect should be taken into account by performing more tests under more various testing conditions.

Due to the above mentionned limitations, the proposed solution should not be used to evaluate the maximum allowable waste rock mass in terms of ratio between in place paste backfill and dumped waste rock because a large portion of paste backfill may not participate in the mixing activity, especially when the horizontal cross section is large. As such, using the total volume of the in place paste backfill may result in an over estimation of the maximum allowable waste rock mass, leading a non-conservative design.

The large-scale validation tests were designed to examine whether the proposed empirical solution could still provide reasonable predictions under conditions different from the small-scale tests and closer to field conditions. Therefore, the large-scale validation tested were conducted with larger paste backfill thickness, larger maximum particle size of waste rock, and wider PSD curve. . The paste backfill was prepared from a mixture of non-sulfate and sulfate tailings, which contained a higher proportion of fine particles than the tailings used in the small-scale tests. The waste rock was obtained from a different mine. Nevertheless, additional validation tests using tailings and waste rock from different mines are still recommended to further assess the general applicability of the proposed solution under more varying conditions.

In this study, uncemented paste backfill was used to facilitate sample cutting after drying and to allow visual observation of the internal distribution of waste rock particles within the paste backfill. However, in underground mining operations, cemented paste backfill is commonly used, particularly in primary stopes. The presence of binder can affect the rheological and mechanical properties of paste backfill, including yield stress, stiffness, bonding behavior, and early-age strength development, which may influence waste rock penetration and mixing behavior. Nevertheless, before significant cementation and strength development occur, the proposed empirical solution may still provide a preliminary estimate of the maximum allowable waste rock mass for early-aged cemented paste backfill. However, further experimental work using cemented paste backfill is required to evaluate the influences of binder content, curing time, and paste rheology on the mixing behavior and maximum allowable waste rock mass, as well as to validate, calibrate, or improve the proposed solution.

Although the large-scale tests extended the experimental conditions, the dimensions of the experimental setup were still much smaller than those of underground mine stopes, which are typically several and tens of meters in both vertical and horizontal directions. Therefore, further larger-scale or field tests are required to evaluate the applicability of the proposed solution under field mining conditions.

Another limitation of this study is related to the non consideration of the quality of mixing between dumped waste rock and paste backfill. The spatial distribution and homogeneity of the mixture were not systematically analyzed. Future study is necessary and ongoing to quantify the mixing quality of dumped waste in paste backfill.

3.6 Conclusions

In this study, the natural mixing between dumped waste rock and paste backfill was evaluated through small- and large- scale tests. An empirical solution was proposed to estimate the maximum allowable waste rock mass that can mix with paste backfill without causing significant poor mixture between the two materials. The results show that increasing the solids content of paste backfill reduces the maximum allowable waste rock mass, while increasing the paste backfill thickness leads to an increase in the maximum allowable waste rock mass. However, the mold dimensions did not show significant effect on the maximum allowable waste rock mass. The results also show that the maximum allowable waste rock mass can be increased through increasing the falling height of waste rock or through increasing the maximum particle size of waste rock.

The experimental data were used to obtained the empirical coefficients of the proposed solution. The applicability and predictability of the proposed solution along with the calibrated coefficients were successfully validated with new and independent small-scale and large-scale test results. The proposed solution can thus be used to estimate the maximum allowable mass of waste rock to avoid significant poor mixture between dumped waste rock and paste backfill. Further studies are necessary to take into account receiving area and to test its validity in field conditions.

Acknowledgements

The authors acknowledge the financial support from the Natural Sciences and Engineering Research Council of Canada (RGPIN-2024-06859 and ALLRP 580767-22), and industrial partners of the Research Institute on Mines and the Environment (RIME UQAT–Polytechnique; http://rime-irme.ca). The anonymous reviewers are also gratefully acknowledged for their constructive comments and suggestions, which are very helpful for improving the quality and coherences of the manuscript.

Appendix A: Quality control and improved procedure

Figure 3-25 illustrates the initial small-scale physical model used to study the natural mixing of waste rock poured into paste backfill. Figure 3-25(a) shows a schematic representation of the experimental setup, while Figure 3-25(b) presents a photograph of the laboratory model.

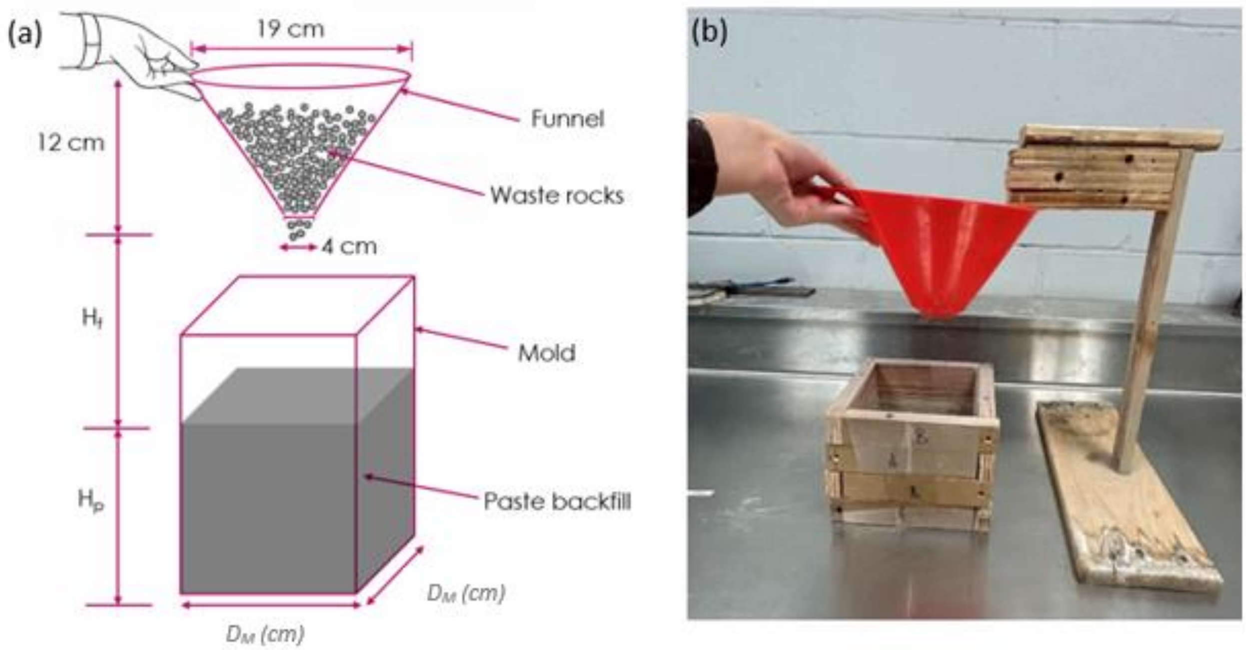

Figure 3-25 A small-scale physical model used to study the natural mixing of waste rocks poured into paste backfill: (a) schematic presentation; (b) photograph

A series of preliminary experiments were conducted with this physical model to investigate the influence of the solids content of paste backfill on the maximum allowable waste rock mass. Figure 3-26 show the variation of the maximum allowable waste rock mass as a function of solids content of paste backfill. The results did not show a consistent trend. As the solids content increased, the maximum allowable waste rock mass first increased and then sharply decreased with a small additional increase in solids content. Such behavior was not physically reasonable and indicated possible experimental uncertainties.

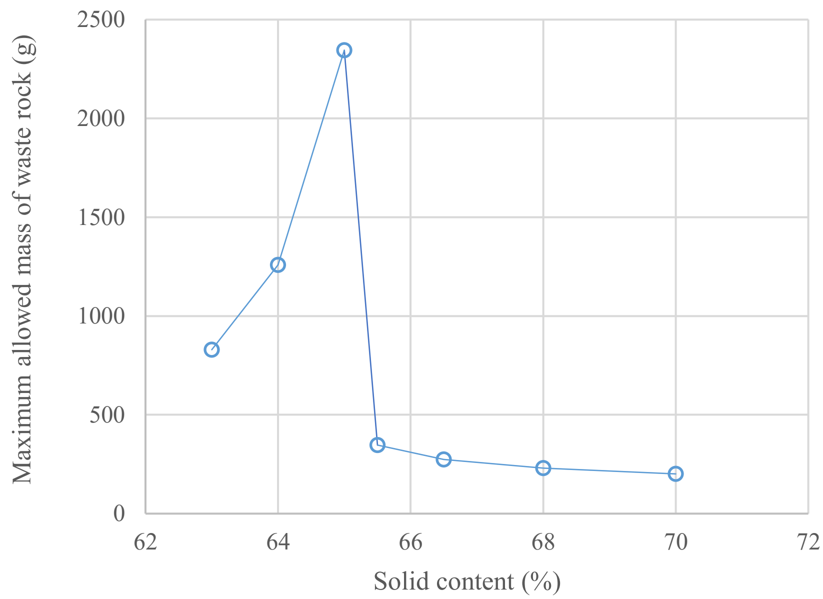

Figure 3-26 Relationship between paste backfill solids content and maximum allowable waste rock mass observed in the preliminary tests

This irregular behavior was attributed to limitations in the initial experimental setup. At the beginning of the study, the funnel used to pour the waste rock was not fixed on the stand and was held manually during the tests (Figure 3-25). As a result, small movements of the hand could occur, leading to changes in the falling height of the waste rock or pouring position. These variations affected the test conditions and led to unreliable results.

To reduce this source of error, the experimental setup was improved by rigidly fixing the funnel on the stand. This modification ensured that the funnel position remained stable throughout each test and that the falling height of the waste rock was kept constant. The improved experimental configuration is shown in Figure 3-27, including a schematic representation of the setup (Figure 3-27a) and a photograph of the physical model used in the laboratory (Figure 3-27b). After this improvement, the experiments were repeated under controlled conditions.

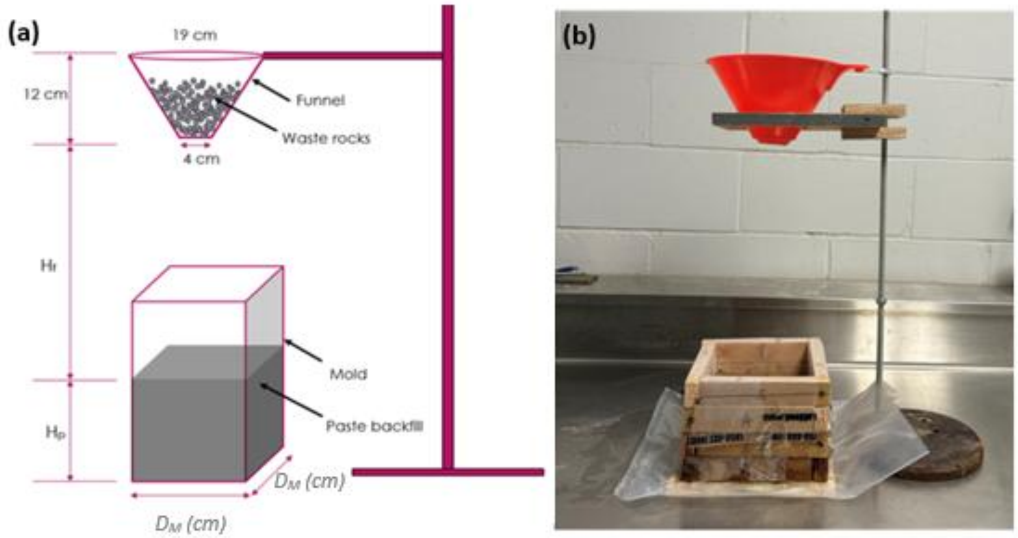

Figure 3-27 Improved experimental setup with the funnel fixed to the stand: (a) schematic view, (b) laboratory photograph

Following this improvement, the results showed a clearer trend in which an increase in solids content led to a decrease in the maximum allowable waste rock mass. However, the reproducibility of the results was still limited, as repeated tests performed under the same conditions produced different values (Figure 3-38). This behavior revealed that this poor reproducibility was mainly caused by inconsistencies in the pouring location. In some tests, the waste rock was not poured exactly at the center of the mold, which resulted in non-uniform distribution within the paste backfill (Figure 3-29).

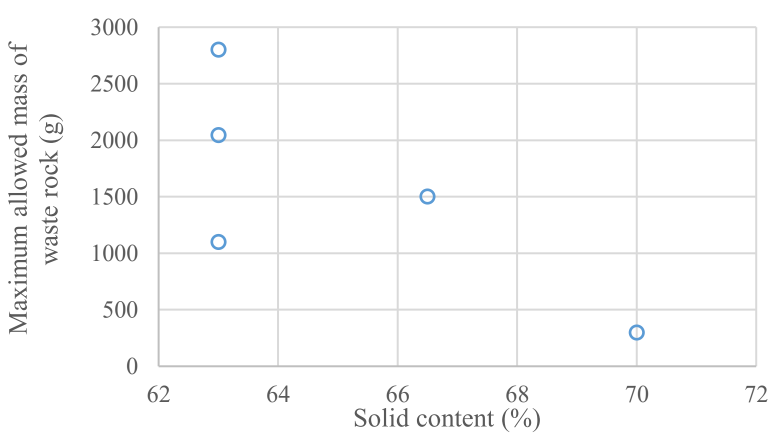

Figure 3-28 Relationship between paste backfill solids content and maximum allowable waste rock mass after the first improvement of the test setup: variation of maximum allowable waste rock mass measured under the same solids contents

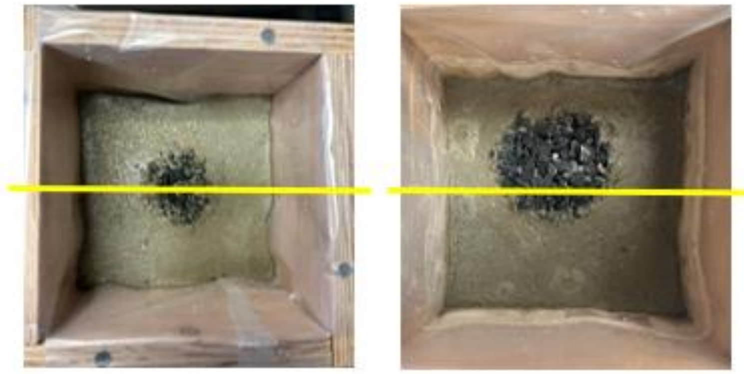

Figure 3-29 Top-view images showing centered and off-centered waste rock pouring

To address this issue, a second improvement was introduced. The exact center of the mold was clearly marked, and the funnel was carefully aligned with this point before each test. This ensured that the waste rock was consistently poured at the center of the mold in all experiments (see Figure 3-3b). By controlling both the falling height and the pouring location, the experimental conditions were further stabilized, allowing a more reliable evaluation of the effect of solids content on the maximum allowed waste rock mass.

It should be mentioned that all the test results reported in this study were obtained using the improved procedure.

Appendix B: Verification of experimental repeatability

Figure 3-30 shows the initial test results with a jump in the maximum allowable waste rock mass at a paste backfill thickness. This is not expected because the paste backfill with a solids content of 70% does no behave as a highly fluid material.

To verify the reliability of these observations and eliminate possible experimental errors, all data points in the paste backfill thickness series were repeated two more times under the same controlled conditions. All the experimental results are successfully reproduced, as shown in Fig. 3-8, except the test results at the paste backfill thickness of 13 cm.

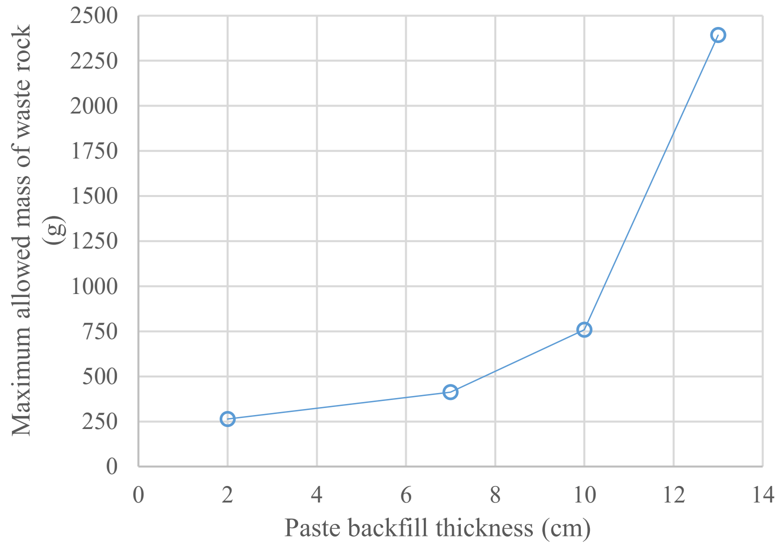

Figure 3-30 Relationship between paste backfill thickness and maximum allowable waste rock mass ob-served during preliminary tests; details given in Table 3-1 for Case 2

To ensure the repeatability and reliability of the experimental results, a total of 14 repetition tests were conducted by arbitrarily choosing testing points, as shown in Figures 3-6, 3-8, 3-10, and 3-12.

CHAPTER 4 EFFECT OF RECEIVING AREA ON THE MAXIMUM ALLOWABLE WASTE ROCK MASS

4.1 Introduction

Based on the observations from the falling height experiments presented in Chapter 3, it was found that an additional parameter influences the maximum allowable waste rock mass, namely the receiving area. The receiving area is defined as the surface area over which the waste rock initially lands on the paste backfill.

In the previous experiments, this parameter was not explicitly controlled. However, it was observed that changes in falling height could indirectly affect the spreading of waste rock particles on the paste surface, suggesting that receiving area may play an important role in the mixing process. Therefore, a dedicated experimental program was designed to investigate the effect of receiving area on the maximum allowable waste rock mass.

4.2 Materials

The same materials used in the small-scale experiments presented in Chapter 3 were adopted in this study.

The paste backfill was prepared using non-sulfidic tailings collected from an underground mine (Mine A) located in Québec, Canada. The tailings have a specific gravity of 2.77 and a dry density of approximately 1,550 $kg \cdot m^{-3}$ with a maximum particle size of about 0.6 mm and approximately 75% of particles finer than 80 μm. The waste rock was obtained from an open pit mine (Mine B) in Québec, Canada. The material was prepared using a double truncation procedure, in which particles larger than 4.75 mm and smaller than 1 mm were removed. The particle size distribution (PSD) of the tailings and waste rocks are presented in Figure 4-1.

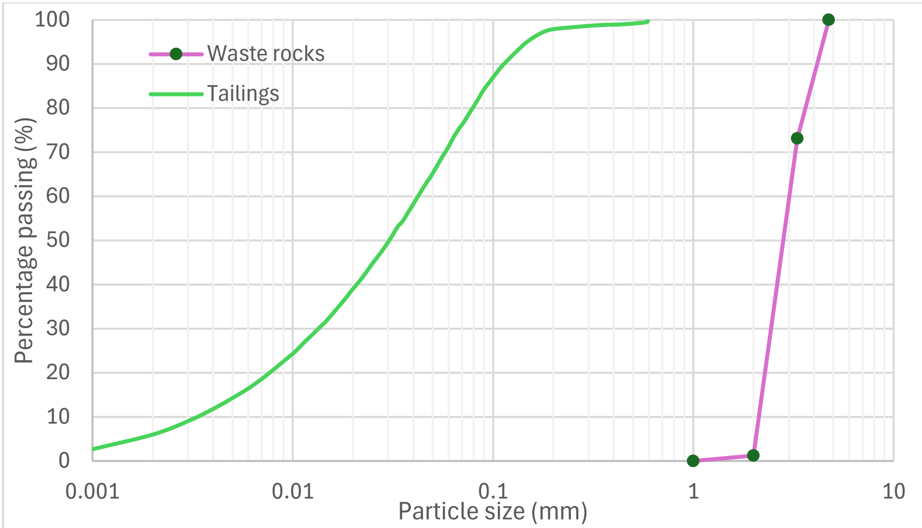

Figure 4-1 Particle size distribution of tailings and waste rocks

4.3 Experimental setup

A mold with internal dimensions of 30 cm × 15 cm × 20 cm (length × width × height) was used to represent a simplified mine stope at laboratory scale. An initial physical model was first designed to investigate the effect of receiving area by distributing waste rock over the paste backfill surface using a slinger system. Figure 4-2 illustrates this initial setup. Figure 4-2(a) presents a schematic representation of the system, while Figure 4-2(b) shows a photograph of the laboratory apparatus. In this configuration, waste rock particles were discharged from a funnel and transported through the slinger to spread over the paste backfill surface.

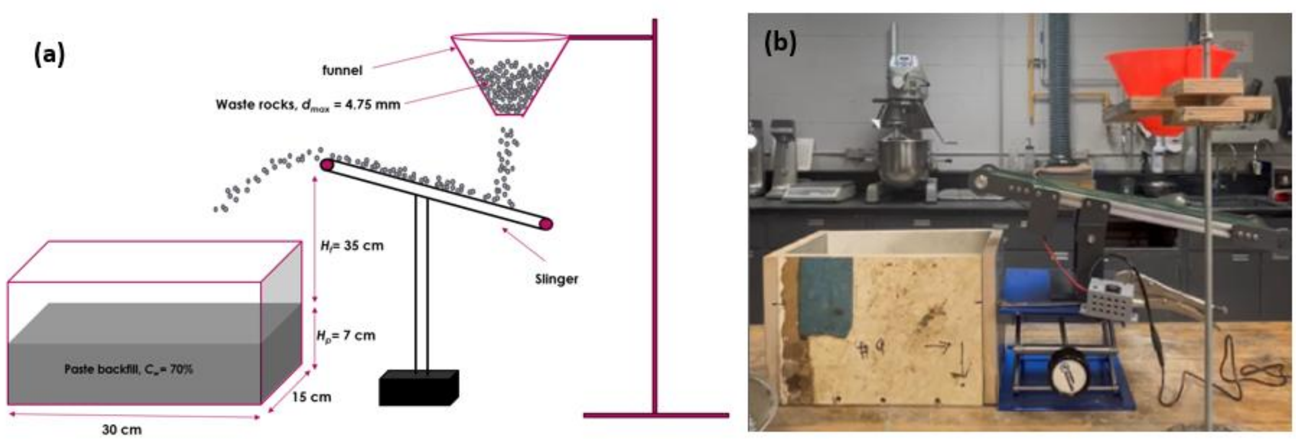

Figure 4-2 Slinger system used for study the influence the receiving area on the natural mixing of waste rocks poured into paste backfill: (a) schematic presentation; (b) photograph

However, this setup and testing procedure were not adopted because the slinger system exhibited several limitations and did not provide stable control over particle distribution.

First, a significant portion of the waste rock particles was scattered outside the mold. Although the particles falling outside the mold were manually collected and subtracted from the total initial mass, some material loss was unavoidable (Figure 4-3). This made it difficult to accurately track the total mass of waste rock contributing to the test, thereby reducing measurement accuracy.

In addition, frequent mechanical issues were encountered with the slinger system. Waste rock particles often became trapped within the conveyor mechanism, causing interruptions and, in some cases, complete stoppage of the system during the tests. As a result, a stable and uniform particle distribution could not be achieved. Therefore, an alternative approach was adopted. Figure 4-4 shows the final experimental setup used in this study.

These limitations explain why the slinger setup was not retained for the main experimental program and why a manual and more controlled placement method was adopted. However, the observations are still relevant from an operational point of view because similar issues may occur in underground conditions when waste rock is placed mechanically. Particle blockage, non-uniform distribution, equipment interruptions, and intermittent waste rock supply may affect the actual placement of waste rock in paste backfill. Therefore, although the slinger system was abandoned in this study to improve experimental control, these operational factors should be considered in future field-scale investigations.

Figure 4-3 Distribution of waste rock into the mold using the slinger system

A rigid stand was installed above the mold and fixed at a height that ensured a constant falling height of 35 cm throughout all tests. A funnel was attached to a movable handle mounted on the stand, allowing controlled horizontal movement of the funnel while ensuring that the falling height remained unchanged during the tests.

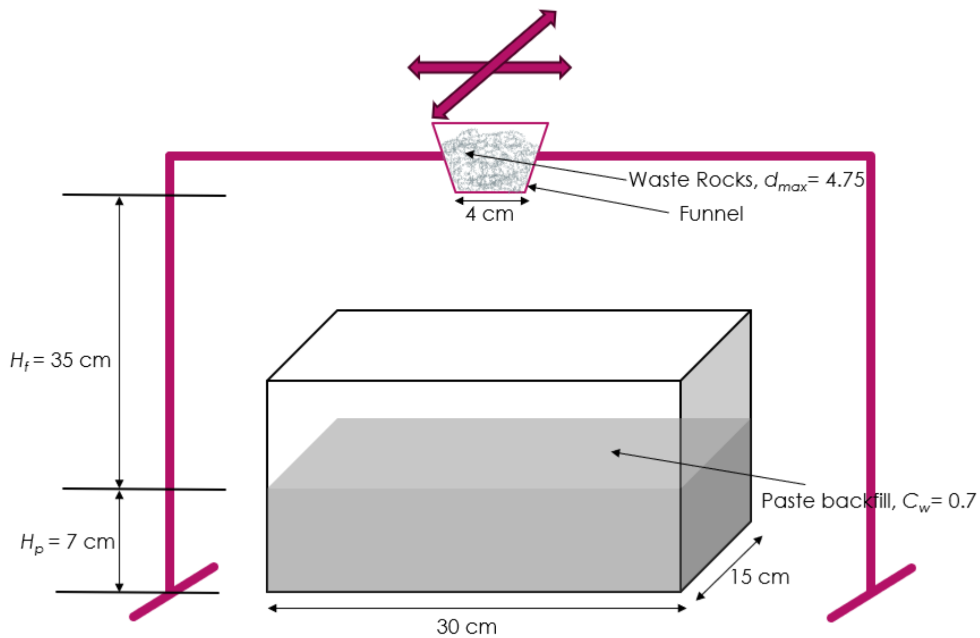

Figure 4-4 schematic view of an alternative experimental setup used for study the influence the re-ceiving area on the natural mixing of waste rocks poured into paste backfill

To control the receiving area of waste rock particles on the surface of the paste backfill, vertical cardboard partitions were inserted inside the mold to divide the mold surface into several sections. They were positioned above the paste backfill surface and did not penetrate into the paste backfill. Therefore, they did not restrict the natural mixing behavior of waste rock after deposition. This configuration allowed clearly identifying the target deposition area where the waste rock should be poured during each test. Figure 4-5 illustrates one example of the experimental configuration used to control the receiving area. Figure 4-5(a) presents a photograph of the mold with the cardboard partitions installed, while Figure 4-5(b) shows the corresponding schematic representation. The purple area in Figure 4-5(b) represents the target receiving area where the waste rock was deposited during the test.

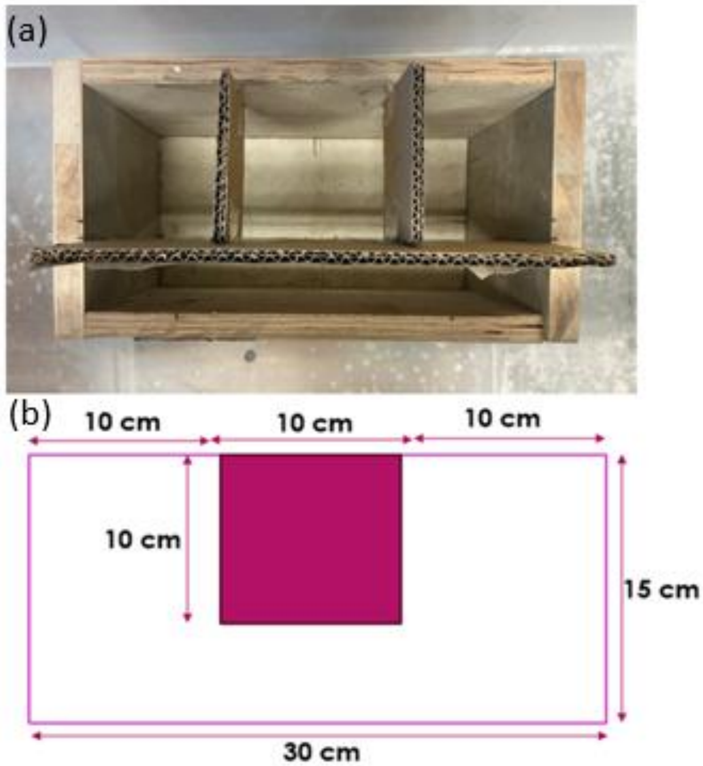

Figure 4-5 Experimental configuration used to control the receiving area of waste rock deposition: (a) photograph of the mold with vertical cardboard partitions used to divide the paste backfill surface; (b) schematic illustration of the mold surface

Figure 4-6 shows a few configurations to simulate the possible variation in receiving areas with a slinger, which can spread and control waste rock over the surface of paste backfill within a stope. The possible spreading patterns of waste rock on the paste backfill surface can thus depend on the position of conveyor and stope shape. In all configurations, the arrow indicates the location and discharge direction of the slinger.

- Model a: Represents a condition where waste rock is uniformly distributed over the entire surface. This occurs when the conveyor discharge is well positioned and the operating conditions allow sufficient lateral spreading.
- Model b: Represents a case where most of the surface is covered, but corner regions remain empty. This occurs because the lateral movement of the slinger is slightly limited, preventing waste rock from reaching the corner areas near the slinger.

- Model c: Represents a condition where waste rock is deposited mainly in a central strip. This occurs when the discharge energy is not sufficient to reach the far wall and not low enough to accumulate near the discharge side.
- Model d: Represents a condition where waste rock spreads in a triangular shape toward the far wall. This occurs when lateral spreading is more limited than in Model b, resulting in reduced side coverage.
- Model e: Represents a condition where waste rock accumulates near the discharge location. This occurs under low discharge velocity, resulting in limited spreading.
- Model f: Represents a condition where waste rock is deposited within a very small central area. This occurs when both discharge velocity and lateral spreading are limited.
- Model g: Represents a deposition pattern similar to Model e, with the difference that the conveyor is located along the shorter side of the stope. In this configuration, the conveyor speed is low, and as a result, waste rock particles are deposited mainly in the central region and near the wall closest to the conveyor.

4.4 Test procedure

Before conducting the experiments, the tailings were dried in an oven for 24 hours and then left to reach room temperature. This procedure was carried out to remove the initial moisture and to use the dry mass of tailings as the basis for solids content calculation. After drying, the tailings were weighed, and the required amount of water was added to prepare a backfill mixture with a target solids content of 70% by mass. The solids content was therefore controlled based on the measured dry mass of tailings and the added water mass.

A series of controlled laboratory experiments was conducted in which all parameters were kept constant and only the receiving area was varied. In all tests, the paste backfill had a fixed thickness of 7 cm, the falling height of the waste rock was maintained at 35 cm, and the maximum particle size of the waste rock was 4.75 mm.

After preparation, the paste backfill was placed in the mold. Waste rock was then poured through the funnel onto the selected target area defined by the cardboard partitions. By changing the position of the funnel and the partition arrangement, different receiving areas were created on the paste backfill surface.

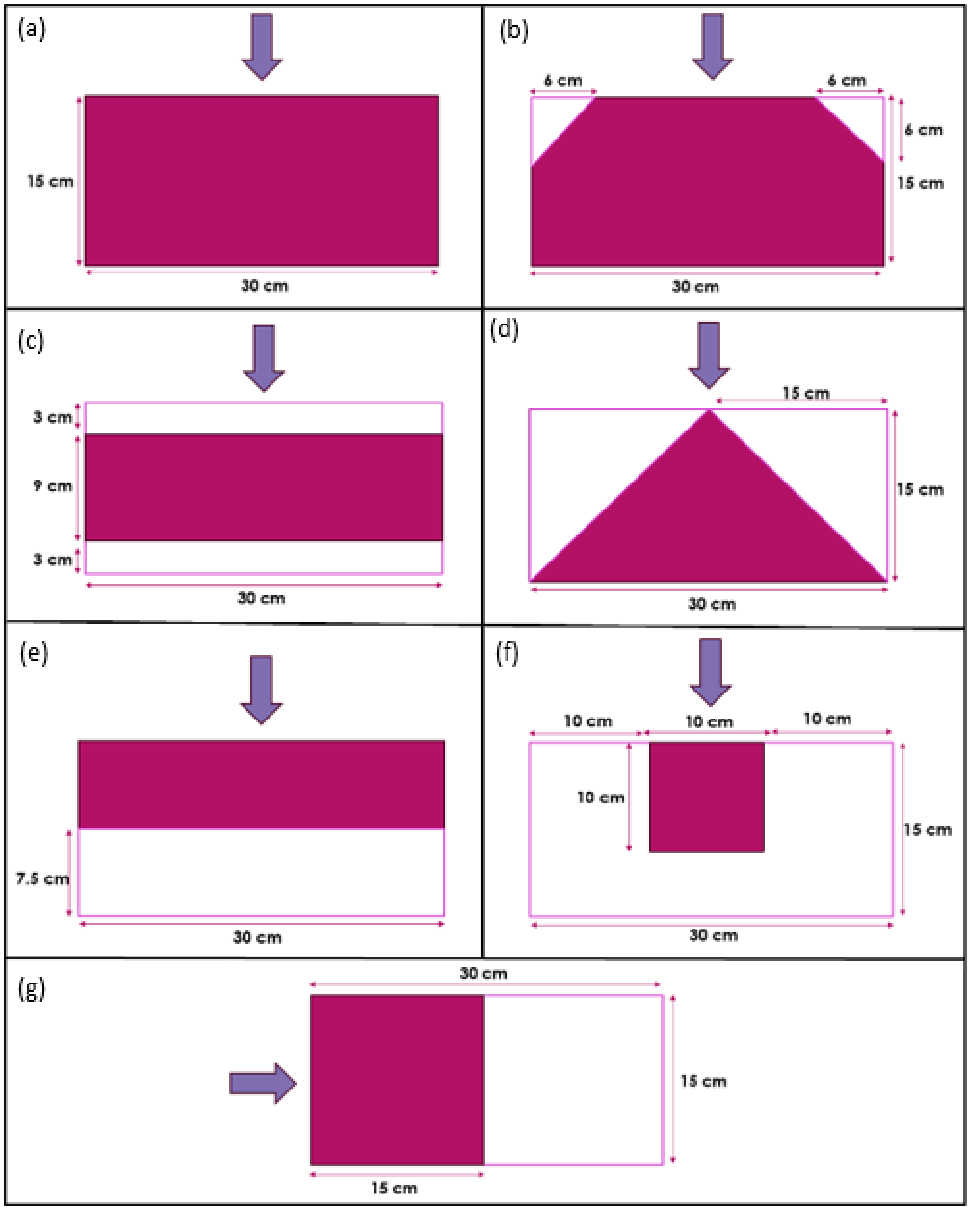

Figure 4-6 Different configurations used to have different receiving areas. The purple shaded area indicates the target receiving area where waste rock was poured

4.5 Results and observations

Figure 4-7 presents the internal structure of the samples corresponding to Models e and f of Figure 4-6 after one week of resting time. The samples were cut along the indicated blue line to examine the internal distribution of waste rock within the paste backfill.

For Model f, where waste rock was deposited within a small square receiving area, the particles penetrated vertically and reached the bottom of the mold, but showed very limited lateral spreading. The waste rock remained concentrated directly beneath the deposition zone. The maximum allowable waste rock mass for this configuration was 726.34 g.

For Model e, where waste rock was deposited over a larger, strip-shaped receiving area, the maximum allowable waste rock mass increased to 972.7 g. A similar penetration behavior was observed, with particles reaching the bottom of the mold within the deposition zone. However, no significant lateral spreading into adjacent regions was observed.

It is important to note that the cardboard partitions used to define the receiving areas were positioned above the paste backfill surface and did not penetrate into it. Therefore, they did not physically restrict the movement of waste rock particles after deposition. The absence of lateral spreading is thus attributed to the resistance of the paste backfill (Cw = 70%), rather than any physical constraint.

A similar behavior was previously observed in Chapter 3 (Figure 3-13), where waste rock was deposited at a single point during the investigation of mold size. In that case, the particles also penetrated vertically and reached the bottom of the mold while remaining confined beneath the initial deposition area, without significant lateral spreading.

Figure 4-8 shows the variation of the maximum allowable waste rock mass as a function of receiving area. The experimental results indicate a clear increasing trend, where the maximum allowable waste rock mass increases with increasing receiving area. This behavior is physically consistent. When the receiving area is larger, waste rock is distributed over a wider surface, reducing localized loading and allowing a greater amount of material to penetrate and mix with the paste backfill.

A comparison between Models d, e, and g shows that, although their deposition shapes are different, they have similar receiving areas (Figure 4-6). As a result, their maximum allowable waste rock masses are also similar, approximately 972.7 g, 923.91 g, and 942.8 g, respectively (Figure 4-8). This observation confirms that the receiving area plays a more dominant role than the exact shape of the deposition pattern.

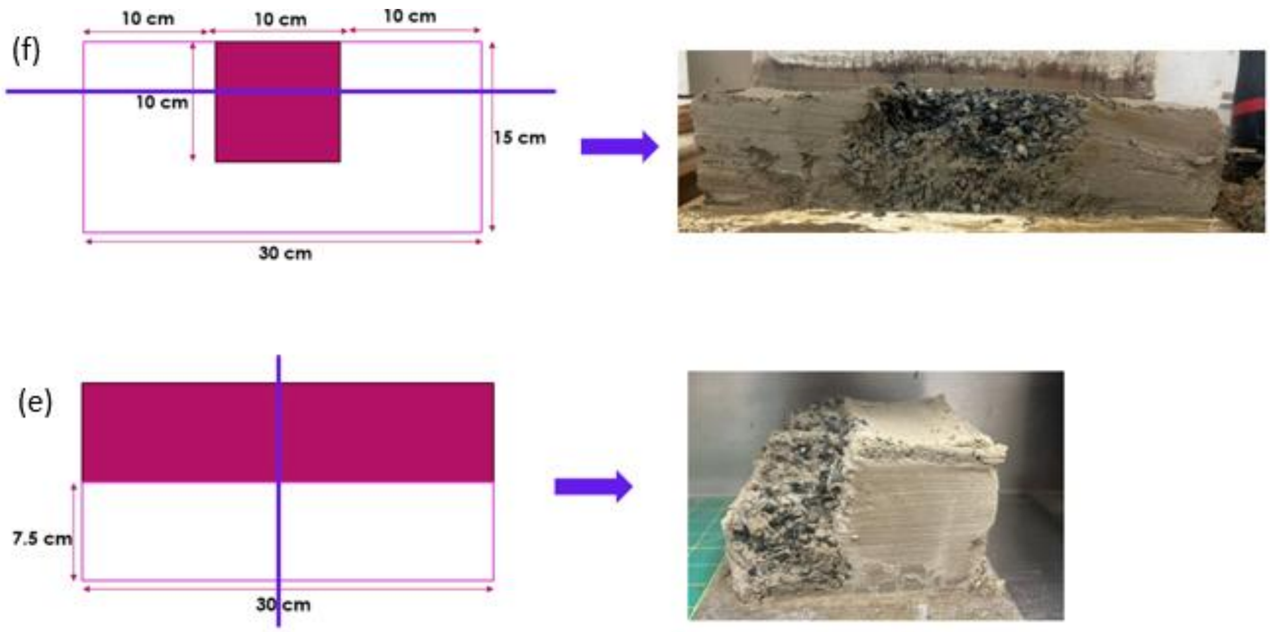

Figure 4-7 Internal texture structure of model f and model e

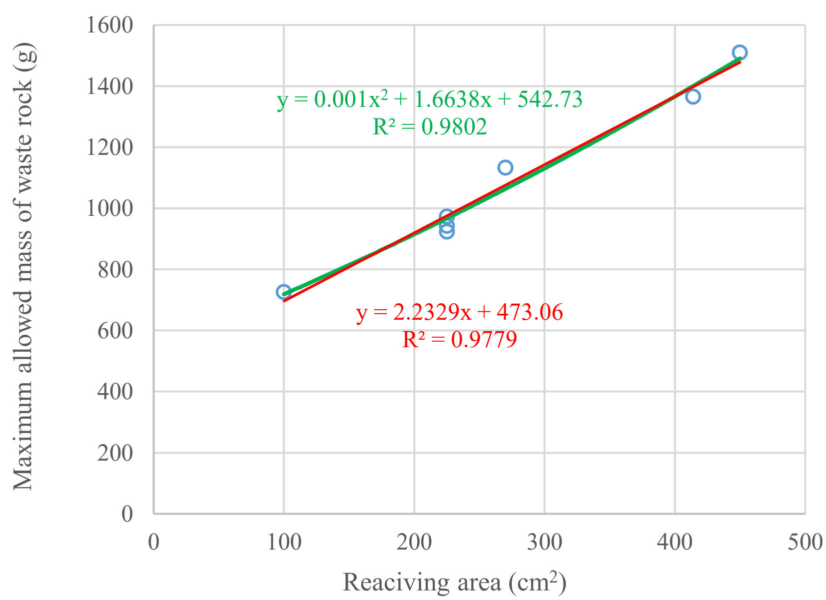

Figure 4-8 Variation in the maximum allowable waste rock mass as a function of receiving area

4.6 Conclusions and discussions

In this chapter, the effect of receiving area on the maximum allowable waste rock mass was investigated through a series of controlled laboratory experiments. This parameter was identified based on the observations from the falling height experiments presented in Chapter 3, where it was found that, in addition to the previously studied parameters, the surface area over which waste rock is initially deposited can influence the mixing behavior.

To isolate the effect of receiving area, a dedicated experimental setup was developed in which all parameters (C_w, H_f, H_p, and d_{max}) were kept constant, and only the receiving area was varied. Different deposition configurations were designed to represent possible spreading patterns of waste rock under various operational conditions.

The experimental results showed a clear increasing trend between receiving area and the maximum allowable waste rock mass. As the receiving area increases, waste rock is distributed over a wider surface, which allows a larger quantity of waste rock to penetrate and mix with the paste backfill. In addition, it was observed that configurations with different shapes but similar receiving areas resulted in comparable values of maximum allowable waste rock mass, indicating that the total receiving area plays a more dominant role than the specific shape of the deposition pattern.

Overall, this chapter demonstrates that receiving area is an important parameter controlling the natural mixing behavior between waste rock and paste backfill. However, since this parameter was not measured in the earlier experimental program, it was not included in the empirical equation developed in Chapter 3. Therefore, further work is required to explicitly incorporate receiving area into the predictive model and to evaluate its effect under field-scale conditions.

In addition, further investigations are required using materials from different mines, as well as a wider range of solids contents, paste backfill thicknesses, waste rock particle sizes, and falling heights, in order to improve the general applicability of the proposed model.

Furthermore, future studies should investigate the influence of operational parameters related to the slinger system. In particular, the effect of conveyor velocity on waste rock distribution should be examined, as higher velocities may increase particle spreading and enlarge the receiving area. The influence of the slinger angle relative to the horizontal should also be studied, as it can affect the trajectory, impact energy, and landing distribution of waste rock particles. In addition, the distance between the slinger and the stope and its position within the stope, whether located on the smaller or larger side, should be evaluated.

CHAPTER 5 GENERAL DISCUSSION

The main objective of this thesis was to develop a practical and quantitative solution to estimate the maximum allowable waste rock mass that can be dumped into paste backfill without causing significant poor mixture. To achieve this objective, a comprehensive experimental program was conducted. The test results showed that the maximum allowable waste rock mass is mainly controlled by the solids content and thickness of paste backfill as well as the maximum particle size and falling height of waste rock. Based on preliminary experimental results of small-scale tests on available materials, an empirical solution was proposed along with empirical coefficients obtained by best-fitting technique. The validity and predictive capability were confirmed by addition experimental results obtained by new and independent small- and large-scale tests. The proposed solution can thus be considered as a useful tool to guide waste rock dumping operation to avoid significant poor mixture between dumped waste rock and in-place paste backfill.

It is interesting to note that the proposed empirical solution may also be relevant to the design of paste backfill as a working platform. This function is mainly considered from a bearing-capacity perspective, focusing on the ability of paste backfill to support mining equipment and personnel without excessive surface penetration (Hassani & Archibald 1998; Belem & Benzaazoua 2008). The proposed empirical solution can be used to estimate the minimum required mass of waste rock used to pave a pathway onto paste backfill. Further studies are required to evaluate the validity and applicability under field loading conditions, including equipment loads.

Although this study did not directly investigate the strength or stability of the mixed material, the results suggest that controlled mixing between waste rock and paste backfill may potentially improve the mechanical properties of the backfill mass.

However, one needs to keep in mind that the proposed solution is empirical and contains several limitations.

First of all, it is important to notice that the proposed empirical solution was established under specific conditions. With one position dumping, the maximum allowable waste rock mass was shown to be insensitive to stope width and length, which are absent in the proposed solution. This is because only a portion of the paste backfill below the dumped waste rock participates in the mixing process, especially when the horizontal dimensions are large. Therefore, the proposed solution should not be generalized to estimate the ratio between the total volume of paste backfill and maximum allowable waste rock mass. Using the total paste backfill volume may lead to overestimation of maximum allowable waste rock mass and non-conservative design.

Although the empirical solution was validated with large-scale test results, the dimensions of the experimental setups remain much smaller than actual underground stopes. In real mining conditions, stopes can have dimensions of tens of meters. Large uncertainty can be expected when one makes use of a model established with laboratory setups of tens of centimeters to predict the maximum allowable waste rock mass by extrapolation to field stopes of tens of meters.

In this study, uncemented paste backfill was used in the experiments to facilitate the cutting of the samples after drying and allow visual observation of the internal distribution of waste rock particles within paste backfill. However, in underground mining operations, cemented paste backfill is commonly used, especially in primary stopes. The presence of binder can significantly affect the mechanical properties of the paste backfill, including stiffness, yield stress, and bonding behavior. Nevertheless, the proposed empirical solution may represent the early-age behavior of CPB before significant cementation and strength development occur. In this sense, the proposed empirical solution can still be applied for a rough estimation of the maximum allowed mass of waste rock. However, more work is necessary with cemented paste backfill to validate or calibrate the proposed solution.

This study mainly focused on determining the maximum allowable waste rock mass to avoid poor mixture. Although the internal structure of the samples was visually examined, the quality of mixing was not quantified using a defined parameter or index. In practice, the stability of the backfilled stope depends not only on how much waste rock is mixed, but also on how uniformly the materials are distributed. A non-uniform mixture may still lead to weak zones, even if the total amount of waste rock is within the allowable limit. Therefore, the absence of a quantitative mixing quality index represents an important limitation.

The experimental program was conducted using tailings and waste rock materials obtained from mines in Québec, Canada. Although these materials are representative of certain mining conditions, the properties of waste rock and tailings can vary significantly between different sites. Parameters such as particle shape, mineral composition, grain size distribution, and paste rheology may influence the mixing behavior. Therefore, the empirical coefficients obtained in this study may not be directly applicable to all mining conditions. To improve the general applicability of the proposed solution, additional tests should be conducted using a wider range of materials.

In this study, the tests were limited to the case where a uniform paste backfill is a priori placed in a stope, quickly followed by the dumping of waste rock. In practice, a stope is seldom fully filled instantaneously. Self-weight consolidation and cementation can take place during the pour of cemented paste backfill. Moreover, waste rock can also be placed in stope before pour of paste backfill. More work is necessary to study the mixing behavior between waste rock and paste backfill to take into account these conditions.

Direct dumping of waste rock into paste backfill can increase the underground use of waste rock and reduce the amount of waste rock transported to the surface. However, this also means that waste rock partially replaces paste backfill in the stope, resulting in a reduced amount of tailings used underground. Consequently, a larger volume of tailings may need to be stored on the surface in tailings storage facilities or tailings impoundments, which can increase storage requirements, construction costs, monitoring needs, and long-term management costs.

Another limitation associated with co-disposal of waste rock and paste backfill is related to placement of waste rock. Paste backfill can generally be pumped continuously through a pipeline system once the backfill plant and distribution system are established. In contrast, waste rock dumping is usually an intermittent operation that depends on underground equipment availability, access conditions, haulage logistics, and operator presence. Therefore, although the co-disposal of waste rock and paste backfill can reduce waste rock handling and paste backfill consumption underground, its implementation could also increase surface disposal of tailings and energy consumption and operation cost due to the discontinuous nature of waste rock placement compared to the continuous pipe transportation of paste backfill.

In practice, the dumping of waste rock in stope being filled with waste rock is seldom continuous. After each dumping, a new layer of paste backfill forms between the top of the dumped waste rock and the surface of the paste backfill at the moment of a new dumping of waste rock. In such case, the proposed empirical solution can still be applied to estimate the new maximum allowed mass of waste rock by updating the thickness of paste backfill and the failing height of waste rock. Nevertheless, the proposed solution cannot account for the timing of waste rock placement on the mixing behavior between waste rock and paste backfill. Placing waste rock at the beginning, at the end, or intermittently throughout the backfilling process may create different contact conditions between the two materials, leading to different penetration depths and mixing patterns. More experimental work, especially field work, is necessary to validate or calibrate the proposed solution.

Still for the case of staged dumping of waste rock when an excessive mass of waste rock is dumped onto the paste backfill, the unmixed waste rock above the surface of the paste backfill can be submerged by later paste backfill. The same phenomenon applies exactly to the case where waste rock is first placed in a stope, followed by the pour of paste backfill. More work is necessary to qualify and quantify the mixing behavior between the two materials, mostly due to the penetration and migration of paste backfill through the pores of waste rock.

In this study, solids content was used as the main parameter to describe the consistency of the tested mixtures. However, measuring yield stress through slump would provide a more complete characterization of the material for cemented and uncemented paste backfill at their early stage.

Finally, the proposed solution does not take into account the receiving area. The experimental results presented in Chapter 4 clearly show that the receiving area has a significant influence on the maximum allowable waste rock mass. A larger receiving area allows waste rock to be distributed over a wider surface and increasing the amount of material that can penetrate into the paste backfill. Using the proposed solution may largely underestimate the allowable waste rock mass when the receiving area is increased through the use of spreading equipment such as slinger. Receiving area needs to be taken into account in the proposed solution in future work.

CHAPTER 6 CONCLUSIONS AND RECOMMENDATIONS

6.1 Conclusion

The results of this study provide several important findings.

First, the maximum allowable waste rock mass is strongly controlled by the properties of the paste backfill. Increasing the solids content significantly reduces the allowable waste rock mass, as the paste backfill becomes more resistant to particle penetration. In contrast, increasing the thickness of the paste backfill increases the allowable waste rock mass by providing more space for particle penetration.

Second, the characteristics of waste rock also play an important role. Increasing the maximum particle size and falling height enhances the penetration of particles into the paste backfill due to higher kinetic energy, which leads to an increase in the allowable waste rock mass. However, the effect of particle size becomes limited beyond a certain threshold.

Third, the results show that the horizontal dimension of the stope has a limited influence on the maximum allowable waste rock mass in this study.

Fourth, this study identified the receiving area as an important parameter controlling the mixing behavior. Increasing the receiving area allows waste rock to be distributed over a wider surface, which increases the maximum allowable waste rock mass. It was also observed that the total receiving area is more influential than its shape.

Based on these findings, an empirical solution was developed to estimate the maximum allowable waste rock mass as a function of key parameters, including solids content, paste backfill thickness, falling height, and maximum particle size. The proposed solution was calibrated using experimental data and validated using independent small-scale and large-scale tests. The results showed a strong agreement between predicted and measured values, indicating that the proposed model can reasonably predict the allowable waste rock mass under different conditions.

From an engineering perspective, this study provides a practical tool that can assist mining engineers and dumping operator in controlling waste rock dumping operations in stopes filled with paste backfill. The proposed solution can help reduce the risk of poor mixture between dumped waste rock and in-place paste backfill.

6.2 Recommendation and future work

Based on the findings and limitations of this study, several recommendations and directions for future work are proposed to improve the understanding of natural mixing behavior and to extend the applicability of the proposed empirical solution.

First, it is recommended to explicitly incorporate the receiving area into the empirical model. The results of this study showed that receiving area plays an important role in controlling the maximum allowable waste rock mass. Future work should focus on developing a modified empirical equation that includes receiving area as an independent parameter.

Second, future studies should investigate the influence of operational parameters related to the slinger system. In particular, the effect of conveyor velocity on waste rock distribution should be examined, as higher velocities may increase the spreading of particles and consequently enlarge the receiving area, while lower velocities may result in more localized deposition. The influence of the slinger angle relative to the horizontal should also be studied, since upward or downward inclination can modify the trajectory, impact energy, and landing distribution of waste rock particles.

In addition, the position of the slinger within the stope, whether located on the smaller or larger side, should be evaluated, as it may affect the spatial distribution and coverage of waste rock over the paste backfill surface. The distance between the slinger and the stope is another important parameter, as it directly controls the falling height and particle dispersion, which in turn influence both the receiving area and the penetration behavior of waste rock.

A systematic investigation of these parameters would provide a better understanding of the relationship between operational conditions and mixing behavior, and would help improve the applicability of the proposed model under real mining conditions.

Third, further investigations at field scale are strongly recommended. Although the proposed solution was validated at laboratory and large scales, real underground stopes involve more complex conditions. Field tests or in-situ monitoring are necessary to evaluate the reliability of the proposed model under actual mining conditions.

Fourth, the effect of cemented paste backfill on the mixing behavior should be examined. In this study, uncemented paste backfill was used, while in practice cemented paste backfill is applied.

The presence of binder and/or chemical admixtures, such as superplasticizers, may affect the mechanical and rheological properties of the paste and consequently influence the mixing process.

Fifth, it is recommended to focus on developing a quantitative index to evaluate the quality of mixing between dumped waste rock and paste backfill, including the assessment of spatial distribution and mixture homogeneity.

Sixth, it is recommended to include cemented mixtures and UCS testing on core samples taken from different locations within the waste rock–paste backfill mass for each test condition. This would help evaluate how different factors, such as waste rock content, particle size, paste thickness, solids content, falling height, and mixing quality, influence the strength development.

Seventh, it is recommended to extend the study to a wider range of waste rock and tailings materials. Since material properties can vary significantly between mining sites, additional experiments using different materials would improve the general applicability of the proposed empirical solution.

Finally, future work should also investigate the case where waste rock is placed in the stope before paste backfill is poured. In this sequence, the paste must flow through and fill the voids between waste rock particles. Therefore, the maximum waste rock tonnage may depend on factors such as porosity and particle-size distribution of the waste rock, the flowability of the paste, the degree of void filling. This method may increase underground waste rock storage, but it may also lead to incomplete filling, segregation, or weak zones. Further tests are needed to evaluate this placement sequence.

REFERENCES

Abzalov, M. (2016). Applied mining geology (Vol. 12). *Modern approaches in solid earth sciences, Springer*.

Akcil, A., & Koldas, S. (2006). Acid mine drainage (AMD): causes, treatment and case studies. *Journal of cleaner production, 14*(12-13), 1139-1145.

Annor, A. (1999). A study of the characteristics and behaviour of composite backfill material. Ph.D thesis, McGill University, Montreal, QC, Canada.

Arteaga, F., Nehring, M., Knights, P., & Camus, J. (2014). Schemes of exploitation in open pit mining. Paper presented at the mine planning and equipment selection. Proceedings of the 22nd MPES conference, Dresden, Germany.

Aubertin, M. (2013). Waste rock disposal to improve the geotechnical and geochemical stability of piles. *23rd world mining congress*, Montréal, QC, Canada.

Aubertin, M., Bussière, B., & Bernier, L. (2002). Environnement et gestion des rejets miniers. *Presses internationales Polytechnique*.

Aubertin, M., Bussière, B., Bernier, L., Chapuis, R., Julien, M., Belem, T., Simon, R., Mbonimpa, M., Benzaazoua, M., Li, L. (2002). La gestion des rejets miniers dans un contexte de développement durable et de protection de l'environnement. *Congrès annuel de la Société canadienne de génie civil*, 5-8.

Azam, S., & Li, Q. (2010). Tailings dam failures: a review of the last one hundred years. *Geotechnical news, 28*(4), 50-54.

Baldwin, G., & Grice, A. (2000). Engineering the new Olympic Dam backfill system. *Proceedings massmin*, 705-711.

Béket Dalcé, J., Li, L., & Yang, P. (2019). Experimental study of uniaxial compressive strength (UCS) distribution of hydraulic backfill associated with segregation. *Minerals, 9*(3), 147.

Belem, T., & Benzaazoua, M. (2008). Design and application of underground mine paste backfill technology. *Geotechnical and geological engineering, 26*(2), 147-174.

Berger, K. C. (2017). Study of tailings management technologies (MEND Report 2.50. 1).

Bernd, G., & Bernd, G. (2007). Mine wastes, characterization, treatment and environmental impacts. *Springer*.

Blowes, D., Ptacek, C., Jambor, J., Weisener, C., Paktunc, D., Gould, W., & Johnson, D. (2003). The geochemistry of acid mine drainage. *Environmental geochemistry, 9*, 149-204.

Boakye, K. (2008). Large in situ direct shear tests on rock piles at the Questa Min, Taos county, New Mexico. M.Sc. thesis, New Mexico institute of mining and technology, Socorro, New Mexico.

Brady, B. H., & Brown, E. T. (2006). Rock mechanics: for underground mining. *Science & business media, Springer.*

Bussiere, B. (2007). Colloquium 2004: Hydrogeotechnical properties of hard rock tailings from metal mines and emerging geoenvironmental disposal approaches. *Canadian geotechnical journal, 44*(9), 1019-1052.

Cacciuttolo, C., & Marinovic, A. (2023). Experiences of underground mine backfilling using mine tailings developed in the Andean region of Peru: A green mining solution to reduce socio-environmental impacts. *Sustainability, 15*(17), 12912.

Darling, P. (2011). SME mining engineering handbook (Vol. 1). *Society for Mining, Metallurgy & Exploration (SME*.)

Deiminiat, A., & Li, L. (2022). Experimental study on the reliability of scaling down techniques used in direct shear tests to determine the shear strength of rockfill and waste rocks. *CivilEng, 3*(1), 35-50.

Fala, O., Aubertin, M., Molson, J., Bussière, B., Wilson, G. W., Chapuis, R., & Martin, V. (2003). Numerical modelling of unsaturated flow in uniform and heterogeneous waste rock piles. *Paper presented at the sixth international conference on acid rock drainage (ICARD),* Australasian institute of mining and metallurgy, Cairns, Australia, Publication Series.

Fala, O., Molson, J., Aubertin, M., & Bussière, B. (2005). Numerical modelling of flow and capillary barrier effects in unsaturated waste rock piles. *Mine water and the environment, 24*(4), 172-185.

Falaknaz, N., Aubertin, M., & Li, L. (2015). Numerical analyses of the stress state in two neighboring stopes excavated and backfilled in sequence. *International journal of geomechanics, 15*(6), 04015005.

Fall, M., Adrien, D., Célestin, J., Pokharel, M., & Touré, M. (2009). Saturated hydraulic conductivity of cemented paste backfill. *Minerals engineering,* 22(15), 1307-1317.

Fan, C., Li, L., Liu, G., Yang, X., Guo, L., & Tang, J. (2025). Analytical solution for estimating the minimum required strength of sill mat by considering failure due to rock wall closure. *Journal of rock mechanics and geotechnical engineering, 17*(2), 996-1007.

Fan, C., Li, L., Yang, X., Liu, G., Guo, L., & Tang, J. (2025). Analytical solution for determining wall closure associated with stope excavation underneath sill mat constructed by cemented backfill. *Journal of rock mechanics and geotechnical engineering, 17*(2), 983-995.

Gamache-Rochette, A. (2004). Une étude de caractérisation en laboratoire et sur le terrain des écoulements de l'eau dans les roches stériles. *Mémoire de maîtrise.* Département des génies civil, géologique et des mines. École Polytechnique de Montréal, Montreal, QC, Canada.

Grabinsky, M., Bawden, W., & Thompson, B. (2021). Required plug strength for continuously poured cemented paste backfill in longhole stopes. *Mining, 1*(1), 80-99.

Grice, A. G. (2001). Recent mine fill developments in Australia. *Paper presented at the proceedings of the 7th international symposium on mining with backfill*.

Grimalt, J. O., Ferrer, M., & Macpherson, E. (1999). The mine tailing accident in Aznalcollar. *Science of the Total Environment, 242*(1-3), 3-11.

Hamrin, H. (1980). Guide to underground mining: methods and applications. *Atlas copco*.

Hamrin, H., Hustrulid, W., & Bullock, R. (2001). Underground mining methods and applications. *Underground mining methods: engineering fundamentals and international case studies*, 3-14.

Hane, I., Belem, T., Benzaazoua, M., & Maqsoud, A. (2017). Laboratory characterization of cemented tailings paste containing crushed waste rocks for improved compressive strength development. *Geotechnical and Geological Engineering, 35*(2), 645-662.

Hartman, H. L., & Mutmansky, J. M. (2002). Introductory mining engineering. *John Wiley & Sons*.

Hawley, M., & Cunning, J. (2017). Guidelines for mine waste dump and stockpile design. *Csiro publishing*.

Hudson-Edwards, K. A., Jamieson, H. E., & Lottermoser, B. G. (2011). Mine wastes: past, present, future. *Elements, 7*(6), 375-380.

Hustrulid, W. A., & Bullock, R. L. (2001). Underground mining methods: Engineering fundamentals and international case studies. *SME*.

Investigation, M. P. I. E. E., & Panel, R. (2015). Report on Mount Polley tailings storage facility breach. Government of British Columbia.

Iqbal, A., Mashaan, N. S., & Paraskeva, T. (2025). Mining waste in asphalt pavements: A critical review of waste rock and tailings applications. *Journal of composites science, 9*(8), 402.

Jakubick, A. T., McKenna, G., & Robertson, A. M. (2003). Stabilisation of tailings deposits: International experience. *Paper presented at the mining and the environment conference*, Sudbury.

James, M., & Aubertin, M. (2012). The use of waste rock inclusions to improve the seismic stability of tailings impoundments. *GeoCongress 2012: State of the art and practice in geotechnical engineering* (pp. 4166-4175).

James, M., Aubertin, M., & Bussière, B. (2013). On the use of waste rock inclusions to improve the performance of tailings impoundments. *Paper presented at the proceedings of the 18th international conference on soil mechanics and geotechnical engineering*, Paris, France.

Johnson, D. B., & Hallberg, K. B. (2005). Acid mine drainage remediation options: a review. *Science of the total environment, 338*(1-2), 3-14.

Joughin, W. (2017). Dealing with uncertainty and risk in the design of deep and high stress mining excavations. Proceedings of the 8th international conference on deep and high stress mining, Australian centre for geomechanics, Perth, pp. 489-507.

Kazemi, P. (2026). *Empirical solution to estimate the maximum allowed mass of dumped waste rock to avoid significant poor mixture between dumped waste rock and paste backfill in stopes*. M.Sc. thesis, Ecole Polytechnique de Montéal, Montreal, QC, Canada.

Keita, A. M. T., Jahanbakhshzadeh, A., & Li, L. (2021). Numerical analysis of the stability of arched sill mats made of cemented backfill. *International journal of rock mechanics and mining sciences, 140*, 104667.

Kuganathan, K., & Sheppard, I. (2001). A non-segregating'rocky paste fill'(RPF) produced by co-disposal of cemented de-slimed tailings slurry and graded rockfill. *7th international symposium on mining with backfill, .*

Kumar, A., Das, S. K., Nainegali, L., Raviteja, K., & Reddy, K. R. (2023). Probabilistic slope stability analysis of coal mine waste rock dump. *Geotechnical and geological engineering, 41*(8), 4707-4724.

Landriault, D. (1995). Paste backfill mix design for Canadian underground hard rock mining. *Paper presented at the 97th annual general meeting of CIM, rock mechanics and strata control session,* Halifax, Nova Scotia.

Lèbre, É., Corder, G. D., & Golev, A. (2017). Sustainable practices in the management of mining waste: A focus on the mineral resource. *Minerals engineering, 107*, 34-42.

Lee, C., & Gillot, P. (2014). Case study–a high strength paste aggregate backfill at Randgold's Loulo mine in Mali. *Proceedings of the 11th international symposium on mining with backfill,* Perth, Australia.

Lee, C., & Gu, F. (2017). Co-disposal of waste rock with backfill. Proceedings of the first international conference on underground mining technology, Sudbury, Canada

Lee, C., & Pieterse, E. (2005). Commissioning and operation experience with a 400 tph paste backfill system at kidd creek mine. *Proceedings of the international seminar on paste and thickened tailings*, Australia,

Lewin, J., Davies, B., & Wolfenden, P. (1977). Interactions between channel change and historic mining sediments. *River channel changes*, 353-367.

Li, L. (2014a). Analytical solution for determining the required strength of a side-exposed mine backfill containing a plug. *Canadian geotechnical journal, 51*(5), 508-519.

Li, L. (2014b). Generalized solution for mining backfill design. *International journal of geomechanics, 14*(3), 04014006.

Li, L. (2024). Méthodes de minage en souterrain avec remblai, GML8301. Course lecture notes, École Polytechnique de Montréal, Montreal, QC, Canada.

Li, L., & Aubertin, M. (2011). Limit equilibrium analysis for the design of backfilled stope barricades made of waste rock. *Canadian geotechnical journal, 48*(11), 1713-1728.

Li, L., & Aubertin, M. (2012). A modified solution to assess the required strength of exposed backfill in mine stopes. *Canadian geotechnical journal, 49*(8), 994-1002.

Li, L., & Aubertin, M. (2014). An improved method to assess the required strength of cemented backfill in underground stopes with an open face. *International journal of mining science and technology, 24*(4), 549-558.

Li, L., Aubertin, M., & Belem, T. (2005). Formulation of a three dimensional analytical solution to evaluate stresses in backfilled vertical narrow openings. *Canadian geotechnical journal, 42*(6), 1705-1717.

Li, L., Aubertin, M., Simon, R., Bussière, B., & Belem, T. (2003). Modeling arching effects in narrow backfilled stopes with FLAC. *Flac and numerical modeling in geomechanics*, 211-219.

Liu, G., Li, L., Yang, X., & Guo, L. (2018). Required strength estimation of a cemented backfill with the front wall exposed and back wall pressured. *International journal of mining and mineral engineering, 9*(1), 1-20.

Liu, G., Li, L., Yao, M., Landry, D., Malek, F., Yang, X., & Guo, L. (2017). An investigation of the uniaxial compressive strength of a cemented hydraulic backfill made of alluvial sand. *Minerals, 7*(1), 4.

Lottermoser, B. G. (2010). Introduction to mine wastes. *Mine wastes, Characterization, treatment and environmental impacts* (pp. 1-41).

Lyu, Z., Chai, J., Xu, Z., Qin, Y., & Cao, J. (2019). A comprehensive review on reasons for tailings dam failures based on case history. *Advances in civil engineering, 2019*(1), 4159306.

Ma, Q., Liu, G., Yang, X., Guo, L., & Fourie, A. (2025). Stability of base-exposed backfill roof considering interfaces between adjacent drifts in underhand drift-and-fill mining. *Journal of rock mechanics and geotechnical engineering*.

Maknoon, M. (2016). Slope stability analyses of waste rock piles under unsaturated conditions following large precipitations. Ph.D thesis, Ecole Polytechnique de Montéal, Montreal, QC, Canada

Manaviparast, H. R., Miranda, T., Pereira, E., & Cristelo, N. (2024). A comprehensive review on mine tailings as a raw material in the alkali activation process. *Applied sciences, 14*(12), 5127.

Martin, T., & McRoberts, E. (1999). Some considerations in the stability analysis of upstream tailings dams. *Paper presented at the proceedings of the 6th international conference on tailings and mine waste*.

Matyas, E. L., Welch, D. E., & Reades, D. W. (1984). Geotechnical parameters and behaviour of uranium tailings. *Canadian geotechnical journal, 21*(3), 489-504.

Mining, Minerals and Sustainable Development Project. (2002). Breaking new ground: Mining, minerals, and sustainable development: The report of the MMSD project. *Earthscan.*

Ministère de l'Environnement, de la Lutte contre les changements climatiques, de la Faune et des Parcs (MELCCFP). (2025). Directive 019 sur l'industrie minière. *Gouvernement du Québec*.

Mitchell, R. (1991). Sill mat evaluation using centrifuge models. *Mining science and technology, 13*(3), 301-313.

Mitchell, R. J., Olsen, R. S., & Smith, J. D. (1982). Model studies on cemented tailings used in mine backfill. *Canadian geotechnical journal, 19*(1), 14-28.

Moffitt, K. (2000). Mine waste dump instability. M.Sc. thesis, University of British Columbia, BC, Canada.

Nichols, R. (1986). Rock segregation in waste dumps. *Proceedings of the international symposium convened at the inn of the south*, Cranbrook, BC.

Nordstrom, D. K., & Alpers, C. N. (1997). Geochemistry of acid mine waters. *The environmental geochemistry of mineral deposits: Part A: processes, methods and health issues.*

Ouattara, D., Yahia, A., Mbonimpa, M., & Belem, T. (2017). Effects of superplasticizer on rheological properties of cemented paste backfills. *International journal of mineral processing, 161*, 28-40.

Pagé, P., Li, L., Yang, P., & Simon, R. (2019). Numerical investigation of the stability of a base-exposed sill mat made of cemented backfill. *International journal of rock mechanics and mining sciences, 114*, 195-207.

Pakalnis, R., Caceres, C., Clapp, K., Morin, M., Brady, T., Williams, T., Blake, W., MacLaughlin, M. (2005). Design spans–underhand cut and fill mining. *Mining rocks! 107th CIM-AGM,* Toronto, ON, Canada.

Pearce, S., Lehane, S., & Pearce, J. (2016). Waste material placement options during construction and closure risk reduction—quantifying the how, the why and the how much. *Proceedings of the 11th international conference on mine closure*, Perth, Australia

Pengyu, Y., & Li, L. (2015). Investigation of the short-term stress distribution in stopes and drifts backfilled with cemented paste backfill. *International journal of mining science and technology, 25*(5), 721-728.

Peregoedova, A. (2012). Étude expérimentale des propriétés hydrogéologiques des roches stériles à une échelle intermédiaire de laboratoire. M.Sc. thesis, École Polytechnique de Montréal, Montreal, QC, Canada.

Pettibone, H. C., & Kealy, C. D. (1971). Engineering properties of mine tailings. *Journal of the soil mechanics and foundations division, 97*(9), 1207-1225.

Pierce, M., Bawden, W., & Paynter, J. (1998). Laboratory testing and stability analysis of paste backfill at the Golden Giant Mine. *Paper presented at the 6th international symposium on mining with backfill.*

Pornillos, E. (2009). Paste fill plant designs for underground mines—a comparison of batch process and continuous process. *Proceedings of the 12th international seminar on paste and thickened tailings.*

Potvin, Y., Thomas, E., & Fourie, A. (2005). Handbook on mine fill. *Australian centre for geomechanics.*

Qin, J., Zheng, J., & Li, L. (2021). Experimental study of the shrinkage behavior of cemented paste backfill. *Journal of rock mechanics and geotechnical engineering, 13*(3), 545-554.

Qiu, H., Zhang, F., Liu, L., Hou, D., & Tu, B. (2020). Influencing factors on strength of waste rock tailing cemented backfill. *Geofluids, 2020*(1), 8847623.

Qiu, H., Zhang, F., Sun, W., Liu, L., Zhao, Y., & Huan, C. (2022). Experimental study on strength and permeability characteristics of cemented rock-tailings backfill. *Frontiers in earth science, 10*, 802818.

Rankine, K. J. (2005). An investigation into the drainage characteristics and behaviour of hydraulically placed mine backfill and permeable minefill barricades. Ph.D thesis, James Cook University, Australia.

Rankine, R. M., & Sivakugan, N. (2007). Geotechnical properties of cemented paste backfill from cannington mine, Australia. *Geotechnical and geological engineering, 25*(4), 383-393.

Rask, A. (2019). Indirect methods as quality control of cemented hydraulic fill: Renström mine, Boliden mineral AB. M.Sc thesis, Luleå University of Technology, Sweden.

Raymond, K. E., Seigneur, N., Su, D., & Mayer, K. U. (2021). Investigating the influence of structure and heterogeneity in waste rock piles on mass loading rates—a reactive transport modeling study. *Frontiers in water, 3*, 618418.

Rico, M., Benito, G., Salgueiro, A., Díez-Herrero, A., & Pereira, H. (2008). Reported tailings dam failures: a review of the European incidents in the worldwide context. *Journal of hazardous materials, 152*(2), 846-852.

Robinsky, E. (1975). Thickened discharge. A new approach to tailings disposal. *Pascal and francis bibliographic databases.*

Sadrossadat, E., Basarir, H., Luo, G., Karrech, A., Durham, R., Fourie, A., & Elchalakani, M. (2020). Multi-objective mixture design of cemented paste backfill using particle swarm optimisation algorithm. *Minerals engineering, 153*, 106385.

Sainsbury, B.-A., Gharehdash, S., & Sainsbury, D. (2021). Large-scale characterisation of cemented rock fill performance for exposure stability analysis. *Construction and building materials, 308*, 124995.

Salama, A. (2014). Haulage system optimization for underground mines: A discrete event simulation and mixed integer programming approach. Ph.D thesis, Luleå University of Technology, Sweden.

Saw, H., & Villaescusa, E. (2013). Geotechnical properties of mine fill. *Paper presented at the proceedings of the 18th southeast asian geotechnical conference*, Singapore.

Sivakugan, N. (2008). Drainage issues and stress developments within hydraulic fill mine stopes. *Australian journal of civil engineering, 5*(1), 61-72.

Sivakugan, N., Veenstra, R., & Naguleswaran, N. (2015a). Underground mine backfilling in Australia using paste fills and hydraulic fills. *International journal of geosynthetics and ground engineering, 1(2)*, 18.

Sivakugan, N., Veenstra, R., & Naguleswaran, N. (2015b). Underground mine backfilling in Australia using paste fills and hydraulic fills. *International journal of geosynthetics and ground engineering, 1*(2), 18.

Skawina, B. (2017). Rock mass transportation systems in underground mines: consequences and solutions when mining at greater depths. Licentiate thesis, Luleå University of Technology, Sweden.

Smith, L. (2021). Hydrogeology and mineral resource development. *The groundwater project: Guelph, ON, Canada*.

Sun, W., Wang, H., & Hou, K. (2018). Control of waste rock-tailings paste backfill for active mining subsidence areas. *Journal of cleaner production, 171*, 567-579.

Tachie-Menson, S. (2006). Characterization of the acid-producing potential and investigation of its effect on weathering of the goathill north rock pile at the questa molybdenum mine, New Mexico. M.Sc thesis, New Mexico Institute of Mining and Technology, Socorro, New Mexico.

Tatiya, R. R. (2005). Surface and underground excavations: methods, techniques and equipment. *CRC press*.

Tomaschitz, J. d. O. P., Mannich, M., & Ota, J. J. (2018). Experimental results for guidance and design criteria of horizontal end-dumping type river closure. *RBRH, 23*, e48.

Turner, J., Brewer, P., & Macklin, M. (2008). Fluvial-controlled metal and as mobilisation, dispersal and storage in the Río Guadiamar, SW Spain and its implications for long-term contaminant fluxes to the Doñana wetlands. *Science of the total environment, 394*(1), 144-161.

Veenstra, R. L., & Grobler, J. J. (2021). Paste-waste design and implementation at Newmont Goldcorp's Tanami Operation. *CRC Press*.

Vick, S. G. (1990). Planning, design, and analysis of tailings dams. *BiTech Publishers Ltd*

Wang, R., Zeng, F., & Li, L. (2021). Stability analyses of side-exposed backfill considering mine depth and extraction of adjacent stope. *International journal of rock mechanics and mining sciences, 142*, 104735.

Williams, D., & Kuganathan, V. (1992). Co-disposal of coal mine tailings and coarse reject. Third large open pit mining conference, Mackay, Australia.

Williams, D. J., & Walker, L. (1985). Laboratory and field strength of mine waste rock. *Civil engineering transactions, 27*(3), 299-304.

Wu, A., Cheng, H., Yang, Y., & Zhang, L.-F. (2017). Development and challenge of paste technology in China. Proceedings of the 20th international seminar on paste and thickened tailings.

Yang, P. (2016). Investigation of the geomechanical behavior of mine backfill and its interaction with rock walls and barricades. Ph.D thesis, Ecole Polytechnique de Montéal, Montreal (Canada).

Yang, P., & Li, L. (2015). Investigation of the short-term stress distribution in stopes and drifts backfilled with cemented paste backfill. *International journal of mining science and technology, 25*(5), 721-728.

Yang, P., & Li, L. (2017). Numerical and limit equilibrium stability analyses of cemented mine backfill upon vertical exposure. Proceedings of the first international conference on underground mining technology.

Yang, P., Li, L., & Aubertin, M. (2017). A new solution to assess the required strength of mine backfill with a vertical exposure. *International journal of geomechanics, 17*(10), 04017084.

Yang, P., Li, L., Aubertin, M., Brochu-Baekelmans, M., & Ouellet, S. (2017). Stability analyses of waste rock barricades designed to retain paste backfill. *International journal of geomechanics, 17*(3), 04016079.

Zhang, S., & Liu, W. (2017). Application of aerial image analysis for assessing particle size segregation in dump leaching. *Hydrometallurgy, 171*, 99-105.

Zhang, Y. (2024). Investigation of the natural mixing behavior of dumped waste rock and paste backfill. Ph.D thesis, Ecole Polytechnique de Montéal, Montreal (Canada).

Zhang, Y., & Li, L. (2023). Experimental study on the natural mixing behaviour of waste rocks poured in a paste backfill. *International journal of mining, reclamation and environment, 37*(10), 953-977.

Zhang, Y., & Li, L. (2024). Optimization of discrete element method model to obtain stable and reliable numerical results of mechanical response of granular materials. *Minerals, 14*(8), 758.

Zhang, Y., Li, L., Gélinas, L.-P., & Ouellet, S. (2026b). Numerical and experimental studies of the natural mixing behavior between an uncemented paste backfill and dumped waste rock in stopes from laboratory toward field conditions. Part II: Application and prediction of the validated and calibrated numerical model. *Deep resources engineering*, 100236.

Zhang, Y., Li, L., Ouellet, S., & Gélinas, L.-P. (2026a). Numerical and experimental studies of the natural mixing behavior between an uncemented paste backfill and dumped waste rock in stopes from laboratory toward field conditions. Part I: Calibration and validation of a numerical model. *Deep resources engineering*, 3(1), 100232.